Chapter 4

TOTAL OPTIMAL SYNTHESIS METHOD FOR TRUSS STRUCTURES CONSIDERING SHAPE, SIZING AND MATERIAL VARIABLES SUBJECTED TO STATIC LOADS

4-1. INTRODUCTION

In problems of optimal synthesis of structures, the most fundamental and significant design variables are the geometry of structures, mechanical and economical properties of materials and cross-sectional dimensions that are available for each member element. Therefore, the establishment of a structural optimization method which can optimize the design problem considering all three types of design variables simultaneously, is a significant task.

During the past decades, a number of contributions have been made exclusively to the sizing optimization since the earliest study by Schmit[1] in 1960 and, in the last two decades, the shape optimization and topology optimization have been studied considerably[2-5]. However, only a bit of focus has been on optimization with material selection which requires a discrete/continuous formulation of the problem [6-13].

In this study an optimal structural synthesis method is presented to determine the optimum solutions for the design problems of truss structures considering the coordinates of the panel points, cross-sectional areas and discrete material kinds of member elements simultaneously as design variables. The stress and displacement constraints due to static loads are taken into account in the optimization process.

The primary design problem is transformed into an approximate subproblem of convex and separable form by using mixed direct/reciprocal design variables, shape, material and sizing sensitivities. The approximate subproblem is solved by a dual method, where the separable Lagrangian function for each element is introduced. In this study, shape and sizing variables are dealt with as continuous variables and material variables as discrete variables. Therefore, the following two-stage minimization process of the Lagrangian function is proposed to solve the design problem including the continuous and discrete variables. At the first stage minimization process, the product of modulus of elasticity E and cross-sectional area A, EA, is treated as one continuous design variable and the optimum values of

EA and shape variable are determined by minimizing the Lagrangian function with respect to EA and shape variable. Then, at next stage the shape variable is maintained constant, and the better combination of cross-sectional area and material kind for each member element is searched independently to reduce the Lagrangian function by comparing the values of discretized Lagrangian function while keeping the activeness of the constraints which are determined by the first minimization process. This separable minimization of the element Lagrangian function with respect to material and sizing variables simplifies the inherent combinatorial complexity associated with the discrete material-selection problems.

The generality, rigorousness and reliability of the proposed optimal structural synthesis method are illustrated by applying the method to various minimum cost design problems of 31-bar trusses subject to stress and displacement constraints and investigations of the optimum solutions at various design conditions. It is also demonstrated that the optimum solutions can be obtained after 15-25 iterations efficiently even when the algorithm is initialized with the worst possible material distribution.

4-2. FORMULATION OF PRIMARY OPTIMUM DESIGN PROBLEM

(1) Design variables

In the design problems of truss structures, the vertical coordinates of panel points **Y**, material kinds **M** and cross-sectional areas **A** of member elements are considered as design variables.

$$\mathbf{A} = \left[A_1, \cdots, A_n\right]^T \tag{4-1}$$

$$\mathbf{Y} = \left[Y_1, \cdots, Y_P\right]^T \tag{4-2}$$

$$\mathbf{M} = \left[M_1, \cdots, M_n\right]^T \tag{4-3}$$

where n is the number of member elements, P denotes the number of coordinates of panel points considered as the design variables **Y**.

Depending on the characteristics of these design variables, **Y** and **A** are dealt with as continuous variables and **M**, which represent the physical and economical properties of the material, are dealt with as discrete variables.

(2) Stress and displacement constraints

The stress constraints on all member elements in truss structures are given as

$$g_{\sigma j}(\mathbf{A},\mathbf{Y},\mathbf{M}) = |N_j(\mathbf{A},\mathbf{Y},\mathbf{M})/A_j| - |\sigma_{aj}(M_j)| \le 0 \qquad (j = 1,\cdots,n) \tag{4-4}$$

where $\sigma_{aj}(M_j)$ and $N_j(\mathbf{A},\mathbf{Y},\mathbf{M})$ are, respectively, the maximum allowable stress and axial force in the jth member element.

The displacement constraints are expressed as

$$g_{\delta d}(\mathbf{A},\mathbf{Y},\mathbf{M}) = |\delta_d(\mathbf{A},\mathbf{Y},\mathbf{M})| - |\delta_{ad}| \le 0 \qquad (d = 1,\cdots,u) \tag{4-5}$$

where δ_{ad} and $\delta_d(\mathbf{A},\mathbf{Y},\mathbf{M})$ are the maximum allowable displacement and actual displacement at the dth panel point, respectively. u is the number of displacement constraints to be taken into account.

(3) Primary optimum design problem

In this study, the total cost of a structure is considered as the objective function **W** and it is expressed as the summation of the costs of member elements. The behavior constraints are stress and displacement constraints $\mathbf{g}_\sigma$ and $\mathbf{g}_\delta$, and the upper and lower limits of the design variables are imposed as their side constraints. The behaviors of trusses, such as member forces and displacements of panel points, are expressed as functions of the lengths, cross-sectional areas and moduli of elasticity of materials of member elements. The upper or lower limitations in the design constraints, such as allowable stresses σ_a and minimum rigidity requirements for stability of the member elements, also depend on the mechanical properties and element sizes. Furthermore, the objective function, such as cost or weight of structure, is also a function of the element sizes and material costs or unit weights. Therefore, the objective function **W**, behavior constraints **g** and upper or lower limit constraints on the design variables can be expressed as functions of **A**, **Y** and **M**. The primary design problem can be then formulated as

Find **A**, **Y**, **M**, which

minimize $$\mathbf{W}(\mathbf{A},\mathbf{Y},\mathbf{M}) = \sum_{i=1}^{n} \rho_{ai}(M_i) l_i(\bar{Y}_i) A_i \tag{4-6}$$

subject to $$g_j(\mathbf{A},\mathbf{Y},\mathbf{M}) \le 0 \qquad (j = 1,\cdots,m) \tag{4-7}$$

$$\left.\begin{array}{ll} A_i^l \le A_i \le A_i^u & (i=1,\cdots,n) \\ Y_k^l \le Y_k \le Y_k^u & (k=1,\cdots,p) \\ M_i \in \mathbf{MS} & (i=1,\cdots,n) \end{array}\right\} \tag{4-8}$$

where $\tilde{\mathbf{Y}}_i = [Y_{i+}, Y_{i-}]^T$

$$\mathbf{g} = [g_1,\cdots,g_m]^T = [g_{\sigma 1},\cdots,g_{\sigma m}, g_{\delta 1},\cdots,g_{\delta u}]^T$$

In the above expressions, $\rho_{ci}(M_i)$, M_i and $l_i(\tilde{Y}_i)$ are, respectively, the unit cost, material kind and member length of the ith member element. Y_{i+} and Y_{i-} are the coordinates of panel points to which the ith member element is connected. **MS** is the set of available candidate materials. m is the number of behavior constraints. Superscripts l and u represent the lower and upper limits of the design variables.

In the material set **MS**, the material components need to be arranged and numbered in order of the ratio between allowable stress σ_a and $\rho_{ci}(M_i)$ or the ratio between modulus of elasticity E and $\rho_{ci}(M_i)$ to ensure a smooth convergence to the optimum materials through iterative improvements.

4-3. OPTIMAL STRUCTURAL SYNTHESIS METHOD FOR TRUSS STRUCTURES SUBJECTED TO STATIC LOADS[19,20]

(1) Convex and separable approximate subproblem

An optimal structural synthesis method combining the concept of convex and linear approximation[14-20], dual method, multilevel optimization concept[21] and discrete sensitivity analysis is developed to determine the optimum solution for structural design problem described in section 4-2.

Utilizing the convex and linear approximation concept, shape, material and sizing sensitivities, the objective function in eq.(4-6) and the behavior constraints in eq.(4-7) are approximated by using the first-order terms of the Taylor series expansions with respect to the direct variables of **A**,**Y**,**M** and the reciprocal variables of **Y** and **A**. In the objective function the constant term can be neglected in the optimization process and only the change in the objective function $\Delta\mathbf{W}$ is dealt with in place of the objective function, $\mathbf{W}(\mathbf{A},\mathbf{Y},\mathbf{M})$. Then, the following convex and separable approximate subproblem can be derived.

Find $\mathbf{A}, \mathbf{Y}, \Delta\mathbf{M}$, which

minimize
$$\Delta W(\mathbf{A},\mathbf{Y},\mathbf{M}^0+\Delta\mathbf{M}) = \sum_{i=1}^{n} \omega_{Ai}\left(M_i^0+\Delta M_i\right)A_i$$
$$+\sum_{K=1}^{p}\left[\omega_{YK_{(+)}}(\mathbf{M}^0+\Delta\mathbf{M})Y_K - \omega_{YK_{(-)}}(\mathbf{M}^0+\Delta\mathbf{M})\left(Y_K^0\right)^2\frac{1}{Y_K}\right] \qquad (4\text{-}9)$$

subject to
$$\bar{g}_j(\mathbf{A},\mathbf{Y},\mathbf{M}^0+\Delta\mathbf{M}) = \sum_{i=1}^{n}\left[a_{ji_{(+)}}A_i - a_{ji_{(-)}}\left(A_i^0\right)^2\frac{1}{A_i} + m_{ji}\Delta M_i\right]$$
$$+\sum_{k=1}^{p}\left[y_{jk_{(+)}}Y_k - y_{jk_{(-)}}\left(Y_k^0\right)^2\frac{1}{Y_k}\right] + \overline{U}_j \le 0 \qquad (j=1,\cdots,m) \qquad (4\text{-}10)$$

$$\left.\begin{aligned} &A_i^l \le A_i \le A_i^u && (i=1,\cdots,n)\\ &Y_k^l \le Y_k \le Y_k^u && (k=1,\cdots,P)\\ &M_i \in \mathbf{MS} && (i=1,\cdots,n)\end{aligned}\right\} \qquad (4\text{-}11)$$

where
$$\overline{U}_j = g_j(\mathbf{A}^0,\mathbf{Y}^0,\mathbf{M}^0) - \sum_{i=1}^{n}A_i^0\left[a_{ji_{(+)}} - a_{ji_{(-)}}\right] - \sum_{k=1}^{p}Y_k^0\left[y_{jk_{(+)}} - y_{jk_{(-)}}\right]$$

$$\omega_{Ai}\left(M_i^0+\Delta M_i\right) = \frac{\partial \mathbf{W}}{\partial A_i} = \rho_{ci}\left(M_i^0+\Delta M_i\right)l_i\left(\tilde{Y}_i\right)$$

$$\omega_{Yk}(\mathbf{M}^0+\Delta\mathbf{M}) = \frac{\partial \mathbf{W}}{\partial Y_k} = \sum_{i\in\mathbf{S}_k}\rho_{ci}\left(M_i^0+\Delta M_i\right)A_i\frac{\partial l_i\left(\tilde{Y}_i\right)}{\partial Y_k}$$

$$a_{ji} = \frac{\partial g_j}{\partial A_i}, \quad y_{jk} = \frac{\partial g_j}{\partial Y_k}, \quad m_{ji} = \frac{\partial g_j}{\partial M_i}, \quad \mathbf{M} = \mathbf{M}^0 + \Delta\mathbf{M}$$

In the above expressions, the symbols (+) and (-) express the signs of the first-order partial derivatives and $\mathbf{S}_k$ is the set of elements connected to the kth panel point. In the above approximate formulation the changes $\Delta\mathbf{M}$ in material kinds are dealt with as material variables.

(2) Calculation of behavior sensitivities

Utilizing the concept of convex linearization, the stress and displacement constraints (eqs.(4-4) and (4-5)) are transformed into their approximated forms as shown in eq.(4-7), in which the sensitivities with respect to design variables are calculated by the following expressions:

if j indicates the stress constraint : $g_j(j=1,\cdots,n)$

$$a_{ji}=-|N_j|\frac{1}{\left(A_j^0\right)^2}+\frac{\partial|N_j|}{\partial A_j}\frac{1}{A_j^0}\quad(i=j),\quad a_{ji}=\frac{\partial|N_j|}{\partial A_i}\frac{1}{A_j^0}\qquad(i\neq j),\tag{4-12}$$

$$y_{jk}=\frac{\partial|N_j|}{\partial A_k}\frac{1}{A_j^0}\tag{4-13}$$

$$m_{ji}=-\left[\sigma_a(M_i)-\sigma_a\left(M_i^0\right)\right]+\frac{1}{A_j^0}\frac{\partial|N_j|}{\partial A_i}\frac{A_i^0}{E_i\left(M_i^0\right)}\left[E_i(M_i)-E_i\left(M_i^0\right)\right]\quad(i=j),$$

$$m_{ji}=\frac{1}{A_j^0}\frac{\partial|N_j|}{\partial A_i}\frac{A_i^0}{E_i\left(M_i^0\right)}\left[E_i(M_i)-E_i\left(M_i^0\right)\right]\qquad(i\neq j)\tag{4-14}$$

if j indicates the displacement constraint : $g_j(j=n+1,\cdots,n+u)$

$$a_{ji}=\frac{\partial|\delta_d|}{\partial A_i}\qquad(d=j-n)\tag{4-15}$$

$$y_{jk}=\frac{\partial|\delta_d|}{\partial Y_k}\qquad(d=j-n)\tag{4-16}$$

$$m_{ji}=\frac{\partial|\delta_d|}{\partial A_i}\frac{A_i^0}{E_i\left(M_i^0\right)}\left[E_i(M_i)-E_i\left(M_i^0\right)\right]\qquad(d=j-n)\tag{4-17}$$

where

$$\frac{\partial|N_j|}{\partial A_i}=\frac{\partial N_j}{\partial A_i},\qquad\frac{\partial|N_j|}{\partial Y_k}=\frac{\partial N_j}{\partial Y_k}\qquad\text{if}\quad N_j\geq 0$$

$$\frac{\partial|N_j|}{\partial A_i}=-\frac{\partial N_j}{\partial A_i},\qquad\frac{\partial|N_j|}{\partial Y_k}=-\frac{\partial N_j}{\partial Y_k}\qquad\text{if}\quad N_j<0$$

$$\frac{\partial|\delta_d|}{\partial A_i}=\frac{\partial D_{Sd}}{\partial A_i},\qquad\frac{\partial|\delta_d|}{\partial Y_k}=\frac{\partial D_{Sd}}{\partial Y_k}\qquad\text{if}\quad \delta_d\geq 0$$

$$\frac{\partial|\delta_d|}{\partial A_i}=-\frac{\partial D_{Sd}}{\partial A_i},\qquad\frac{\partial|\delta_d|}{\partial Y_k}=-\frac{\partial D_{Sd}}{\partial Y_k}\qquad\text{if}\quad \delta_d<0$$

In the above expressions, $\frac{\partial N_j}{\partial A_i}$, $\frac{\partial N_j}{\partial Y_k}$, $\frac{\partial D_{Sd}}{\partial A_i}$ and $\frac{\partial D_{Sd}}{\partial Y_k}$ are calculated analytically by the following expressions:

$$\frac{\partial\mathbf{N}}{\partial A_i}=\frac{\partial\mathbf{K}_m}{\partial A_i}\mathbf{Q}\mathbf{D}_S+\mathbf{K}_m\mathbf{Q}\frac{\partial\mathbf{D}_S}{\partial A_i}\tag{4-18}$$

$$\frac{\partial \mathbf{N}}{\partial Y_k} = \frac{\partial \mathbf{K}_m}{\partial Y_k}\mathbf{Q}\mathbf{D}_S + \mathbf{K}_m \frac{\partial \mathbf{Q}}{\partial Y_k}\mathbf{D}_S + \mathbf{K}_m \mathbf{Q}\frac{\partial \mathbf{D}_S}{\partial Y_k} \tag{4-19}$$

$$\frac{\partial \mathbf{D}_S}{\partial A_i} = -\mathbf{K}_S^{-1}\left[\mathbf{Q}^{\mathrm{T}}\frac{\partial \mathbf{K}_m}{\partial A_i}\mathbf{Q}\mathbf{D}_S\right] \tag{4-20}$$

$$\frac{\partial \mathbf{D}_S}{\partial Y_k} = -\mathbf{K}_S^{-1}\left[\left\{\frac{\partial \mathbf{Q}^{\mathrm{T}}}{\partial Y_k}\mathbf{K}_m\mathbf{Q} + \mathbf{Q}^T\frac{\partial \mathbf{K}_m}{\partial Y_k}\mathbf{Q} + \mathbf{Q}^{\mathrm{T}}\mathbf{K}_m\frac{\partial \mathbf{Q}}{\partial Y_k}\right\}\mathbf{D}_S\right] \tag{4-21}$$

where $\mathbf{K}_S$ and $\mathbf{K}_m$ are, respectively, the system stiffness matrices expressed in terms of the structure-oriented coordinate system and the member-oriented coordinate system. $\mathbf{D}_S$ is the displacement expressed in terms of the structure-oriented coordinate system and $\mathbf{Q}$ is the angular transformation matrix of the total system.

(3) Improvements of **A**, **Y** and **M** by a two-stage minimization process of the Lagrangian function

(a) Two-stage minimization process of the Lagrangian function

The stresses of member elements and displacements at the free nodes of truss structure are expressed as the functions of **Y** and the product of modulus of elasticity E and **A**, EA, and the objective function is also expressed as the function of **A**, **Y** and **M**. As stated previously, in this study **A** and **Y** are dealt with as continuous variables and $\Delta\mathbf{M}$ as a discrete variable. Therefore, the design variables **A**, **Y** and $\Delta\mathbf{M}$ are improved by a two-stage minimization process of the Lagrangian function which uses a dual method and incorporate discrete sensitivity analysis. At the first stage minimization process, EA is treated as one continuous design variable and the optimum values of EA and **Y** are determined by minimizing the Lagrangian function with respect to EA and **Y**. In the optimization algorithm of first stage minimization process, E is constant and **A** is improved for improvement of EA. Thereafter, the better combination of **A** and $\Delta\mathbf{M}$ for each member element is searched independently to reduce the Lagrangian function by comparing the values of discretized Lagrangian function while keeping the activeness of the constraints which are determined by the first minimization process.

(b) Lagrangian function **L**

The design variables **A**, **Y** and $\Delta\mathbf{M}$ are improved by solving the convex and separable approximate subproblem (eqs.(4-9)-(4-11)). A separable Lagrangian function can be introduced for the subproblem as

$$\mathbf{L}\left(\mathbf{A},\mathbf{Y},\mathbf{M}^0+\Delta\mathbf{M},\lambda\right)=\sum_{i=1}^{n}L_i\left(A_i,\Delta M_i,\lambda\right)+\sum_{k=1}^{p}L_k\left(Y_k,\Delta\mathbf{M},\lambda\right)+\sum_{j=1}^{m}\lambda_j\overline{U}_j \qquad (4\text{-}22)$$

$$\text{where} \quad \lambda_j\geq 0 \qquad (j=1,\cdots,m)$$

where L_i and L_k are, respectively, the element Lagrangian functions with respect to the $A_i,\Delta M_i$ and $Y_k,\Delta\mathbf{M}$. λ_j is the Lagrange multiplier(dual variable) for the jth behavior constraint. L_i and L_k are in turn given by

$$L_i\left(A_i,\Delta M_i,\lambda\right)=\omega_{Ai}\left(M_i^0+\Delta M_i\right)A_i+\sum_{j=1}^{m}\lambda_j\left[a_{ji_{(+)}}A_i-a_{ji_{(-)}}\left(A_i^0\right)^2\frac{1}{A_i}+m_{ji}\Delta M_i\right] \qquad (4\text{-}23)$$

$$L_k\left(Y_k,\Delta\mathbf{M},\lambda\right)=\omega_{Yk_{(+)}}\left(\mathbf{M}^0+\Delta\mathbf{M}\right)Y_k-\omega_{Yk_{(-)}}\left(\mathbf{M}^0+\Delta\mathbf{M}\right)\left(Y_k^0\right)^2\frac{1}{Y_k}$$
$$+\sum_{j=1}^{m}\lambda_j\left[y_{jk_{(+)}}Y_k-y_{jk_{(-)}}\left(Y_k^0\right)^2\frac{1}{Y_k}\right] \qquad (4\text{-}24)$$

The solutions of the subproblem, $\mathbf{A}^*,\mathbf{Y}^*,\mathbf{M}^*$ and λ^*, can be obtained by maximizing $\mathbf{L}\left(\mathbf{A},\mathbf{Y},\mathbf{M}^0+\Delta\mathbf{M},\lambda\right)$ with respect to λ and minimizing it with respect to **A**, **Y** and $\Delta\mathbf{M}$.

(c) First stage min.-max. process of **L** with respect to ***EA***, **Y** and λ

At the first stage of the minimization process, $L_i\left(A_i,\Delta M_i,\lambda\right)$ and $L_k\left(Y_k,\Delta\mathbf{M},\lambda\right)$ are, respectively, minimized with respect to A_i and Y_k. At this stage, $\Delta\mathbf{M}$ is maintained constant, namely, ***E*** is constant, and **A** is improved for improvement of ***EA***. A_i, which minimizes $L_i\left(A_i,\Delta M_i,\lambda\right)$, is given by the simple expression in eq. (4-25) which is derived from the necessary condition for the minimum of $L_i\left(A_i,\Delta M_i,\lambda\right)$, namely, $\partial L_i/\partial A_i=0$, and the side constraint.

$$\left.\begin{array}{ll}\text{if} \quad \left[A_i^l\left(M_i^0\right)\right]^2<Z_{Ai}\left(M_i^0\right)<\left[A_i^u\left(M_i^0\right)\right]^2, & A_i^*=\sqrt{Z_{Ai}\left(M_i^0\right)}\\ \text{if} \quad Z_{Ai}\left(M_i^0\right)\leq\left[A_i^l\left(M_i^0\right)\right]^2, & A_i^*=A_i^l\left(M_i^0\right)\\ \text{if} \quad Z_{Ai}\left(M_i^0\right)\geq\left[A_i^u\left(M_i^0\right)\right]^2, & A_i^*=A_i^u\left(M_i^0\right)\end{array}\right\} \qquad (4\text{-}25)$$

where

$$Z_{Ai}\left(M_i^0\right)=\frac{-\sum_{j=1}^{m}\lambda_j a_{ji(-)}\left(A_i^0\right)^2}{\omega_{Ai}\left(M_i^0\right)+\sum_{j=1}^{m}\lambda_j a_{ji(+)}}$$

Y_k, which minimizes L_k, is also calculated by similar expression shown below:

$$\left.\begin{array}{lll} \text{if} & \left[Y_k^l\right]^2 < Z_{Yk}\left(\mathbf{M}^0\right) < \left[Y_k^u\right]^2, & Y_k^* = \sqrt{Z_{Yk}\left(\mathbf{M}^0\right)} \\ \text{if} & Z_{Yk}\left(\mathbf{M}^0\right) \le \left[Y_k^l\right]^2, & Y_k^* = Y_k^l \\ \text{if} & Z_{Yk}\left(\mathbf{M}^0\right) \ge \left[Y_k^u\right]^2, & Y_k^* = Y_k^u \end{array}\right\} \quad (4\text{-}26)$$

where

$$\text{if} \quad \omega_{Yk}\left(\mathbf{M}^0\right) \ge 0, \qquad Z_{Yk}\left(\mathbf{M}^0\right)=\frac{-\sum_{j=1}^{m}\lambda_j y_{jk(-)}\left(Y_k^0\right)^2}{\omega_{Yk_{(+)}}\left(\mathbf{M}^0\right)+\sum_{j=1}^{m}\lambda_j y_{jk(+)}},$$

$$\text{if} \quad \omega_{Yk}\left(\mathbf{M}^0\right) < 0, \qquad Z_{Yk}\left(\mathbf{M}^0\right)=\frac{-\left(\omega_{Yk_{(-)}}\left(\mathbf{M}^0\right)+\sum_{j=1}^{m}\lambda_j y_{jk(-)}\right)\left(Y_k^0\right)^2}{\sum_{j=1}^{m}\lambda_j y_{jk(+)}}$$

The minimized Lagrangian function with respect to **A** and **Y** by the above expressions is denoted as $l(\lambda)$:

$$l(\lambda)=\min_{\mathbf{A},\mathbf{Y}}\mathbf{L}\left(\mathbf{A},\mathbf{Y},\mathbf{M}^0+\Delta\mathbf{M},\lambda\right) \quad (4\text{-}27)$$

Following the minimization process with respect to A_i and Y_k, the Lagrangian function $l(\lambda)$ is maximized with respect to the dual variables λ by using a Newton-type algorithm. In the Newton-type algorithm, the dual variables $\bar{\lambda}$ corresponding to the active behavior constraints at the current stage are modified iteratively as

$$\bar{\lambda}^{(t+1)}=\bar{\lambda}^{(t)}+\alpha^{(t)}\cdot\mathbf{S}^{(t)} \quad . \quad (4\text{-}28)$$

or in a scalar form

$$\bar{\lambda}_j^{(t+1)} = \bar{\lambda}_j^{(t)} + \alpha^{(t)} \cdot S_j^{(t)} \qquad (j \in \boldsymbol{S}_{AG}) \tag{4-29}$$

where $\mathbf{S}^{(t)}$ denotes the search direction of λ for active constraints, $\boldsymbol{S}_{AG}$ is the set of active behavior constraints and α represents the step length parameter. The search direction $\mathbf{S}^{(t)}$ is given by

$$\mathbf{S}^{(t)} = -\left[\mathbf{H}\left(\bar{\lambda}^{(t)}\right)\right]^{-1} \cdot \nabla l\left(\bar{\lambda}^{(t)}\right) \tag{4-30}$$

where $\nabla l(\bar{\lambda})$ is the vector of first derivatives of $l(\lambda)$ with respect to $\bar{\lambda}$ and the components of the vector are simply given by the approximate active constrains, namely,

$$\frac{\partial l(\bar{\lambda})}{\partial \bar{\lambda}_j} = \sum_{i=1}^{n}\left[a_{j\beta_{(-)}} A_i^* - a_{j\beta_{(-)}}\left(A_i^0\right)\frac{1}{A_i^*}\right] + \sum_{k=1}^{p}\left[y_{j\beta_{(+)}} Y_k^* - y_{j\beta_{(-)}}\left(Y_k^0\right)^2 \frac{1}{Y_k^*}\right] + \bar{U}_j \tag{4-31}$$

H in eq.(4-30) is the Hessian matrix of $l(\bar{\lambda})$ with respect to $\bar{\lambda}$ and its jkth element is given by

$$H_{jk} = \frac{\partial^2 l(\bar{\lambda})}{\partial \lambda_j \partial \lambda_k} = \sum_{i=1}^{n} P_i + \sum_{i=1}^{p} Q \qquad (j,k \in \boldsymbol{S}_{AG}) \tag{4-32}$$

The expressions used in the calculations of P_i and Q in eq.(4-32) are given in the Appendix 4-1.

The search direction $\mathbf{S}^{(t)}$ is calculated by using Cholesky decomposition described in section 4-3.(3).(d).

The step length α is first set as 1.0; however, its maximum allowable value is restricted by

$$\alpha_{\max}^{(t)} = \min_{S_j^{(t)} < 0}\left|\frac{\bar{\lambda}_j^{(t)}}{S_j^{(t)}}\right| \qquad (j \in \boldsymbol{S}_{AG}) \tag{4-33}$$

to ensure the non-negativity of λ when $\mathbf{S}^{(t)}$ includes negative components.

Based on the modifications of dual variables λ through the above search procedure, the primary design variables **A** and **Y** are improved by eqs.(4-25) and (4-26). The set of active constraints $\boldsymbol{S}_{AG}$ in the currently approximated design space also has to be updated. The min.-mix. process described above is iterated until **A**, **Y** and λ converge to constant values.

In the above optimization algorithm, it should be noted that if the changing rates in **Y** calculated as per eq.(4-26) are too large in any one iteration of the improvement process, the successive solutions oscillate and in some cases smooth convergence may not be obtained. For this reason, the adaptive move limit constraints are restricted such that the maximum rate of change in **Y** is limited to less than 5%.

(d) Calculation of search direction $\mathbf{S}^{(t)}$ by using Cholesky decomposition

In this study, the search direction $\mathbf{S}^{(t)}$ for improvement of $\bar{\lambda}$ is calculated by using Cholesky decomposition[22]. In the process, eq.(4-30) is transformed into eq.(4-34).

$$\left[\mathbf{H}\left(\bar{\lambda}^{(t)}\right)\right]\cdot\mathbf{S}^{(t)} = -\nabla l\left(\bar{\lambda}^{(t)}\right) \tag{4-34}$$

If **H** is a symmetrical matrix and positive definite, then **H** is factorized as eq.(4-35) by using lower triangular matrix $\mathbf{L}_C$ and upper triangular matrix $\mathbf{L}_C^T$.

$$\left[\mathbf{H}\left(\bar{\lambda}^{(t)}\right)\right] = \mathbf{L}_C\cdot\mathbf{L}_C^T \tag{4-35}$$

The elements of $\mathbf{L}_C$ and $\mathbf{L}_C^T$ can be calculated by the followings.

$$L_{11} = \sqrt{h_{11}} \tag{4-36}$$

$$L_{1j} = \frac{h_{1j}}{L_{11}} \tag{4-37}$$

$$L_{ii} = \sqrt{h_{ii} - \sum_{k=1}^{i-1} L_{ki}^2} \qquad \left(i = 2,\cdots,\bar{q}\right) \tag{4-38}$$

$$L_{ij} = \frac{h_{ij} - \sum_{k=1}^{i-1} L_{ki}L_{kj}}{L_{ii}} \qquad \left(i < j\right) \tag{4-39}$$

where L_{ij} and h_{ij} are, respectively, the ijth element of $\mathbf{L}_C$ and **H**. $\bar{q}$ denotes the number of active constraints.

We can use the decomposition in eq.(4-35) to solve the linear set in eq.(4-34), namely,

$$\left[\mathbf{H}\left(\bar{\lambda}^{(t)}\right)\right]\cdot\mathbf{S}^{(t)} = \left(\mathbf{L}_C\cdot\mathbf{L}_C^T\right)\cdot\mathbf{S}^{(t)} = \mathbf{L}_C\cdot\left(\mathbf{L}_C^T\cdot\mathbf{S}^{(t)}\right) = -\nabla l\left(\bar{\lambda}^{(t)}\right) \tag{4-40}$$

by first solving for vector **V** such that

$$\mathbf{L}_C \cdot \mathbf{V} = -\nabla l\left(\overline{\lambda}^{(t)}\right) \tag{4-41}$$

and then solving

$$\mathbf{L}_C^T \cdot \mathbf{S}^{(t)} = \mathbf{V} \tag{4-42}$$

Eq.(4-41) can be solved by forward substitution, while eq.(4-42) can then be solved by backsubstitution.

It is very important to note that, in the maximizing process of the Lagrangian function with respect to λ, the Hessian matrix **H** can become singular and then the search direction $\mathbf{S}^{(t)}$ can not be determined by eq.(4-30). **H** can become singular if one or more gradient vectors of the active constraints become linearly dependent on the others. In this case, in the process of factorization of **H** by Cholesky decomposition, the *i*th element of diagonal, L_{ii}, in the lower triangular matrix can not be calculated by eq.(4-38) because of the complex number. To overcome the complication associate with this singularity, in this study, if L_{ii} can not be calculated by eq.(4-38), the *i*th active constraint is deleted from the set of active constraints $\mathbf{S}_{AG}$. Then, the Hessian matrix **H** is re-calculated and the calculation of search direction **S** is tried again.

(e) Second stage minimizaition of **L** with respect to **M** and **A**

In the second stage minimization process of the Lagrangian function, the values of **S** and λ improved by the first stage minimization process are maintained constant, and the Lagrangian function $\mathbf{L}(\mathbf{A}, \mathbf{Y}, \mathbf{M}^0+\Delta\mathbf{M}, \lambda)$ given by eq.(4-22) is minimized with respect to **A** and $\Delta\mathbf{M}$ while keeping the activeness of the constraints which are determined by the first stage minimization process, namely,

Find $\mathbf{A}, \Delta\mathbf{M},$ which

minimize $\mathbf{L}(\mathbf{A}, \overline{\mathbf{Y}}, \mathbf{M}^0+\Delta\mathbf{M}, \overline{\lambda})$ (4-43)

subject to $\overline{g}_j(\mathbf{A}, \overline{\mathbf{Y}}, \mathbf{M}^0+\Delta\mathbf{M}) \le 0 \qquad (j \in \mathbf{S}_{AG})$ (4-44)

$$\left.\begin{aligned} A_i^l \le A_i^l \le A_i^u \qquad & (i=1,\cdots,n) \\ M_i \in \mathbf{MS} \qquad & (i=1,\cdots,n) \end{aligned}\right\} \tag{4-45}$$

In the above expression, $\overline{\lambda}$ and $\overline{\mathbf{Y}}$ are the solutions obtained by the first stage

minimization process and these values are maintained constant during the second stage minimization process.

After the first stage improvement of $\mathbf{A}$, $\mathbf{Y}$ and λ, the approximate constraint $\overline{g}_j(\mathbf{A}, \overline{\mathbf{Y}}, \mathbf{M}^0+\Delta\mathbf{M})$ in the set of active constraints $\boldsymbol{S}_{AG}$, namely, $j \in \boldsymbol{S}_{AG}$, becomes zero, and λ_j for the inactive constraint $\overline{g}_j$, namely, $j \notin \boldsymbol{S}_{AG}$, becomes zero. By substituting these relations into $\mathbf{L}(\mathbf{A}, \overline{\mathbf{Y}}, \mathbf{M}^0 + \Delta\mathbf{M}, \overline{\lambda})$ in eq.(4-22), the minimization problem in eqs.(4-43)-(4-45) is solved by minimizing only the term of objective function for each member element in $\mathbf{L}(\mathbf{A}, \overline{\mathbf{Y}}, \mathbf{M}^0 + \Delta\mathbf{M}, \overline{\lambda})$ independently, namely, $\overline{L}_i(\overline{A}_i, \Delta M_i)$ $(i=1,\cdots,n)$ given by eq.(4-46) subject to the constraints in eqs.(4-44) and (4-45).

$$\overline{L}_i(\overline{A}_i, \Delta M_i) = \omega_{Ai}(M_i^0 + \Delta M_i) \cdot \overline{A}_i(M_i^0 + \Delta M_i) \qquad (i=1,\cdots,n) \qquad (4\text{-}46)$$

$\overline{A}_i$ and ΔM_i which minimize $\overline{L}_i(\overline{A}_i, \Delta M_i)$ are determined by comparing the discrete value of $\overline{L}_i(\overline{A}_i, \Delta M_i)$ calculated by using the new material kind $(M_i^0 + \Delta M_i)$ and $\overline{A}_i\left(M_i^0 + \Delta M_i\right)$ improved so as to satisfy the constraints in eqs.(4-44) and (4-45).

The calculation of $\overline{A}_i\left(M_i^0 + \Delta M_i\right)$ is made in the manner described below in order to satisfy the active constraints.

(i) For the case that only stress constraints are active

For the case that only stress constraints are active after the first stage minimization process, the necessary condition which maintains the stress constraints active for a discrete change ΔM_i in material kind M_i is given as

$$g_{\sigma i}\left(\overline{A}_i^{\sigma}, \Delta M_i\right) = \frac{\sigma_i \cdot A_i^{*}\left(M_i^0\right)}{\overline{A}_i^{\sigma}\left(M_i^0 + \Delta M_i\right)} - \sigma_{ai}\left(M_i^0\right) + m_{ii} = 0 \qquad (i=1,\cdots,n) \qquad (4\text{-}47)$$

where σ_i and $\sigma_{ai}\left(M_i^0\right)$ are, respectively, the working stress and allowable stress of the ith member element with material kind M_i^0. m_{ii} given by eq.(4-14) is the sensitivity of stress constraint of the ith member element with respect to a discrete change in material kind M_i. Considering the lower and upper limits on A_i in eq.(4-8), the improved A_i for $M_i^0 + \Delta M_i$, $\overline{A}_i^{\sigma}\left(M_i^0 + \Delta M_i\right)$, is calculated by the following expressions.

$$
\left.
\begin{aligned}
&\text{if} \quad A_i^l\left(M_i^0+\Delta M_i\right) < A_{Si} < A_i^u\left(M_i^0+\Delta M_i\right), \\
&\qquad \overline{A}_i^{\sigma}\left(M_i^0+\Delta M_i\right) = A_{Si} \\
&\text{if} \quad A_{Si} \le A_i^l\left(M_i^0+\Delta M_i\right), \\
&\qquad \overline{A}_i^{\sigma}\left(M_i^0+\Delta M_i\right) = A_i^l\left(M_i^0+\Delta M_i\right) \\
&\text{if} \quad A_{Si} \ge A_i^u\left(M_i^0+\Delta M_i\right), \\
&\qquad \overline{A}_i^{\sigma}\left(M_i^0+\Delta M_i\right) = A_i^u\left(M_i^0+\Delta M_i\right)
\end{aligned}
\right\} \qquad (4\text{-}48)
$$

where

$$
A_{Si} = A_i^{*} \cdot \sigma\left(M_i^0\right) / \left[\sigma_{ai}\left(M_i^0\right) - m_{ii}\right]
$$

$$
A_i^{*} = \sqrt{\frac{-\sum_{j=1}^{q} \lambda_j a_{ji(-)} \left(A_i^0\right)^2}{\omega_{Ai}\left(M_i^0\right) + \sum_{j=1}^{q} \lambda_j a_{ji(+)}}}
$$

(ii) For the case that only displacement constraints are active

For the case that displacement constraint(s) is(are) active after the first stage minimization process, the necessary condition required to maintain the displacement constraint(s) to be active for a discrete change ΔM_i is to keep the value of $E_i A_i$ constant, namely

$$
E_i\left(M_i^0\right) A_i^{*}\left(M_i^0\right) = E_i\left(M_i^0+\Delta M_i\right) \overline{A}_i^{\delta}\left(M_i^0+\Delta M_i\right) \qquad (i=1,\cdots,n) \qquad (4\text{-}49)
$$

Considering the lower and upper limits on A_i, the improved A_i for $M_i^0+\Delta M_i$, $\overline{A}_i^{\delta}\left(M_i^0+\Delta M_i\right)$, is calculated as

$$
\left.
\begin{aligned}
&\text{if} \quad A_i^l\left(M_i^0+\Delta M_i\right) < A_{\delta i} < A_i^u\left(M_i^0+\Delta M_i\right), \\
&\qquad \overline{A}_i^{\delta}\left(M_i^0+\Delta M_i\right) = A_{\delta i} \\
&\text{if} \quad A_{\delta i} \le A_i^l\left(M_i^0+\Delta M_i\right), \\
&\qquad \overline{A}_i^{\delta}\left(M_i^0+\Delta M_i\right) = A_i^l\left(M_i^0+\Delta M_i\right) \\
&\text{if} \quad A_{\delta i} \ge A_i^u\left(M_i^0+\Delta M_i\right), \\
&\qquad \overline{A}_i^{\delta}\left(M_i^0+\Delta M_i\right) = A_i^u\left(M_i^0+\Delta M_i\right)
\end{aligned}
\right\} \qquad (4\text{-}50)
$$

where

$$A_{\delta i} = \frac{A_i^* \cdot E_i\left(M_i^0\right)}{E_i\left(M_i^0 + \Delta M_i\right)}$$

(iii) For the case that both stress and displacement constraints are active

For the case that both stress and displacement constraints are active after the first stage minimization process, the improved A_i for $M_i^0 + \Delta M_i$, $\overline{\mathrm{A}}_i^{\sigma,\delta}\left(M_i^0 + \Delta M_i\right)$, chooses a larger value of $\overline{A}_i^{\sigma}$ and $\overline{A}_i^{\delta}$. Namely,

$$\left.\begin{array}{l} \text{if} \quad \overline{\mathrm{A}}_i^{\sigma}\left(M_i^0 + \Delta M_i\right) \geq \overline{\mathrm{A}}_i^{\delta}\left(M_i^0 + \Delta M_i\right), \quad \overline{\mathrm{A}}_i^{\sigma,\delta}\left(M_i^0 + \Delta M_i\right) = \overline{\mathrm{A}}_i^{\sigma}\left(M_i^0 + \Delta M_i\right) \\ \text{if} \quad \overline{\mathrm{A}}_i^{\delta}\left(M_i^0 + \Delta M_i\right) > \overline{\mathrm{A}}_i^{\sigma}\left(M_i^0 + \Delta M_i\right), \quad \overline{\mathrm{A}}_i^{\sigma,\delta}\left(M_i^0 + \Delta M_i\right) = \overline{\mathrm{A}}_i^{\delta}\left(M_i^0 + \Delta M_i\right) \end{array}\right\} \tag{4-51}$$

The discrete changes in the mechanical and economical properties of materials considerably affect the design space and, therefore, the range of ΔM_i for the minimizaition of $\overline{L}_i(\overline{A}_i, \Delta M_i)$ in one iterative improvement is restricted to the nearest discrete values, namely stronger $(\Delta M_i = +1)$ and weaker $(\Delta M_i = -1)$ materials, only.

The reformulation of approximate subproblem and improvements of **A**, **Y**, **M** and λ by the above two-stage minimization process are repeated until the convergence criteria are satisfied. Thus, the final optimum solutions, $\mathbf{A}^*, \mathbf{Y}^*, \mathbf{M}^*$ and λ^*, can be obtained.

(f) Scaling of initial design variables

In the Newton-type algorithm for the first stage min.-max. process of the Lagrangian function, at least one of the behavior constraints must be active, that is, at least one component of λ must have a non-trivial positive value for the formation of the Hessian matrix. For this purpose, a simple scaling technique given by eq.(4-52) can be devised for modifying the initial cross-sectional areas $\mathbf{A}^0$ so that at least one of the behavior constraints is active.

$$\left.\begin{array}{lll} \text{if} \quad (\sigma/\sigma_a)_{\max} \geq (\delta/\delta_a)_{\max}, & A_i = A_i^0 \cdot (\sigma/\sigma_a)_{\max} & (i = 1, \cdots, n) \\ \text{if} \quad (\sigma/\sigma_a)_{\max} < (\delta/\delta_a)_{\max}, & A_i = A_i^0 \cdot (\delta/\delta_a)_{\max} & (i = 1, \cdots, n) \end{array}\right\} \tag{4-52}$$

In the above expressions, $(\sigma/\sigma_a)_{\max}$ is the maximum ratio between actual stress and allowable stress in all member elements and $(\delta/\delta_a)_{\max}$ is the maximum ratio

between actual displacement and allowable displacement at the aimed points of displacement constraints.

The macro flow diagram of the optimal structural synthesis method proposed in this study is shown in Fig. 4-1.

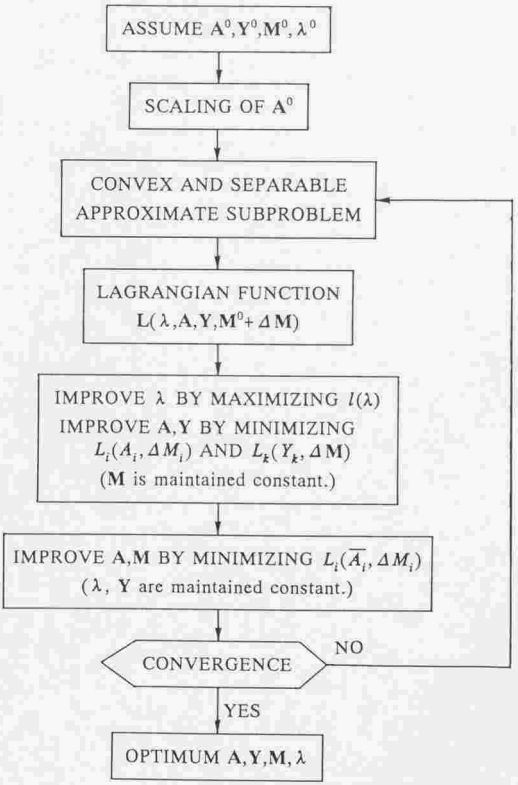

Fig.4-1 Macro flow diagram of proposed optimal structural synthesis method

4-4. NUMERICAL DESIGN EXAMPLES

The optimal structural synthesis method described in section 4-3 has been applied to the minimum-cost designs of statically indeterminate trusses subjected to stress and displacement constraints. In this section, the details of problems and results are discussed. In the design problems, the lower limits of cross-sectional areas are set as $0.10\,\mathrm{cm}^2$ and the objective is to find the optimum topological member arrangements of truss structures for various design conditions.

(1) Material sets

In structural design, several types of material sets may be available, such as a set of steel kinds in which the moduli of elasticity E are the same, and another set could have materials with different E. The optimum structural synthesis method developed in this study can select the optimum material kind for each member element from either types of material sets.

The properties of material which affect the optimum solution of the minimum-cost designs of trusses are the allowable stress σ_a, modulus of elasticity E and cost per unit volume ρ_c. In general, the ratios of σ_a / ρ_c and E / ρ_c represent the effectivenesses of the stress and displacement constraints, respectively. Materials with high values of σ_a / ρ_c are more advantageous in situations in which the stress constraints are dominant, while those with high E / ρ_c are more advantageous when the displacement constraints are dominant. For this reason, the components of material set must be arranged and numbered in ascending order of σ_a / ρ_c or descending order of E / ρ_c for the simplification of algorithm for material improvement and smooth convergence to the optimum solution. Table 4-1 shows two types of material sets (A) and (B) which are used for the numerical examples. Material set (A) consists of five components with the same moduli of elasticity and set (B) consists of seven components with different moduli of elasticity. The allowable tensile and compressive stresses of the materials are assumed to be the same. Fig.4-2 shows the properties of σ_a / ρ_c and E / ρ_c for material sets (A) and (B).

In the material sets, σ_a / ρ_c increases with material number; therefore, the larger numbered material is more economical than the smaller for problems in which only stress constraints are active. On the contrary, E / ρ_c decreases with material number

Table 4-1 Material sets (A) and (B)

	Material number	σ_a (kgf/cm^2)	E (kgf/cm^2)	ρ_c (1/cm^3)	$\frac{\sigma_a}{\rho_c}$	$\frac{E}{\rho_c}$
Set (A)	1	1500	2.0×10^6	2.50	600	800 000
	2	2000	2.0×10^6	3.00	667	666 667
	3	2500	2.0×10^6	3.50	714	571 428
	4	3000	2.0×10^6	4.00	750	500 000
	5	3500	2.0×10^6	4.50	778	444 444
Set (B)	1	140	0.4×10^6	0.75	186	533 333
	2	200	0.5×10^6	1.00	200	500 000
	3	400	0.7×10^6	1.45	275	482 759
	4	850	1.1×10^6	2.50	340	440 000
	5	1300	1.4×10^6	3.20	406	437 500
	6	1700	1.7×10^6	4.00	425	425 000
	7	2400	2.1×10^6	5.10	470	411 765

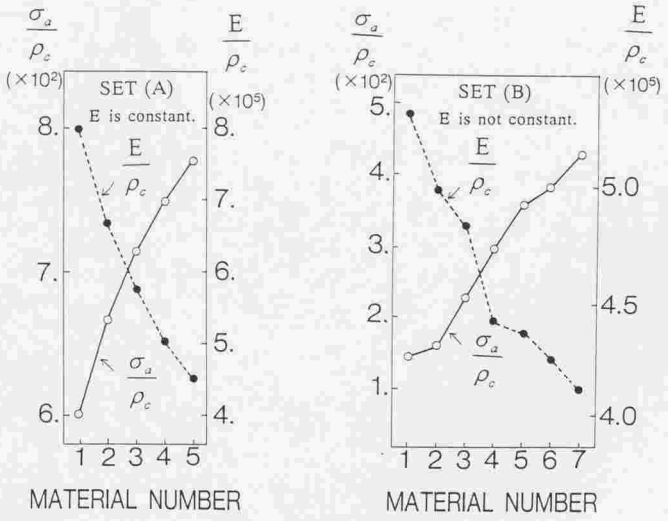

Fig.4-2 Properties of σ_a/ρ_c and E/ρ_c for material sets (A) and (B)

and the smaller numbered materials are more economical when only displacement constraints are active. In problems where both stress and displacement constraints are active, the optimum materials are selected such that a balance is maintained between the values of σ_a / ρ_c and E / ρ_c.

(2) Effect of the initial material kinds on the optimum solution

The rigorousness, reliability and efficiency of the proposed design method are investigated by comparing the optimum solutions which are optimized from extremely different material kinds.

The iteration histories for 31-bar truss with 4 fixed-ends, truss A shown in Fig.4-3, are summarized in Table 4-2, where three different initial material kinds are assumed, namely, the initial material kinds for all member elements are, respectively, assumed as 7, 5 and 1 in material set (B). In this problem, the maximum vertical displacement limit, δ_{2max}, is set as 2.0cm and both stress and displacement constraints are active at the optimum solutions.

As seen from Table 4-2, the optimum solutions for initial material kinds 7, 5 and 1 are, respectively, obtained after 19, 19 and 24 iterations efficiently even if the adaptive move limit constraints, maximum 5%, are imposed on **Y**. The optimum **A**, **Y**, **M** and total cost are converged to the quite similar values in each case. Therefore, it can be said that the global optimum solution can be obtained by the proposed design method even when any material kinds are assumed as the initial material kinds. This result emphasizes the reliability, rigorousness and efficiency of the proposed design method.

Fig.4-3 shows the iteration history for initial material 7, in which the thickness of member element indicates the size of cross-sectional area and the number associated with the member element represents the material kind. **Y**, **M** and **A** are improved quite reasonably and the material kinds for almost all member elements are improved from 7 to 4 in 5 iterations. Thereafter, the material kinds for redundant member elements are improved and converged to 1, while the material kinds for all non-trivial member elements remain at 4. After 11 iterations the move limit on **Y** is reduced adaptively and the optimum solution is obtained at 19 iterations at which stage the optimum shape of the truss, namely the optimum values of **Y**, and the optimum topological member arrangement are quite reasonable. The cross-sectional areas of redundant member elements converged to 0.1 cm^2 which is the lower limit of **A**.

Table 4-2 Iteration histories for initial material kinds 7, 5 and 1 in material set (B)

(Truss A, $\delta_{a\,max}$=2.0cm, Active constraints: σ, δ)

Material number	Iteration number	Cross-sectional area (cm^2) and material kind				Height of panel point (cm)				Total cost
		$A_1(M_1)^1$	$A_{18}(M_{18})^1$	$A_{24}(M_{24})^1$	$A_{31}(M_{31})^1$	Y_1	Y_2	Y_3	Y_4	
ALL 7	INIT.[2]	100.0(7)	100.0(7)	100.0(7)	100.0(7)	600.0	600.0	600.0	600.0	9.003×10^8
	3	110.9(6)	101.7(6)	34.4(6)	182.0(6)	661.5	541.5	541.5	661.5	5.633×10^8
	8	159.7(4)	156.8(4)	0.1(2)	299.7(4)	670.7	454.2	557.5	691.1	4.965×10^8
	13	168.5(4)	164.1(4)	0.1(1)	298.7(4)	651.6	411.4	586.6	663.6	4.885×10^8
	OPT.[3]19	169.7(4)	165.3(4)	0.1(1)	305.6(4)	650.3	405.4	573.9	676.9	4.955×10^8
ALL 5	INIT.[2]	100.0(5)	100.0(5)	100.0(5)	100.0(5)	600.0	600.0	600.0	600.0	5.649×10^8
	3	184.0(4)	168.7(4)	46.0(4)	268.4(4)	661.5	541.5	541.5	661.5	5.449×10^8
	8	164.5(4)	160.7(4)	0.1(2)	303.0(4)	659.5	429.8	533.6	691.1	4.953×10^8
	13	169.2(4)	164.7(4)	0.1(1)	296.3(4)	649.8	408.2	553.4	663.6	4.849×10^8
	OPT.[3]19	169.7(4)	165.3(4)	0.1(1)	305.8(4)	650.5	405.1	542.3	676.0	4.954×10^8
ALL 1	INIT.[2]	100.0(1)	100.0(1)	100.0(1)	100.0(1)	600.0	600.0	600.0	600.0	1.324×10^8
	3	404.9(3)	357.6(3)	49.4(3)	581.4(3)	601.6	550.8	598.5	617.4	5.582×10^8
	8	328.4(3)	325.2(3)	0.1(1)	580.7(3)	676.6	481.6	577.9	678.6	5.000×10^8
	13	151.2(4)	150.5(4)	0.1(1)	213.0(4)	680.3	502.0	588.8	728.3	4.089×10^8
	OPT.[3]24	169.2(4)	164.8(4)	0.1(1)	305.8(4)	651.0	407.7	561.9	692.8	4.946×10^8

$(M)^1$: Material number, INIT.[2] : Initial values, OPT.[3] : Optimum solution

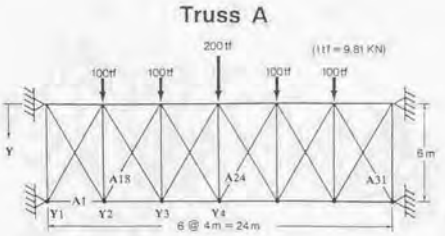

δ_a = 2.0cm
Material set (B)
All of initial material kinds = 7

ITE. 3

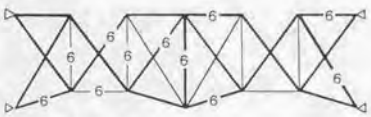

ITE. 8

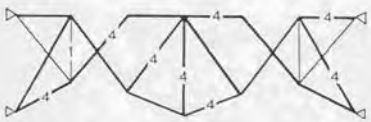

OPT.
ITE. 19

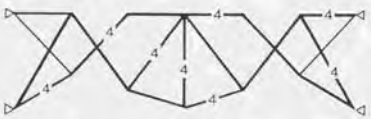

Fig.4-3 Iteration history for truss A with initial material kinds 7

(3) Optimum solutions for three types of 31-bar simple span trusses

The design examples for three types of 31-bar trusses, trusses A, B and C, are shown in Fig.4-4 and Table 4-3, where the iteration histories and the final optimum solutions are given.

In the problem for truss A shown in Fig.4-4, the maximum vertical displacement limit, $\delta_{z\max}$, is set as 0.7cm, and the material set (B) is used for the candidate

materials. In this problem, the active constraints at the optimum solution are displacement constraints only. Even when the design process is initialized with the worst material distribution for displacement constraints, namely , $M_i = 7(i = 1,\cdots,31)$, **Y**, **M** and **A** are improved quite reasonably. After 6 iterations the material kinds of almost all member elements converged to 1, which is the most economical material in situations when only the displacement constraints are active. **Y** and **A** begin to oscillate around the optimum solution at iteration 8, after which the move limit on **Y** is reduced adaptively. The optimum solution is obtained at iteration 15 at which stage the optimum shape of truss and the optimum topological member arrangement are quite reasonable. The cross-sectional areas of redundant member elements at the optimum solution are reduced to $0.1\,cm^2$. The final optimum solution is determined as shown in Table 4-3 and Fig.4-4.

In the problem for truss B, the maximum vertical displacement limit is set as 15.0cm and the material set (B) is used. The active constraints at the optimum solution are stress constraints only in this problem. In contrast with truss A, the initial material kinds are assumed as 1 for all member elements, which is the worst material distribution when stress constraints are active. **Y**, **M** and **A** are improved quite reasonably and steadily, and the material kinds for almost all member elements are imposed from 1 to 7 in 7 iterations. Thereafter, the material kinds for almost all non-trivial member elements remain at 7, which is the most economical material in this situation. After 7 iterations **M** for the redundant member elements, **Y** and **A** are improved steadily and oscillations are absent in successive solutions. The final optimum solution is reached after 19 iterations and the cross-sectional areas of redundant member elements at the optimum solution are reduced to $0.1cm^2$.

In the problem for truss C, the maximum vertical displacement limit is set as 10.0cm and material set (A) is used for the candidate materials. Both stress and displacement constraints are active at the optimum solution. The material kinds for almost all member elements are improved from 1 to 3 in 3 iterations, after which **M** for all non-trivial member elements remain at 3. After 3 iterations **M** for the redundant member elements, **Y** and **A** are improved steadily and the optimum solution is reached at 25 iterations without oscillations on **Y**. The cross-sectional areas of redundant member elements at the optimum solution are reduced to $0.1\,cm^2$ as the same as the problems for trusses A and B.

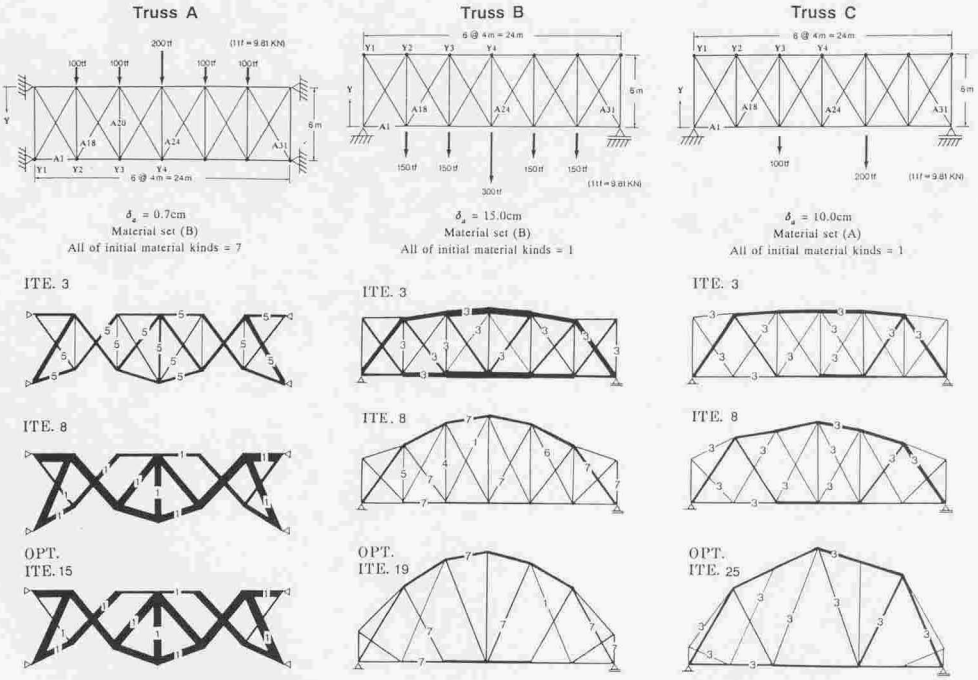

Fig.4-4 Iteration histories for trusses A, B and C

Table 4-3 Iteration histories for trusses A, B and C

	ITE.[1]	Cross-sectional area (cm^2) and material kind				Height of panel point (cm)				Total cost
		$A_1(M_1)^2$	$A_{18}(M_{18})^2$	$A_{24}(M_{24})^2$	$A_{31}(M_{31})^2$	Y_1	Y_2	Y_3	Y_4	
TRUSS A	INIT.[3]	100.0 (7)	100.0 (7)	100.0 (7)	100.0 (7)	600.0	600.0	600.0	600.0	9.003×10^8
	3	376.4 (5)	358.0 (5)	122.9 (5)	648.4 (5)	661.5	541.5	541.5	661.5	15.55×10^8
Material set (B)	8	944.0 (1)	943.1 (1)	0.1 (1)	2348.3 (1)	711.6	463.7	561.1	691.1	11.09×10^8
$\delta_{a\,max}$=0.7cm	13	965.0 (1)	963.6 (1)	0.1 (1)	2368.6 (1)	697.9	462.4	560.8	662.5	11.10×10^8
S_{AG}^5 : δ only	OPT.[4]15	954.2 (1)	949.2 (1)	0.1 (1)	2363.8 (1)	708.8	461.5	459.3	675.1	11.11×10^8
TRUSS B	INIT.[3]	100.0 (1)	100.0 (1)	100.0 (1)	100.0 (1)	600.0	600.0	600.0	600.0	1.324×10^8
	3	638.4 (3)	166.3 (3)	327.4 (3)	917.7 (3)	541.5	542.8	598.5	627.7	12.74×10^8
Material set (B)	8	92.0 (7)	3.2 (6)	55.4 (7)	156.4 (7)	419.6	549.9	749.7	801.1	6.314×10^8
$\delta_{a\,max}$=15.0cm	13	75.5 (7)	0.1 (1)	44.0 (7)	141.7 (7)	336.5	636.9	870.0	927.8	5.979×10^8
S_{AG}^5 : σ only	OPT.[4]19	52.3 (7)	0.1 (1)	40.6 (7)	105.9 (7)	282.6	704.3	957.9	1028.4	5.794×10^8
TRUSS C	INIT.[3]	100.0 (1)	100.0 (1)	100.0 (1)	100.0 (1)	600.0	600.0	600.0	600.0	4.413×10^8
	3	36.4 (3)	11.7 (3)	0.7 (3)	76.0 (3)	541.5	584.3	598.5	600.2	1.796×10^8
Material set (A)	8	30.6 (3)	2.4 (3)	0.1 (3)	80.5 (3)	419.0	611.6	670.5	766.1	1.471×10^8
$\delta_{a\,max}$=10.0cm	13	27.4 (3)	2.0 (3)	0.1 (1)	78.2 (3)	324.2	713.0	831.0	970.7	1.368×10^8
S_{AG}^5 : σ, δ	OPT.[4]25	28.3 (3)	0.6 (3)	0.1 (1)	73.4 (3)	166.4	718.6	902.5	1095.8	1.461×10^8

ITE.[1] : Iteration number. $(M)^2$: Material number. INIT.[3] : Initial values. OPT.[4] : Optimum solution.

S_{AG}^5 : Set of active constraint(s)

(4) Effect of displacement constraints at arbitrary panel points on optimum solution

In the previous design examples, the maximum vertical displacements in 31-bar trusses are restricted. In this example, the effect of displacement constraints at arbitrary panel points in truss A on the optimum solution is investigated by comparing the optimum solutions given in Figs.4-3, 4-4 and 4-5.

Fig.4-5 shows the iteration history for truss A in which the displacements at panel points A and B are limited to 0.5cm. Material set (B) is used for the candidate materials and the active constraints at the optimum solution are both stress and displacement constraints. **Y**, **M** and **A** are also improved quite reasonably and steadily in this problem, and the optimum solution is reached after 12 iterations without oscillations on **Y**. As seen in Fig.4-5, in the optimum solution, the final topological member arrangement is different from those in truss A shown in Figs.4-3 and 4-4. The cross-sectional areas for only four member elements are found to be 0.1cm^2 and these member elements are deleted. Almost all member elements for material kind 4 are fully stressed and all member elements for material kind 3 are distributed for the displacement constraints at panel points A and B. Some member elements whose material kind are 1, also require considerable cross-sectional areas in order to satisfy the displacement constraints. The maximum vertical displacement at the optimum solution is 1.99cm. From this investigation, it is confirmed that the optimum topological member arrangement and distribution of optimum material kinds are considerably affected by the aimed points of displacements constraints.

(5) Optimum solutions for 31-bar 2-span continuous trusses

The iteration histories and final optimum solutions for 31-bar 2-span continuous trusses with different design conditions are given in Fig.4-6 and Table 4-4, where the maximum vertical displacements are, respectively, limited to 1.0cm, 3.0cm and 10.0cm. The material set (A) is used for the candidate material.

For case in which the displacement limit is set as 1.0cm, the displacement constraint is active at the optimum solution. Even when the design process is started from the worst material distribution for displacement constraints, namely $M_i = 5$ $(i = 1, \cdots, 31)$, **Y**, **M** and **A** are improved quite reasonably, and after 5 iterations the material kinds for all member elements converged to 1. After 7 iterations the move limit on **Y** is reduced adaptively and the final optimum solution is obtained at 21

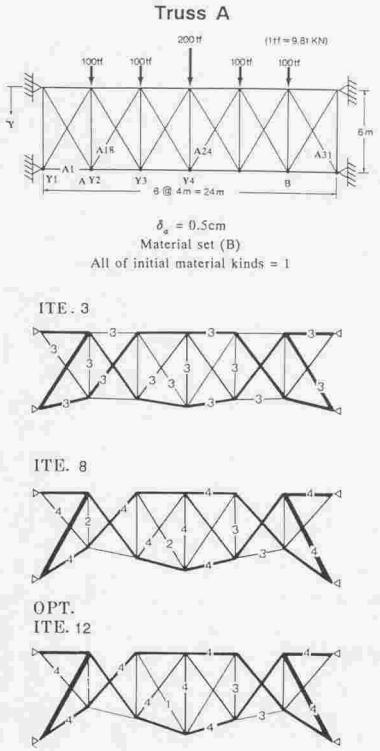

Fig.4-5 Iteration history for truss A in which the displacements at panel points A and B are limited to 0.5cm

iterations. Although the truss is optimized from a 2-span continuous truss, the cross-sectional areas of all redundant member elements are reduced to 0.1 cm^2 by the proposed optimization process, and the final topological member arrangement indicates a simple span statically determinate truss. The total cost converged to 1.544×10^8.

For case in which the displacement limit is set as 10.0cm, the active constraints at the optimum solution are stress constraints only. The initial material kinds for all member elements are set at 1 and after 5 iterations the material kinds of all non-

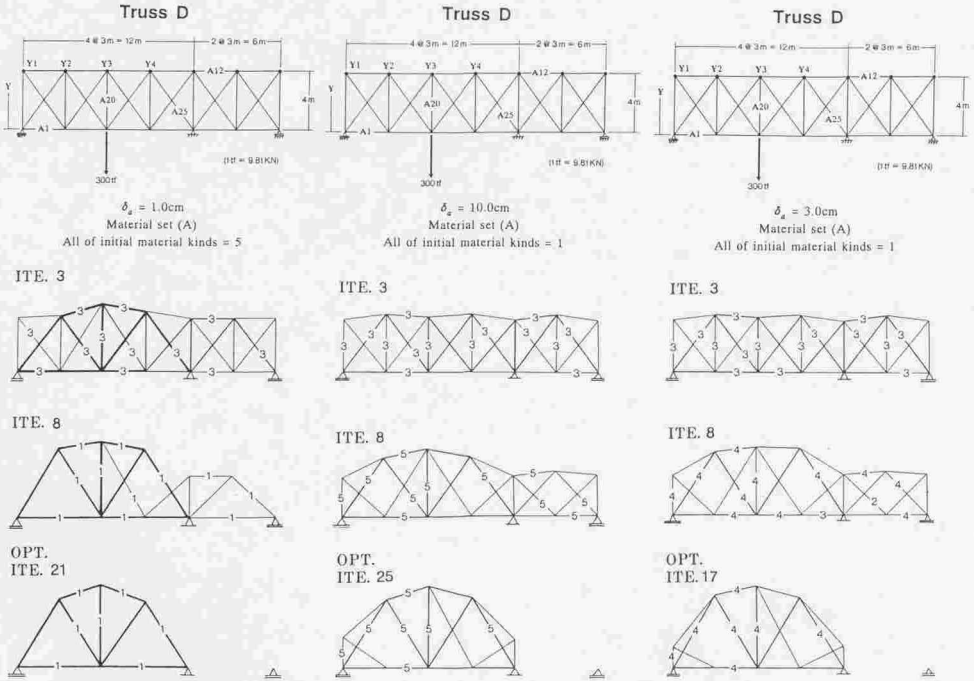

Fig.4-6 Iteration histories for truss D

Table 4-4 Iteration histories for truss D

	ITE.[1]	Cross-sectional area (cm^2) and material kind				Height of panel point (cm)				Total cost
		$A_1(M_1)^2$	$A_{12}(M_{12})^2$	$A_{20}(M_{20})^2$	$A_{25}(M_{25})^2$	Y_1	Y_2	Y_3	Y_4	
TRUSS D	INIT.[3]	100.0 (5)	100.0 (5)	100.0 (5)	100.0 (5)	400.0	400.0	400.0	400.0	5.580×10^8
Material set (A)	3	121.3 (3)	36.0 (3)	142.5 (3)	175.0 (3)	361.0	361.0	441.0	399.0	2.747×10^8
$\delta_{a\,max}$=1.0cm	8	114.3 (1)	3.2 (1)	61.6 (1)	188.8 (1)	279.3	395.2	460.7	393.9	1.610×10^8
$S_{AG}{}^5$: δ only	13	114.3 (1)	0.2 (1)	69.1 (1)	191.3 (1)	247.8	408.7	459.7	407.3	1.599×10^8
	OPT.[4]21	101.6 (1)	0.1 (1)	85.5 (1)	181.8 (1)	215.8	452.4	526.7	451.7	1.544×10^8
TRUSS D	INIT.[3]	100.0 (1)	100.0 (1)	100.0 (1)	100.0 (1)	400.0	400.0	400.0	400.0	3.100×10^8
Material set (A)	3	42.6 (3)	28.8 (3)	41.6 (3)	43.2 (3)	361.0	392.8	386.8	399.0	1.200×10^8
$\delta_{a\,max}$=10.0cm	8	27.1 (5)	15.6 (5)	28.1 (5)	32.8 (5)	279.3	414.0	467.2	450.1	0.895×10^8
$S_{AG}{}^5$: σ only	13	28.5 (5)	19.5 (5)	22.6 (5)	35.5 (5)	216.1	420.3	483.3	496.9	0.959×10^8
	OPT.[4]25	26.6 (5)	0.1 (1)	25.7 (5)	47.3 (5)	110.9	479.6	564.7	483.2	0.785×10^8
TRUSS D	INIT.[3]	100.0 (1)	100.0 (1)	100.0 (1)	100.0 (1)	400.0	400.0	400.0	400.0	3.100×10^8
Material set (A)	3	42.6 (3)	28.8 (3)	41.6 (3)	43.2 (3)	361.0	392.8	386.8	399.0	1.200×10^8
$\delta_{a\,max}$=3.0cm	8	34.8 (4)	19.1 (4)	37.8 (4)	49.8 (4)	279.3	399.6	464.9	446.2	0.998×10^8
$S_{AG}{}^5$: σ, δ	13	31.3 (4)	0.4 (4)	32.2 (4)	56.1 (4)	216.1	482.8	570.9	481.1	0.825×10^8
	OPT.[4]17	31.1 (4)	0.1 (1)	31.4 (4)	57.9 (4)	167.3	480.1	562.0	476.1	0.817×10^8

ITE.[1] : Iteration number, $(M)^2$: Material number, INIT.[3] : Initial values, OPT.[4] : Optimum solution,
$S_{AG}{}^5$: Set of active constraint(s)

trivial member elements selected the most economical kind 5. The final optimum solution is obtained at iteration 25 without oscillations on **Y**. The final topological member arrangement is also a simple span truss. In this case the total cost decreases by 49.2% compared with the case in which the displacement limit is set as 1.0cm.

For case in which the displacement limit is set as 3.0cm, the active constraints at the optimum solution are both stress and displacement constraints. The material kinds for almost all member elements are improved from 1 to 4 in 4 iterations. Thereafter, **M** for the redundant member elements, **A** and **Y** are improved steadily and oscillations are also absent in successive solutions. The final optimum solution is determined at iteration 17 at which stage the optimum shape of the truss and the optimum topological member arrangement are reasonable, and the final optimum solution also indicates a simple span truss. In this case the total cost decreases by 47.1% compared with the case in which the displacement limit is set as 1.0cm.

From the investigations of the optimum solutions for various design conditions, it is clear that the proposed optimal synthesis method can determine the optimum coordinates of panel points, optimum distributions of material kinds and cross-sectional areas of member elements of truss structures efficiently. At the optimum solution the cross-sectional areas of redundant member elements are found to be the imposed lower limit automatically by the proposed optimum design method. Therefore, the optimum topological arrangement of member elements can also be determined by the proposed synthesis method with setting the lower limit of cross-sectional areas of member elements to an extremely small value.

4-5. CONCLUSIONS

In this study an optimal structural synthesis method is presented to determine the optimum solutions for design problems of truss structures considering the coordinates of panel points, cross-sectional areas and discrete material kinds of all member elements simultaneously as design variables. The stress and displacement constraints due to static loads are taken into account in the optimization process. The optimal structural synthesis method has been developed by using the concept of convex and linear approximation, dual method, two-stage minimization process of the Lagrangian function and discrete sensitivity analysis. The generality, rigorousness, reliability and efficiency of the proposed optimal structural synthesis

method are illustrated by applying the method to various minimum-cost design problems of 31-bar trusses subjected to stress and displacement constraints and investigating the optimum solutions at various design conditions.

The conclusions that can be drawn from this study are:

(1) The design method can deal with any combinations of design variables such as shape of the structure, discrete material kinds and cross-sectional areas of member elements, and can optimize the design variables as well as the topological member arrangement simultaneously.

(2) The two-stage minimization process of the Lagrangian function can solve the mixed discrete/continuous variable problems quite systematically and efficiently.

(3) The rigorousness and reliability of the proposed design method have been confirmed by various numerical experiments of 31-bar trusses. The convergence to the optimum solutions is quite excellent and the optimum solutions can be obtained after 15-25 iterations quite efficiently even when the algorithm is initialized with the worst possible material distribution.

(4) Adaptive move limit constraint on **Y** is required to ensure the successive solutions converge to the optimum solution when the displacement constraints are active in the design problem.

APPENDIX 4-1 Calculation of the *jk*th element of Hessian matrix

The *jk*th element of the Hessian matrix (eq.(4-33)) is given by the following expressions:

$$H_{jk} = \frac{\partial^2 l(\overline{\lambda})}{\partial \lambda_j \partial \lambda_k} = \sum_{i=1}^{n} P_i + \sum_{i=1}^{P} Q_i \qquad \text{(A4-1)}$$

where

$$P_i = -\frac{1}{2} a_{ji_{(-)}} a_{ki_{(-)}} \left(A_i^0\right)^4 / \left[A_i^3 \left(\omega_{Ai}\left(M_i^0\right) + \sum_{l=1}^{m} \lambda_l a_{li_{(+)}} \right) \right] \qquad \text{if} \quad a_{ji} < 0,\ a_{ki} < 0$$

$$P_i = -\frac{1}{2} a_{ji_{(+)}} a_{ki_{(-)}} \left(A_i^0\right)^2 / \left[A_i \left(\omega_{Ai}\left(M_i^0\right) + \sum_{l=1}^{m} \lambda_l a_{li_{(+)}} \right) \right] \qquad \text{if} \quad a_{ji} \geq 0,\ a_{ki} < 0,$$

$$P_i = -\frac{1}{2} a_{j i_{(-)}} a_{k i_{(+)}} \left(A_i^0\right)^2 / \left[A_i \left(\omega_{Ai}\left(M_i^0\right) + \sum_{l=1}^{m} \lambda_l a_{l i_{(+)}} \right) \right] \qquad \text{if} \quad a_{ji} < 0,\ a_{ki} \geq 0$$

$$P_i = -\frac{1}{2} a_{j i_{(+)}} a_{k i_{(+)}} A_i / \left(\omega_{Ai}\left(M_i^0\right) + \sum_{l=1}^{m} \lambda_l a_{l i_{(+)}} \right) \qquad \text{if} \quad a_{ji} \geq 0,\ a_{ki} \geq 0$$

$$Q_i = q_i \left(Y_i^0\right)^4 / Y_i^3 \qquad \text{if} \quad y_{ji} < 0,\ y_{ki} < 0$$

$$Q_i = q_i \left(Y_i^0\right)^2 / Y_i \qquad \text{if} \quad y_{ji} \geq 0,\ y_{ki} < 0$$

$$Q_i = q_i \left(Y_i^0\right)^2 / Y_i \qquad \text{if} \quad y_{ji} < 0,\ y_{ki} \geq 0$$

$$Q_i = q_i Y_i \qquad \text{if} \quad y_{ji} \geq 0,\ y_{ki} \geq 0$$

$$q_i = -\frac{1}{2} y_{ji} y_{ki} / \left(\omega_{Yi}\left(\mathbf{M}^0\right) + \sum_{l=1}^{m} \lambda_l y_{l i_{(+)}} \right) \qquad \text{if} \quad \omega_{Yi}\left(\mathbf{M}^0\right) \geq 0$$

$$q_i = -\frac{1}{2} y_{ji} y_{ki} / \sum_{l=1}^{m} \lambda_l y_{l i_{(+)}} \qquad \text{if} \quad \omega_{Yi}\left(\mathbf{M}^0\right) < 0$$

REFERENCES

1. Schmit,L.A., "Structural design by systematic synthesis", *Proc. of 2nd Conf. on Electronic Computation*, ASCE, 1960, pp.105-122.
2. Mota Soares, C. A. et al., "Computer Aided Optimal Design : Structural and Mechanical Systems", *Proc. of the NATO Advanced Study Institute*, Vols.1-3, Troia, Portugal, 1986.
3. Rozvany, G.I.N., "Optimization of Large Structural Systems", *Proc. of the NATO/DFG Advanced Study Institute on Optimization of Large Structural Systems*, Vols.1-2, Berchtesgaden, Germany, 1991.
4. Adeli, H., *Advances in Design Optimization*, Chapman & Hall, 1994.
5. Herskovits, J., *Advances in Structural Optimization*, Kluwer Academic Publishers, 1995.
6. Toakley, A. R., "Optimum design using available sections", *J. Struct. Div. ASCE*, Vol.94, 1968, pp.1219-1241.
7. Reinschmidt, K. F., "Discrete structural optimization", *J. Struct. Div. ASCE*, Vol.97, 1971, pp.133-156.
8. Cella, A. and Logcher, R. D., "Automated optimum design from discrete components". *J. Struct. Div. ASCE*, Vol. 97, 1971, pp.175-190.

9. Cella, A. and Soosaar, K., "Discrete variables in structural optimization", in Gallagher,R.H. and Zienkiewicz,O.C. eds., *Optimum Structural Design - Theory and Application*, New York, Wiley, 1973.
10. Okumura, T. and Ohkubo, S., "Optimum design of steel continuous girders using suboptimization of girder elements", *Proc. Symp. on Analytical Problems for Design of Structures*, compiled by JSCE & AIJ, published by JSPS, 1975, pp. 209-229.
11. Morris, A. J. et al., *Foundations of Structural Optimization*, Chapter 13, New York, Wiley 1982, pp.487-511.
12. Ohkubo, S. and Taniwaki, K., "Optimum material selection of truss by dual approach", *J. Struct. Engng., JSCE & AIJ*, Vol.31A, 1985, pp. 251-262. (in Japanese)
13. Ohkubo, S. and Nakajima, T., "Optimum structural design with element material selection", Structural Engineering & Construction, *Proc. of EASEC* I, Bangkok, Vol.3, 1986, pp.1986-1996.
14. Starnes,J.H. and Haftka,R.T., "Preliminary design of composite wings for buckling, strength, and displacement constraints", *J. Aircraft*, Vol.16, No.8, 1979, pp.564-570.
15. Fleury, C. and Schmit, L. A., "Dual methods and approximation concepts in structural synthesis", CR-3226, NASA, 1980.
16. Prasad,B., "Explicit constraint approximation forms in structural optimization-Part I: Analyses and projections", *Comp. Meth. Appl. Mech. Engng.*, No.40, 1983, pp.1-26.
17. Prasad, B., "Approximation, adaptation and automation concepts for large scale structural optimization", *Eng. Optim.*, Vol. 6, 1983, pp.129-140.
18. Fleury,C. and Braibant,V., "Structural optimization: a new dual method using mixed variables", *Int. J. Numer. Methods Engng.*, Vol.23, 1986, pp.409-428.
19. Ohkubo,S. and Asai,K., "A hybrid optimal synthesis method for truss structures considering shape, material and sizing variables", *Int. J. Numer. Methods Engng.* Vol.34, 1992, pp.839-851
20. Ohkubo,S., Taniwaki,K. and Asai,K., "Optimal structural synthesis utilizing shape, material and sizing sensitivities", in Kleiber,M. and Hisada,T. eds., *Design Sensitivity Analysis*, Atranta Technology Publications, Atlanta, 1993, pp.164-188.
21. Kirsch, U., *Optimum Structural Design*, New York, McGraw-Hill, 1981.
22. William,H.P., Saul,A.T., William,T.V. and Brian,P.F., *Numerical Recipes in Fortoran* (second edition), Cambridge University Press, 1992.

Chapter 5

TOTAL OPTIMAL SYNTHESIS METHOD FOR TRUSS STRUCTURES SUBJECT TO STATIC AND FREQUENCY CONSTRAINTS

5-1. INTRODUCTION

The significant variables in the optimal synthesis of structures are the geometry of structures, distribution of mechanical and economical properties of materials and cross-sectional dimensions of member elements. As noted in Chapter 4, in the past decades, a large number of contributions have been made exclusively to sizing and shape optimization, and in the recent years the sensitivity analysis has been studied considerably. However, very little attention has yet been paid to the optimization problems with material selection which requires a discrete/continuous formulation.

In Chapter 4, a hybrid optimal synthesis method for truss structures is presented in which the coordinates of panel points, cross-sectional areas and discrete material kinds of member elements are optimized simultaneously subject to stress and displacement constraints due to static loads[1,2]. In this Chapter the hybrid optimal synthesis method is applied to solve the optimum design problem of truss structures subject to both static and dynamic constraints.

Optimum design methods with frequency constraints have been studied by many researchers since the earliest study by Turner[3] in 1967. Most of these design methods are developed based on the optimality criteria methods using cross-sectional areas of member elements as the design variable[4-7]. Felix and Vanderplaats[8] studied the optimum configuration design of truss structures subject to stress, Euler buckling, displacement and natural frequency constraints using a multilevel optimization technique. The methods for computing the derivatives of eigenvalues and eigenvectors have also been studied by many researchers[9-15].

In the optimum design method of this study, the primary design problem is transformed into an approximate subproblem of convex and separable form by using mixed direct/reciprocal design variables and the sensitivities of shape, material and sizing variables. The sensitivities of static and frequency constraints with respect to design variables are calculated analytically by using the differentials of the stiffness

and mass matrices. The approximate subproblem is solved by utilizing the two-stage minimization process of the Lagrangian function, concepts of convex and linear approximation, dual method and discrete sensitivity analysis proposed in Chapter 4.

The rigorousness, reliability and efficiency of the proposed optimal structural synthesis method are illustrated by applying the method to various minimum cost design problems of 15-bar truss subject to stress, displacement and natural frequency constraints. It is also emphasized that the vibration mode and frequency of truss structure are very sensitive to the distribution of cross sections and shape of structure, and the vibration mode might be changed by improvements of cross sections and shape of structure at the first stage of the minimization process. Therefore, it is necessary to calculate the exact vibration mode and frequency and to examine the activeness of frequency constraint at the end of the first stage minimization process to ensure the smooth convergence to the optimum solution.

5-2. FORMULATION OF PRIMARY OPTIMUM DESIGN PROBLEM

(1) Design variables

In this study, the design variables for the design of truss structures are assumed as the horizontal and vertical coordinates of panel points, denoted as **X** and **Y**, material kinds **M** representing the physical and economical properties of material and cross-sectional areas **A** of member elements.

$$\mathbf{A} = \left[A_1, \cdots, A_n\right]^T \tag{5-1}$$

$$\mathbf{X} = \left[X_1, \cdots, X_P\right]^T \tag{5-2}$$

$$\mathbf{Y} = \left[Y_1, \cdots, Y_P\right]^T \tag{5-3}$$

$$\mathbf{M} = \left[M_1, \cdots, M_n\right]^T \tag{5-4}$$

where n is the number of member elements, P denotes the number of coordinates of panel points considered as the shape design variables, **X** and **Y**. In order to simplify the expressions of equations the shape design variables, **X** and **Y**, are denoted by **S**, hereafter.

$$\mathbf{S} = \left[S_1, \cdots, S_{2P}\right]^T = \left[X_1, \cdots, X_P, Y_1, \cdots, Y_P\right]^T \tag{5-5}$$

Depending on the characteristics of these design variables, **S** and **A** are treated as continuous design variables and **M** as a discrete design variable.

(2) Stress, displacement and frequency constraints

In the present study, stress on all member elements, displacements at free nodal points and natural frequency are considered as the behavior constraints. The stress constraints on all member elements are expressed as

$$g_{\sigma j}(\mathbf{A},\mathbf{S},\mathbf{M}) = |N_j(\mathbf{A},\mathbf{S},\mathbf{M})/A_j| - |\sigma_{aj}(M_j)| \le 0 \quad (j=1,\cdots,n) \tag{5-6}$$

where $\sigma_{aj}(M_j)$ and $N_j(\mathbf{A},\mathbf{S},\mathbf{M})$ are, respectively, the maximum allowable stress and axial force in the jth member element.

The displacement constraints are expressed as

$$g_{\delta d}(\mathbf{A},\mathbf{S},\mathbf{M}) = |\delta_d(\mathbf{A},\mathbf{S},\mathbf{M})| - |\delta_{ad}| \le 0 \qquad (d=1,\cdots,u) \tag{5-7}$$

where δ_{ad} and $\delta_d(\mathbf{A},\mathbf{S},\mathbf{M})$ are, respectively, the maximum allowable displacement and actual displacement at the dth panel point. u denotes the number of displacement constraints to be taken into account.

The constraints on the natural frequency are specified as

$$g_{fk}(\mathbf{A},\mathbf{S},\mathbf{M}) = (2\pi f_{k\min})^2 - \mu_k^2(\mathbf{A},\mathbf{S},\mathbf{M}) \le 0 \qquad (k=1,\cdots,v) \tag{5-8}$$

where $\mu_k(\mathbf{A},\mathbf{S},\mathbf{M})$ and $f_{k\min}$ are, respectively, the circular frequency and the specified minimum frequency limit of the kth vibration mode. v is the number of vibration mode to be taken into account.

(3)Primary optimum design problem

The behaviors of truss, such as member forces, displacements of panel points and natural frequency, are expressed as functions of the lengths, cross-sectional areas and the moduli of elasticity E of materials of member elements. The total cost is the objective function **W** and it is expressed as the summation of the costs of member elements. The primary design problem can then be formulated as

Find **A, S, M,** which

minimize $$\mathbf{W}(\mathbf{A},\mathbf{S},\mathbf{M}) = \sum_{i=1}^{n} \rho_{ci}(M_i) l_i(\tilde{\mathbf{S}}_i) A_i \tag{5-9}$$

subject to $$g_j(\mathbf{A},\mathbf{S},\mathbf{M}) \le 0 \qquad (j=1,\cdots,m) \tag{5-10}$$

$$\left.\begin{array}{ll} A_i^l \le A_i \le A_i^u & (i=1,\cdots,n) \\ S_k^l \le S_k \le S_k^u & (k=1,\cdots,2P) \\ M_i \in \mathbf{MS} & (i=1,\cdots,n) \end{array}\right\} \tag{5-11}$$

where $\tilde{\mathbf{S}}_i = [S_{i+}, S_{i-}]^T$

$$\mathbf{g} = [g_1,\cdots,g_m]^T = [g_{a1},\cdots,g_{am},g_{\delta 1},\cdots,g_{\delta w},g_{f1},\cdots,g_{fv}]^T$$

$\rho_{ci}(M_i)$ and $l_i(\tilde{\mathbf{S}}_i)$ are, respectively, the unit cost and member length of the ith member element. S_{i+} and S_{i-} are the horizontal and vertical coordinates of panel points to which the ith member element is connected. **MS** is the set of available candidate materials. m denotes the number of behavior constraints. Superscripts l and u represent the lower and upper limits of the design variables.

5-3. OPTIMAL STRUCTURAL SYNTHESIS METHOD FOR TRUSS STRUCTURES SUBJECT TO STATIC AND FREQUENCY CONSTRAINTS[1,2,19,20]

(1) Convex and separable approximate subproblem

Applying the concept of convex and linear approximation[1,2,16-20] the primary optimum design problem defined in eqs.(5-9) to (5-11) can be approximated as the convex and separable optimization subproblem by utilizing the first-order partial derivatives with respect to shape, material and sizing variables and the direct and reciprocal design variables. In the optimization process, the constant term in the objective function will be ignored and only the change in the objective function $\Delta\mathbf{W}$ will be taken into account instead of the total objective function $\mathbf{W}(\mathbf{A},\mathbf{S},\mathbf{M})$. The changes in material kinds, $\Delta\mathbf{M} = (\Delta M_1,\cdots,\Delta M_n)^T$, are also treated as new material variables. Please see eqs.(4-9)-(4-11) in section 4-3.(1) for the detailed expressions of the convex and separable approximate subproblem.

(2)Calculation of the sensitivities of frequency constraints with respect to design variables

The first-order partial derivatives of the frequency constraint $g_j(\mathbf{A},\mathbf{S},\mathbf{M})$ $(j=n+u+1,\cdots,n+u+v)$ with respect to **A**, **S** and **M**, expressed as the eigenvalue derivatives with respect to **A**, **S** and **M**, are obtained by differentiating the following eigenvalue equation of structural dynamics.

$$\left[\mathbf{K}_S - \mu_k^2 \overline{\mathbf{M}}_M\right][\phi]_k = 0 \quad (k = 1, \cdots, \nu) \tag{5-12}$$

where $\mathbf{K}_S$ is the system stiffness matrix and $[\phi]_k$ is the eigenvector of truss structure in the kth vibration mode. μ_k^2 and $\overline{\mathbf{M}}_M$ are, respectively, the eigenvalue in the kth vibration mode and the total system mass matrix.

The total system mass matrix $\overline{\mathbf{M}}_M$ consists of the contributions from structural mass matrix $\overline{\mathbf{M}}_X(\mathbf{A},\mathbf{S},\mathbf{M})$ and nonstructural mass matrix $\overline{\mathbf{M}}_C$.

$$\overline{\mathbf{M}}_M = \overline{\mathbf{M}}_X(\mathbf{A},\mathbf{S},\mathbf{M}) + \overline{\mathbf{M}}_C \tag{5-13}$$

The structural mass matrix is calculated as the lumped masses.

Eq. (5-12) is solved by using an algorithm based on subspace iterative technique given by ref.[21].

Based on the Nelson's technique[9], the sensitivities of eigenvalue and eigenvector with respect to design variables are calculated by differentiating the eigenvalue equation of structural dynamics in eq.(5-12). Namely, the sensitivity of eigenvalue μ_k^2 in the kth vibration mode with respect to design variable $B_i \in \mathbf{B} = [A_1, \cdots, A_n, S_1, \cdots, S_{2P}, M_1, \cdots, M_n]^T$ is given by

$$\frac{\partial \mu_k^2}{\partial B_i} = [\phi]_k^T \left[\frac{\partial \mathbf{K}_S}{\partial B_i} - \mu_k^2 \frac{\partial \overline{\mathbf{M}}_X}{\partial B_i}\right][\phi]_k \tag{5-14}$$

In the case that B_i corresponds to M_i in eq.(5-14), $\partial \mathbf{K}_S / \partial M_i$ is calculated by the following expression using $\partial \mathbf{K}_S / \partial A_i$.

$$\frac{\partial \mathbf{K}_S}{\partial M_i} = \frac{\partial \mathbf{K}_S}{\partial A_i} \cdot \frac{A_i^0}{E_i(M_i^0)} \cdot \left[E_i(M_i) - E_i(M_i^0)\right] \tag{5-15}$$

The sensitivities of frequency constraint $g_j(\mathbf{A},\mathbf{S},\mathbf{M})$ $(j = n+u+1, \cdots, n+u+\nu)$ with respect to $\mathbf{A}$, $\mathbf{S}$ and $\mathbf{M}$ in eq.(4-10), a_{ji}, y_{jk} and m_{ji}, can be expressed as

$$a_{ji} = -[\phi]_q^T \frac{\partial \mathbf{K}_S}{\partial A_i}[\phi]_q + \mu_q^2 [\phi]_q^T \frac{\partial \overline{\mathbf{M}}_X}{\partial A_i}[\phi]_q \qquad (q = j-n-u) \tag{5-16}$$

$$y_{jk} = -[\phi]_q^T \frac{\partial \mathbf{K}_S}{\partial S_k}[\phi]_q + \mu_q^2 [\phi]_q^T \frac{\partial \overline{\mathbf{M}}_X}{\partial S_k}[\phi]_q \qquad (q = j-n-u) \tag{5-17}$$

$$m_{ji} = -[\phi]_q^T \frac{\partial \mathbf{K}_S}{\partial A_i}[\phi]_q \cdot \frac{A_i^0}{E_i(M_i^0)} \cdot \left[E_i(M_i) - E_i(M_i^0)\right] + \mu_q^2 [\phi]_q^T \frac{\partial \overline{\mathbf{M}}_X}{\partial A_i}[\phi]_q$$
$$(q = j-n-u) \tag{5-18}$$

Note that in the above expressions, the eigenvector is normalized such that

$$[\phi]_k^T \overline{\mathbf{M}}_M [\phi]_k = 1.0 \quad (k = 1, \cdots, \nu) \tag{5-19}$$

In the calculation of sensitivity of eigenvector $[\phi]_k$ in the kth vibration mode with respect to B_i, it needs to calculate the inverse matrix of $[\mathbf{K}_S - \mu_k^2 \overline{\mathbf{M}}_M]$. However, the calculation of inverse matrix will not be able to execute because the determinant of $[\mathbf{K}_S - \mu_k^2 \overline{\mathbf{M}}_M]$ becomes zero from eq.(5-12). For this reason, the normalization condition in eq.(5-19) is replaced such that the arbitrary element of eigenvector is equal to 1.0. Hereafter, the arbitrary element of eigenvector is denoted as the jth element. For this normalization condition, all elements of $[\phi]_k$ are divided by the jth element $\phi_k^j (\neq 0)$. Namely, denoting this re-normalized eigenvector $[\bar{\phi}]_k$, $[\bar{\phi}]_k$ is given by

$$[\bar{\phi}]_k = [\phi]_k / \phi_k^j \tag{5-20}$$

Denoting the reduced matrices by deleting the jth row and the jth column of $\mathbf{K}_S$, $\overline{\mathbf{M}}_M$, $\overline{\mathbf{M}}_X$ and deleting the jth element of $[\bar{\phi}]_k$ as $\mathbf{K}_S^S$, $\overline{\mathbf{M}}_M^S$, $\overline{\mathbf{M}}_X^S$ and $[\bar{\phi}']_k$, the inverse matrix of reduced matrix of $[\mathbf{K}_S - \mu_k^2 \overline{\mathbf{M}}_M]$, $[\mathbf{K}_S^S - \mu_k^2 \overline{\mathbf{M}}_M^S]^{-1}$, can be calculated and the sensitivity of $[\bar{\phi}']_k$ with respect to B_i is obtained by

$$\frac{\partial [\bar{\phi}']_k}{\partial B_i} = [\mathbf{K}_S^S - \mu_k^2 \overline{\mathbf{M}}_M^S]^{-1} \left\{ -\left(\frac{\partial \mathbf{K}_S^S}{\partial B_i} - \mu_k^2 \frac{\partial \overline{\mathbf{M}}_X^S}{\partial B_i} \right) [\bar{\phi}]_k + \frac{\partial \mu_k^2}{\partial B_i} \overline{\mathbf{M}}_M^S [\bar{\phi}]_k \right\} \tag{5-21}$$

The jth element $\bar{\phi}_k^j$ of $[\bar{\phi}]_k$ is set at 1.0 and its sensitivity with respect to B_i becomes zero. The sensitivities of other elements of $[\bar{\phi}]_k$ are calculated by eq.(5-21). Therefore, the sensitivities of all elements of $[\bar{\phi}]_k$ with respect to B_i are obtained in the preceding process. Finally, by differentiating eq.(5-20) with respect to B_i, the sensitivities of $[\phi]_k$ with the original normalization are calculated by

$$\frac{\partial [\phi]_k}{\partial B_i} = \frac{\partial \phi_k^j}{\partial B_i} [\bar{\phi}]_k + \phi_k^j \frac{\partial [\bar{\phi}]_k}{\partial B_i} \tag{5-22}$$

By differentiating eq.(5-19) with respect to B_i and considering eq.(5-22), $\partial \phi_k^j / \partial B_i$ in eq.(5-22) is given by

$$\frac{\partial \phi_k^j}{\partial B_i} = -(\phi_k^j)^2 [\phi]_k^T \overline{\mathbf{M}}_M \frac{\partial [\bar{\phi}]_k}{\partial B_i} - \frac{\phi_k^j}{2} [\phi]_k^T \frac{\partial \overline{\mathbf{M}}_X}{\partial B_i} [\phi]_k \tag{5-23}$$

(3) Improvements of **A**, **S** and **M** by a two-stage minimization process of the Lagrangian function

(a) Two-stage minimization process of the Lagrangian function

The stresses of member elements, displacements at the free nodes and frequency of truss structure are expressed as the functions of **S** and the product of modulus of elasticity E and **A**, EA, and the objective function is also expressed as the function of **A**, **S** and **M**. As stated previously, in this study **A** and **S** are dealt with as continuous variables and $\Delta\mathbf{M}$ as a discrete variable. Therefore, the design variables **A**, **S** and $\Delta\mathbf{M}$ are improved by a two-stage minimization process of the Lagrangian function which uses a dual method and incorporates discrete sensitivity analysis. At the first stage minimization process, EA is treated as one continuous design variable and the optimum values of EA and **S** are determined by minimizing the Lagrangian function with respect to EA and **S**. In the optimization algorithm of first stage minimization process, E is constant and **A** is improved for improvement of EA. Thereafter, the better combination of **A** and $\Delta\mathbf{M}$ for each member element is searched independently to reduce the Lagrangian function by comparing the values of discretized Lagrangian function while keeping the activeness of the constraints which are determined by the first minimization process.

(b) Lagrangian Function

The following separable Lagrangian function is introduced for the approximate subproblem.

$$\mathbf{L}(\mathbf{A},\mathbf{S},\mathbf{M}^0+\Delta\mathbf{M},\lambda)=\sum_{i=1}^{n}L_i(A_i,\Delta M_i,\lambda)+\sum_{k=1}^{2p}L_k(S_k,\Delta\mathbf{M},\lambda)+\sum_{j=1}^{m}\lambda_j\overline{U}_j \qquad (5\text{-}24)$$

where $\lambda_j \geq 0 \qquad (j=1,\cdots,m)$

L_i and L_k are, respectively, the element Lagrangian functions with respect to A_i and ΔM_i, S_k and $\Delta\mathbf{M}$. λ_j is the Lagrange multiplier for the jth behavior constraint. L_i and L_k are, respectively, given by

$$L_i(A_i,\Delta M_i,\lambda)=\omega_{M_i}(M_i^0+\Delta M_i)A_i+\sum_{j=1}^{m}\lambda_j\left[a_{j1_{(i-)}}A_i-a_{j1_{(i-)}}(A_i^0)^2\frac{1}{A_i}+m_{ji}\Delta M_i\right] \qquad (5\text{-}25)$$

$$L_k(S_k,\Delta\mathbf{M},\lambda)=\omega_{\omega_{S_{k(-)}}}(\mathbf{M}^0+\Delta\mathbf{M})S_k-\omega_{\omega_{S_{k-1}}}(\mathbf{M}^0+\Delta\mathbf{M})(S_k^0)^2\frac{1}{S_k}$$

$$+\sum_{j=1}^{m}\lambda_j\left[y_{jk_{(+)}}S_k-y_{jk_{(-)}}\left(S_k^0\right)^2\frac{1}{S_k}\right] \tag{5-26}$$

The solutions $\mathbf{A}^*, \mathbf{S}^*, \mathbf{M}^*$ and λ^* can be obtained by maximizing $\mathbf{L}(\mathbf{A},\mathbf{S},\mathbf{M}^0+\Delta\mathbf{M},\lambda)$ with respect to λ and minimizing it with respect to **A**, **S** and $\Delta\mathbf{M}$. Since eq.(5-24) has a simple form of a summation of the separable element Lagrangian functions, L_i and L_k, the minimization of $\mathbf{L}(\mathbf{A},\mathbf{S},\mathbf{M}^0+\Delta\mathbf{M},\lambda)$ with respect to **A**, **S** and $\Delta\mathbf{M}$ can be accomplished by minimizing L_i and L_k, separately.

(c) First stage minimization process of the Lagrangian function

In the first stage minimization process of the Lagrangian function in eq.(5-24), the material kinds of member elements **M** are maintained constant, namely modulus of elasticity $\boldsymbol{E}$ of each member element is assumed as a constant value during the first stage minimization process and **A** is improved for improvement of $\boldsymbol{EA}$. Then, $L_i(A_i,\Delta M_i,\lambda)$ and $L_k(S_k,\Delta\mathbf{M},\lambda)$ are, respectively, minimized with respect to A_i and S_k, independently. A_i^* which minimizes $L_i(A_i,\Delta M_i,\lambda)$ is given by the simple expression which is derived from the necessary condition of the minimization of $L_i(A_i,\Delta M_i,\lambda)$, namely, $\partial L_i/\partial A_i=0$, and the side constraint on A_i. S_k^* which minimizes $L_k(S_k,\Delta\mathbf{M},\lambda)$ is also given in the same manner. The detailed expressions for improvements of A_k^* and S_k^* are described in Chapter 4. The expressions for calculation of A_k^* and S_k^* include λ. Therefore, after λ^* is obtained in the following process, A_k^* and S_k^* should be modified by using λ^*.

The minimized Lagrangian function with respect to **A** and **S** is denoted as $l(\lambda)$: namely,

$$l(\lambda)=\min_{\mathbf{A},\mathbf{S}}\mathbf{L}(\mathbf{A},\mathbf{S},\mathbf{M}^0+\Delta\mathbf{M},\lambda) \tag{5-27}$$

Following the minimization process with respect to A_i and S_k, the Lagrangian function $l(\lambda)$ is maximized with respect to the dual variables λ by using a Newton-type algorithm. In the Newton-type algorithm, the search direction of λ for active constraints $\boldsymbol{S}_{AG}$ can be calculated by a simple expression in terms of the vector of first derivatives of $l(\lambda)$ and the Hessian matrix of $l(\lambda)$ with respect to λ. The details of the expressions of search direction and maximization algorithm of $l(\lambda)$ with respect to λ are also described in Chapter 4.

After the improvements of dual variables λ as λ^* by the Newton-type algorithm and **A** and **S** as $\mathbf{A}^*$ and $\mathbf{S}^*$ using λ^*, the set of active constraints $\boldsymbol{S}_{AG}$ in the currently

approximated primary design space also has to be updated. The min-max process described above is iterated until **A**, **S** and λ converge to constant values.

In this first minimization process, it should be noted that if the rate of change in **S** is too large in any iteration, the successive solutions oscillate and in some cases smooth convergence may not be obtained. For this reason, the adaptive move limit constraints are restricted such that the maximum rate of change in **S** is limited to less than 20%. It is, also, important to note that in the maximizing process of the Lagrangian function, the Hessian matrix can be singular when one or more gradient vectors of the active constraints become linearly dependent. In this case, the maximization process is carried out by deleting one constraint from the set of active constraints $\boldsymbol{S}_{AG}$. Please see section 4-3.(3).(d) for the detailed algorithm in case of singularity of Hessian matrix. Following this, λ should be improved according to the above process.

In the Newton-type algorithm, at least one of the behavior constraints must be active. For this purpose, a simple scaling technique given by eq.(5-28) is used to modify the initial cross-sectional areas $\mathbf{A}^0$.

$$A_i = A_i^0 \cdot R \qquad (i = 1, \cdots, n) \tag{5-28}$$

$$\text{where} \quad R = \max\left(\frac{\sigma_1}{\sigma_a}, \cdots, \frac{\sigma_n}{\sigma_a}, \frac{\delta_1}{\delta_a}, \cdots, \frac{\delta_u}{\delta_a}, \frac{2\pi f_{1\min}}{\mu_1}, \cdots, \frac{2\pi f_{v\min}}{\mu_v}\right)$$

(d) Second stage minimization process of the Lagrangian function

After the first stage improvements of $\boldsymbol{EA}$, **S** and λ by the above min.-max. process, the values of $\mathbf{S}^*$ and λ^* are maintained constant and the Lagrangian function $\mathbf{L}(\mathbf{A}, \mathbf{S}^*, \mathbf{M}^0 + \Delta\mathbf{M}, \lambda^*)$ given by eq.(5-24) is minimized with respect to $\Delta\mathbf{M}$ and **A**. In this stage, the values of λ_p for the inactive constraints, namely, $P \notin \boldsymbol{S}_{AG}$, become zero and the active constraints $\mathbf{g}_a$, namely, $a \in \boldsymbol{S}_{AG}$, also become zero. Therefore, from eq.(5-24), the minimization of $\mathbf{L}(\mathbf{A}, \mathbf{S}^*, \mathbf{M}^0 + \Delta\mathbf{M}, \lambda^*)$ with respect to A_i and ΔM_i is achieved by comparing the discrete values of $\overline{L}_i(\overline{A}_i, \Delta M_i)$ at the neighboring material kinds. The discretized $\overline{L}_i(\overline{A}_i, \Delta M_i)$ is given by

$$\overline{L}_i(\overline{A}_i, \Delta M_i) = \omega_{Ai}(M_i^0 + \Delta M_i) \cdot \overline{A}_i(M_i^0 + \Delta M_i) \tag{5-29}$$

The improved A_i for $M_i^0 + \Delta M_i$, $\overline{A}_i(M_i^0 + \Delta M_i)$, is made in the manner described below in order to satisfy the active constraints.

For the case when only stress constraints are active, the necessary condition

which maintains the stress constraints active for a discrete change ΔM_i in material kind M_i is given as

$$g_{\sigma i}\left(\overline{A}_i^{\sigma}, \Delta M_i\right) = \frac{\sigma_i A_i^*\left(M_i^0\right)}{\overline{A}_i^{\sigma}\left(M_i^0 + \Delta M_i\right)} - \sigma_{ai}\left(M_i^0\right) + m_{ii} = 0 \qquad (i = 1, \cdots, n) \qquad (5\text{-}30)$$

where σ_i and $\sigma_{ai}\left(M_i\right)$ are, respectively, the working stress and allowable stress of the ith member element with material kind M_i. m_{ii} is the sensitivity of stress constraint of the ith member element with respect to a discrete change in material kind M_i. A_i^* is the cross-sectional area of the ith member element which is obtained by the first stage minimization process of the Lagrangian function.

By solving eq.(5-30) with respect to $\overline{A}_i^{\sigma}\left(M_i^0 + \Delta M_i\right)$ and considering the lower and upper limits on M_i, the improved A_i for $M_i^0 + \Delta M_i$, $\overline{A}_i^{\sigma}\left(M_i^0 + \Delta M_i\right)$, is calculated.

For the case when displacement or, and frequency constraint(s) is(are) active, the necessary condition required to maintain the displacement or, and frequency constraint(s) to be active for a discrete change ΔM_i is to keep the value of $E_i A_i$ constant, namely

$$E_i\left(M_i^0\right) A_i^*\left(M_i^0\right) = E_i\left(M_i^0 + \Delta M_i\right) \overline{A}_i^{\delta, f}\left(M_i^0 + \Delta M_i\right) \qquad (i = 1, \cdots, n) \qquad (5\text{-}31)$$

The improved A_i for $M_i^0 + \Delta M_i$, $\overline{A}_i^{\delta, f}\left(M_i^0 + \Delta M_i\right)$, is calculated by solving eq.(5-31) with respect to $\overline{A}_i^{\delta, f}\left(M_i^0 + \Delta M_i\right)$ and considering the lower and upper limits on A_i.

In the case when all three constraints, stress, displacement and frequency, are active, a larger value of $\overline{A}_i^{\sigma}$ and $\overline{A}_i^{\delta, f}$ is chosen.

The discrete changes in the mechanical and economical properties of materials considerably affect the design space and, therefore, in the minimization of $\overline{L}_i\left(\overline{A}_i, \Delta A_i\right)$, the range of ΔM_i in one iteration is restricted to the nearest stronger $\left(\Delta M_i = +1\right)$ or weaker $\left(\Delta M_i = -1\right)$ material only.

There is an important issue that needs to be taken into account when the frequency constraint is active. The vibration mode and frequency of truss structure are very sensitive to the distribution of ***EA*** and **S**, and the vibration mode might be changed as a result of the improvements of ***EA*** and **S** in the first stage minimization process. If the vibration mode has indeed changed, the sensitivities of frequency constraint calculated using the initial ***EA*** and **S** become ineffective and may not satisfy the frequency constraint on the new vibration mode. For this reason, it is

necessary to calculate the exact vibration mode and frequency, and examine the activeness of frequency constraint after the first stage minimization process. If the activeness of frequency constraint is changed, namely the frequency constraint becomes active or inactive, the set of active constraints S_{AG} must be modified before performing the second stage minimization process.

In the two-stage minimization process of the Lagrangian function, the iterative improvements of **A**, **S**, **M** and λ are repeated until the convergence criteria are satisfied. Thus, the solution to the optimum design of truss structures subject to stress, displacement and frequency constraints are obtained.

5-4. NUMERICAL DESIGN EXAMPLES

The proposed optimal structural synthesis method is applied to various minimum-cost designs of statically indeterminate trusses subject to stress, displacement and natural frequency constraints.

In this section numerical results for 15-bar truss are discussed. In the design problem, the configuration of structure is assumed to be symmetrical about a vertical centerline and the horizontal distances **X** from the vertical center line to each panel points are treated as the shape design variables **S**. The lower limits of cross-sectional areas, $\mathbf{A}^l$, and shape variables, $\mathbf{X}^l$, are, respectively, set at 0.1cm^2 and 10.0cm. The structures have nonstructural lumped masses $\overline{\mathrm{M}}_C$ and structural lumped masses $\overline{\mathrm{M}}_{Xi}\,(i=1,\cdots,t)$ and are subjected to static vertical and horizontal loads. The objective here is to determine the optimum shapes and member topology for various design conditions.

(1) Material set

The allowable stress σ_a, modulus of elasticity E and unit cost ρ_c are the properties of material which affect the optimum solutions of minimum-cost designs of trusses. In general, the ratios of σ_a/ρ_c and E/ρ_c represent the effectiveness of stress, displacement and frequency constraints. Materials with high values of σ_a/ρ_c are more advantageous for the problems in which the stress constraints are dominant, whereas those with high E/ρ_c are more advantageous when the displacement or frequency constraints are dominant. In this study, material set (A) shown in Table 4-1 is used. The material set (A) consists of five components with identical modulus

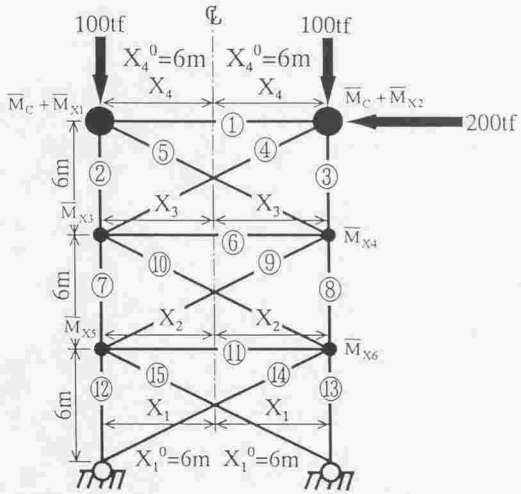

$\overline{M}_C$: non-structural lumped mass (102.04kgf/cm/s^2)

$\overline{M}_{X1}$~$\overline{M}_{X6}$: structural lumped masses

Fig.5-1 Initial 15-bar truss

of elasticity E and weight density ρ_w. ρ_w (kgf/cm^3) is set at 0.00785. The material set is arranged in ascending order of σ_a/ρ_c or descending order of E/ρ_c for the sake of simplification of the algorithm and smooth convergence to the optimum solution. The allowable tensile and compressive stresses of materials are assumed to be the same.

In the material set, σ_a/ρ_c increases with material number, and therefore, in cases where only stress constraints are active, the larger numbered materials are more economical than the smaller ones. On the contrary, E/ρ_c decreases with material number, and as a result, the smaller numbered materials are more economical when displacement or frequency constraints are active. In the problems where the combinations of the stress, displacement and frequency constraints are active, the optimum materials are selected in such a way that a balance is maintained between the values of σ_a/ρ_c and E/ρ_c.

(2) 15-bar truss examples

The 15-bar truss shown in Fig.5-1 is designed for various design conditions. In the problems, the horizontal distances from the vertical center line to each panel point, $\mathbf{X}=[X_1, X_2, X_3, X_4]^T$, are treated as the shape design variables S. The nonstructural lumped mass $\overline{M}_C$ =102.04kgf/cm/s^2 is attached to the top two panel points 1 and 2. The structural lumped masses $\overline{M}_{X1}$ to $\overline{M}_{X6}$ which are calculated using the weight density of material, cross-sectional areas and lengths of member elements, are distributed as shown in Fig.5-1. In the design examples, the fundamental natural frequency constraint g_{f1} is taken into account. The iteration histories and final optimum solutions for various design conditions are presented in Table 5-1 and Fig.5-2. In Fig.5-2, the thickness of a member indicates the cross-sectional area and the number associated with member element represents its material kind. The dotted lines show member elements that are deleted when their cross-sectional areas are equal to or smaller than the lower limit 0.1cm^2.

In case A as shown in Fig.5-2 and Table 5-1, where $f_{1\min}$ and $\delta_{o\max}$ are set at 0.1H$_Z$ and 10.0cm, respectively, the stress constraints are the only ones active at the optimum solution. Noted that the maximum move limit of **X** is set at 20 percent. Even when starting with the worst initial material distribution for stress constraints, namely $M_i^0 = 1 (i = 1, \cdots, 15)$, **X**, **M** and **A** show a steady improvement. After 13 iterations, the material kinds of main member elements are converged to material kind number 5, which is the most economical material kind when only the stress constraints are active. Thereafter, the move limit of **X** is reduced adaptively, which in turn leads to steady improvements of **X** and **A**. After 10 iterations, the optimum solution is obtained. The cross-sectional areas of main member elements, A_1 and A_{12}, are 20 times larger than those of A_8 and A_{13}. The cross-sectional areas of redundant member elements at the optimum solution are reduced to 0.1cm^2 and their material kinds are selected almost as number 1, which is the lowest cost material. The optimum shape of truss is similar to a two-bar truss and the main members A_2, A_3, A_4, A_7, A_8, A_{12} and A_{13} are fully stressed. The cross-sectional areas of A_3, A_8, A_{13} at the optimum solution are almost identical and A_7 and A_{12} are each approximately equal to the sum of the areas of A_2 and A_4 for the balance of axial forces. The maximum horizontal displacement at panel point 2 is 5.9cm.

In case B as shown in Fig.5-2 and Table 5-1, $f_{1\min}$ and $\delta_{o\max}$ are set at 0.1H$_Z$ and 3.8cm, respectively. In this case, both stress and displacement constraints are active

at the optimum solution. The initial material kinds are assumed to be 5 for all member elements. After 30 iterations, the material distribution converge to the optimum and the optimum **X** and **A** are obtained at iteration number 35. In this problem, the maximum horizontal displacement occurred normally at panel point 2, but occasionally at 4. For this reason, the number of iterations required to obtain the optimum solution is larger as compared with other cases. At the optimum solution, the material kinds 4 and 3 are selected, respectively, for the main member elements 2 and 4, and 7 and 12. All of these member elements are fully stressed. For all other member elements, material kind 1 is selected and these member elements are not fully stressed except for member element 8. Material kind 1 is most economical when the displacement constraints are active. The cross-sectional areas of the optimum A_7 and A_{12} are almost the same and are almost 50 times larger than these of member elements 8 and 13. The optimum shape of the truss is similar to a two-bar truss and its X_1 is slightly larger than that for case A. The total cost for case B is 7.3% higher than that for case A.

In case C, shown in Fig.5-2 and Table 5-1, $f_{1\min}$ and $\delta_{a\max}$ are set at 2.0Hz and 10.0cm, respectively. In this case, both stress and frequency constraints are active at the optimum solution. The optimization algorithm is initialized by the material kind distribution $M_i^0 = 5 \quad (i = 1, \cdots, 15)$. In this design problem, the vibration mode of structure in successive solutions is changed according to the improvements of EA and **S** at the first stage minimization process, and then, the sensitivities of frequency constraint calculated with the initial EA and **S** at that iteration become ineffective to satisfy the frequency constraint on new vibration mode. In this kind of situation, the exact vibration mode and frequency of structure must be calculated at each time at the end of first stage minimization process, and the activeness of frequency constraint should be examined. The optimum distribution of material kind is obtained after 18 iterations. The optimum solution is obtained at iteration number 32. At the optimum solution, all non-trivial member elements are fully stressed except member element 3. The optimum cross-sectional areas of A_3, A_5, A_8, and A_{13} are about 12-25 times larger than those chosen in cases A and B, but their optimum material kinds are determined as 1. This optimum solution is quite reasonable in the case where both stress and frequency constraints are active. The total cost in case C is 21.5 percent higher than that in case A.

In case D, shown in Fig.5-2 and Table 5-1, $f_{1\min}$ and $\delta_{a\max}$ are set at 2.0Hz and

Table 5-1 Iteration histories and optimum solutions for cases A, B, C and D

	Iteration number	Total cost	Cross-sectional areas A(cm^2) and material kinds (M)								$X=[X_1,X_2,X_3,X_4]^T$			
			A_2 (M_2)	A_3 (M_3)	A_4 (M_4)	A_5 (M_5)	A_7 (M_7)	A_8 (M_8)	A_{12} (M_{12})	A_{13} (M_{13})	X_1	X_2	X_3	X_4
	INIT.[2]	3.8125×10^8	100.00 (1)	100.00 (1)	100.00 (1)	100.00 (1)	100.00 (1)	100.00 (1)	100.00 (1)	100.00 (1)	600.00	600.00	600.00	600.00
	5	1.1909×10^8	36.62 (5)	11.42 (4)	52.86 (5)	9.54 (5)	85.68 (5)	17.59 (5)	88.18 (5)	25.25 (5)	996.34	690.61	339.68	196.61
(Case A)	10	1.1396×10^8	37.08 (4)	31.55 (5)	67.84 (5)	1.72 (5)	95.25 (5)	6.53 (5)	88.43 (5)	8.21 (5)	1240.66	806.72	348.48	126.62
$f_{1\min} = 0.1$ Hz	15	9.7348×10^7	35.02 (5)	10.41 (5)	48.94 (5)	0.89 (4)	83.26 (5)	11.41 (5)	83.58 (5)	11.28 (5)	1318.47	893.81	449.94	62.24
$\delta_{a\max} = 10.0$ cm	20	9.3057×10^7	37.30 (5)	6.89 (4)	44.35 (5)	0.12 (4)	81.57 (5)	6.86 (4)	93.62 (4)	6.85 (4)	1512.80	1035.38	519.91	21.57
S_{AG}[1]: σ only	OPT.23[3]	9.3844×10^7	38.36 (5)	5.50 (4)	42.88 (5)	0.13 (3)	81.25 (5)	4.24 (4)	81.39 (5)	4.25 (4)	1624.24	1084.49	543.34	11.04
	INIT.[2]	6.8624×10^8	100.00 (5)	100.00 (5)	100.00 (5)	100.00 (5)	100.00 (5)	100.00 (5)	100.00 (5)	100.00 (5)	600.00	600.00	600.00	600.00
	5	1.7691×10^8	45.97 (3)	0.12 (4)	51.84 (4)	34.62 (3)	108.45 (3)	31.05 (3)	113.26 (3)	68.15 (3)	790.61	543.04	443.10	354.29
(Case B)	10	1.5286×10^8	61.73 (3)	0.10 (1)	58.72 (3)	57.72 (1)	114.47 (3)	53.34 (1)	123.02 (3)	71.58 (1)	988.06	698.53	431.30	209.21
$f_{1\min} = 0.1$ Hz	15	1.1429×10^8	57.59 (3)	0.10 (1)	57.33 (3)	22.03 (1)	113.11 (3)	21.53 (1)	115.56 (3)	24.91 (1)	1387.10	934.08	488.36	123.53
$\delta_{a\max} = 3.8$ cm	20	1.0642×10^8	57.34 (3)	0.10 (1)	56.92 (3)	13.23 (1)	113.95 (3)	13.59 (1)	113.43 (3)	15.62 (1)	1559.72	978.20	536.76	72.95
S_{AG}[1]: σ, δ	25	9.3813×10^7	45.18 (4)	0.10 (1)	49.55 (4)	2.91 (1)	101.03 (3)	2.51 (1)	92.12 (4)	9.14 (2)	1537.56	1069.35	620.08	43.07
	30	9.7107×10^7	46.67 (4)	0.10 (1)	47.93 (4)	2.53 (1)	112.69 (3)	0.19 (1)	103.03 (3)	5.16 (1)	1653.14	1143.47	583.90	25.43
	OPT.35[3]	1.0070×10^8	47.09 (4)	1.02 (1)	47.30 (4)	2.12 (1)	113.28 (3)	2.08 (1)	113.05 (3)	2.63 (1)	1735.67	1165.38	585.45	15.02
	INIT.[2]	6.8624×10^8	100.00 (5)	100.00 (5)	100.00 (5)	100.00 (5)	100.00 (5)	100.00 (5)	100.00 (5)	100.00 (5)	600.00	600.00	600.00	600.00
	5	1.6013×10^8	54.88 (4)	24.13 (3)	55.16 (5)	19.69 (3)	95.20 (5)	39.53 (3)	117.80 (4)	56.71 (3)	773.04	509.54	329.59	266.22
(Case C)	10	1.3566×10^8	77.72 (2)	25.11 (1)	58.85 (4)	42.70 (1)	128.56 (3)	61.42 (1)	130.38 (3)	55.91 (1)	927.38	636.10	335.89	159.82
$f_{1\min} = 2.0$ Hz	15	1.1363×10^8	57.08 (3)	24.00 (2)	51.60 (5)	17.21 (2)	89.50 (5)	38.85 (2)	89.19 (5)	40.10 (2)	1024.31	695.95	351.09	70.91
$\delta_{a\max} = 10.0$ cm	20	1.1606×10^8	62.00 (3)	27.04 (1)	52.91 (4)	28.65 (1)	89.66 (5)	53.32 (1)	89.96 (5)	55.03 (1)	1041.68	698.32	354.03	31.46
S_{AG}[1]: σ, f_r	25	1.1507×10^8	63.24 (3)	26.15 (1)	51.37 (4)	29.53 (1)	89.37 (5)	52.38 (1)	89.51 (5)	53.22 (1)	1057.01	708.54	356.94	19.39
	30	1.1434×10^8	64.03 (3)	25.26 (1)	50.22 (4)	30.24 (1)	88.95 (5)	50.96 (1)	89.04 (5)	51.44 (1)	1072.78	719.11	361.43	15.42
	OPT.32[3]	1.1406×10^8	64.38 (3)	24.97 (1)	49.73 (4)	30.54 (1)	88.78 (5)	50.35 (1)	88.87 (5)	50.76 (1)	1079.15	723.25	363.40	13.78
	INIT.[2]	6.8624×10^8	100.00 (5)	100.00 (5)	100.00 (5)	100.00 (5)	100.00 (5)	100.00 (5)	100.00 (5)	100.00 (5)	600.00	600.00	600.00	600.00
	5	1.8560×10^8	45.31 (4)	29.69 (3)	89.13 (4)	15.54 (3)	103.94 (5)	39.46 (3)	100.97 (5)	77.35 (3)	767.72	492.66	320.35	266.22
(Case D)	10	1.4956×10^8	68.17 (2)	44.06 (1)	90.26 (2)	20.26 (1)	121.10 (3)	65.09 (1)	127.11 (3)	86.15 (1)	971.89	686.59	383.45	118.12
$f_{1\min} = 2.0$ Hz	15	1.2890×10^8	91.13 (1)	26.01 (1)	90.82 (2)	22.26 (1)	121.76 (3)	42.08 (1)	121.64 (3)	44.53 (1)	1149.68	770.71	393.24	97.31
$\delta_{a\max} = 3.8$ cm	20	1.2305×10^8	99.39 (1)	22.23 (1)	101.05 (1)	23.05 (1)	119.81 (3)	42.62 (1)	120.88 (3)	43.31 (1)	1194.18	797.91	405.41	47.45
S_{AG}[1]: σ, δ, f_r	OPT.24[3]	1.2075×10^8	97.92 (1)	23.33 (1)	100.49 (1)	19.39 (1)	118.88 (3)	42.43 (1)	119.96 (3)	43.14 (1)	1234.37	823.21	417.01	24.77

1) : Set of active constraint(s), 2) : Initial values, 3) : Optimum solution

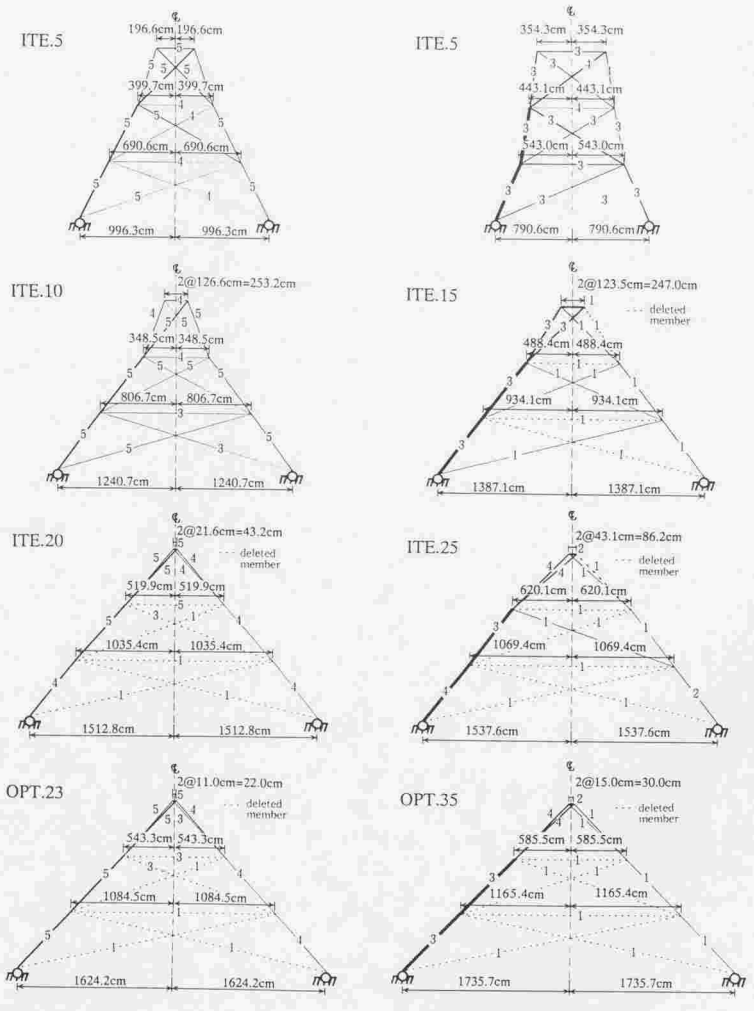

CASE A

$S_{AG} = \sigma$ only

CASE B

$S_{AG} = \sigma$, δ

Fig.5-2 Iteration histories and optimum solutions for cases A, B, C and D (1/2)

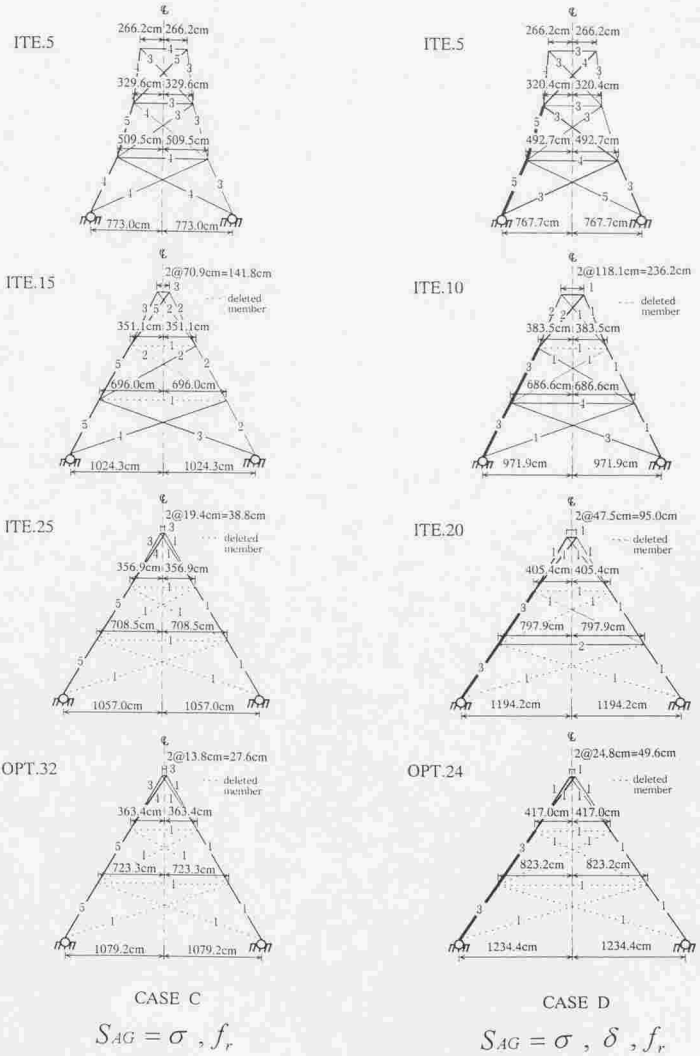

CASE C

$S_{AG} = \sigma , f_r$

CASE D

$S_{AG} = \sigma , \delta , f_r$

Fig.5-2 Iteration histories and optimum solutions for cases A, B, C and D (2/2)

3.8cm, respectively. In this problem, all these constraints on stress, displacement and frequency are active, and the changes in vibration mode are also observed according to the improvements of **A** and **S** in the first stage minimization process. However, the optimum material kind distribution is determined at iteration 13, and the optimum solution is obtained at iteration 24. At the optimum solution, A_2, A_4, A_7 and A_{12} are fully stressed and their material kinds are selected as 1, 1, 3 and 3, respectively. On the contrary, A_3, A_5, A_8 and A_{13} are not fully stressed and their optimum material kinds are selected as 1, which is the most economical material when displacement and frequency constraints are active. As in case C, the cross-sectional areas of A_3, A_5, A_8 and A_{13} are about 8-20 times larger values than those determined in cases A and B. The optimum shape, distribution of material kinds and cross-sectional areas of member elements seem to be quite reasonable for the case in which stress, displacement and frequency constraints are active. The total cost for case D is 29.7 percent higher than that for case A.

In all four cases the quite similar solutions are obtained starting with different initial material distributions. The maximum CPU time in the design examples was 23 seconds on a DEC 3000/300.

From the investigations of the optimum solutions for various number of member trusses subject to different design conditions, it is clear that the proposed optimal synthesis method can efficiently determine the optimum coordinates of the panel points **S**, arrangements of material kinds **M** and cross-sectional areas of member elements **A** of truss structures for optimum design synthesis problems in which both static and frequency constraints are subjected. At the optimum solution the cross-sectional areas of trivial member elements are equal to or less than the imposed lower limit. Therefore, the optimum member topology can, also, be determined by the proposed synthesis method by setting the lower limit of cross-sectional areas of member elements to an extremely small value.

5-5. CONCLUSIONS

In this Chapter the systematic synthesis method proposed in Chapter 4 is applied to the optimization of shape, material and sizing arrangements of truss structures subject to not only stress and displacement constraints due to static loads but also frequency constraints. The design method is developed by utilizing the two-stage

minimization process of the Lagrangian function, the concept of convex and linear approximation, dual method and discrete sensitivity analysis. The rigorousness, reliability and efficiency of the proposed design method have been confirmed by various numerical experiments on statically indeterminate trusses.

The following conclusions can be drawn from this study:

(1) The proposed optimal synthesis method can deal with any combinations of design variables such as shape of structure, discrete material kinds and cross-sectional areas of member elements of truss structure subject to both static and frequency constraints. The application of this method, also, leads to an optimum member topology.

(2) The proposed two-stage optimization process for minimizing the Lagrangian function can also solve the mixed discrete/continuous variable problem subject to stress, displacement and frequency constraints in a systematic and efficient manner.

(3) Adaptive move limit constraint on $\mathbf{S}$ is necessary to ensure that successive solutions converge to the optimum solution when displacement or frequency constraints are active in the design problem.

(4) The vibration mode and frequency of truss structure are very sensitive to the distribution of $\boldsymbol{EA}$ and $\mathbf{S}$, and the vibration mode might be changed by improvements of $\boldsymbol{EA}$ and $\mathbf{S}$ at the first stage of the minimization process. Therefore, it is necessary to calculate the exact vibration mode and frequency and to examine the activeness of frequency constraint at the end of first stage minimization process to ensure the smooth convergence to the optimum solution.

REFERENCES

1. Ohkubo,S. and Asai,K., "A hybrid optimal synthesis method for truss structures considering shape, material and sizing variables", *Int. J. Numer. Methods Engng.* Vol.34, 1992, pp.839-851.
2. Ohkubo,S., Taniwaki,K. and Asai,K., "Optimal structural synthesis utilizing shape, material and sizing sensitivities", in Kleiber,M. and Hisada,T. eds., *Design Sensitivity Analysis*, Atranta Technology Publications, Atlanta, 1993, pp.164-188.
3. Turner,M.J., "Design of minimum mass structures with specified natural frequencies",

AIAA Journal, Vol.5, No.3, 1967, pp.406-412.

4. Khot,N.S., "Optimization of structures with multiple frequency constraints", *Computers & Structures*, Vol.20, No.5, 1985, pp.869-876.
5. Kiusalaas,J. and Shaw,R.C.J., "An algorithm for optimal structural design with frequency constraints", *Int. J. Numer. Methods Engng.*, Vol.13, No.5, 1978, pp.283-295.
6. Rubin,C.P., "Minimum weight design of complex structures subject to a frequency constraint", *AIAA Journal*, Vol.5, No.5, 1970, pp.923-927.
7. Wang,B.P., "Synthesis of truss structures with specified fundamental natural frequency", *Computers & Structures*, Vol.39, No.5, 1991, pp.435-439.
8. Felix,J. and Vanderplaats,G.N., "Configuration optimization of trusses subject to strength, displacement and frequency constraints", *J. Mechanisms, Transmissions, and Automation in Design*, Vol.109, 1987, pp.233-241.
9. Nelson,R.B., "Simplified calculation of eigenvector derivatives", *AIAA Journal*, Vol.14, No.9, 1976, pp.1201-1205.
10. Ojalvo,I.U., "Efficient computation of mode-shape derivatives for large dynamic systems", *AIAA Journal*, Vol.25, No.10, 1987, pp.1386-1390.
11. Sutter,T.R., Camarda,C.J., Walsh,J.L. and Adelman,H.M., "Comparison of several methods for calculating vibrating mode shape derivatives", *AIAA Journal*, Vol.26, No.12, 1988, pp.1506-1511.
12. Mills-Curran,W.C., "Calculation of eigenvector derivatives for structures with repeated eigenvalues", *AIAA Journal*, Vol.26, No.7, 1988, pp.867-871.
13. Murthy,D.V. and Haftka,R.T., "Derivatives of eigenvalues and eigenvectors of a general complex matrix", *Int. J. Numer. Methods Engng.*, Vol.26, 1988, pp.293-311.
14. Dailey,R.L., "Eigenvector derivatives with repeated eigenvalues", *AIAA Journal*, Vol.27, No.4, 1989, pp.486-491.
15. Haftka,R.T. and Gurdal,Z., *Elements of structural optimization* (third revised and expanded edition), Chapter 7, Kluwer Academic Publishers, Dordrecht, 1992.
16. Starnes,J.H. and Haftka,R.T., "Preliminary design of composite wings for buckling, strength, and displacement constraints", *J. Aircraft*, Vol.16, No.8,1979, pp.564-570.
17. Fleury,C. and Schmit,L.A., "Dual methods and approximation concepts in structural synthesis", *CR-3226, NASA*, 1980.
18. Fleury,C. and Braibant,V., "Structural optimization : a new dual method using mixed variables", *Int. J. Numer. Methods Engng.*, Vol.23, 1986, pp.409-428.
19. Ohkubo,S. and Taniwaki,K., "Total optimal synthesis method for truss structures subject

to static and frequency constraints", *Microcomputers in Civil Engineering*, Vol.10, 1995, pp.39-50.

20. Ohkubo,S. and Taniwaki,K., "Structural optimization dealing with shape, material and sizing variables subjected to static and seismic loads", *Proc. of the Tools and Methods for Concurrent Engineering*, TMCE'96, 1996, pp.59-74.
21. Bathe,K.J. and Wilson,E.L., *Numerical Method in Finite Element Analysis*, Prentice-Hall, Englewood Cliffs, New Jersey, 1976.

Chapter 6

TOTAL OPTIMAL SYNTHESIS METHOD FOR TRUSS STRUCTURES SUBJECTED TO STATIC AND SEISMIC LOADS

6-1. INTRODUCTION

In the past decades, a number of contributions to the optimum design of structures subjected to static and seismic loads have been made since the earliest study by Pierson[1], but most of the works have focused to determine the optimum member element size distributions in many types of structures[2-11]. However, from the optimum design viewpoint of structures subjected to static and seismic loads, it is also very important to determine the optimum configuration and discrete material kind distribution of structure as well as the optimum distribution of member element sizes.

In Chapter 4, a total optimal synthesis method for truss structures is presented to determine the optimum values to be used for the coordinates of all panel points, cross-sectional areas and discrete material kinds of all member elements simultaneously satisfying stress and displacement constraints due to static loads [12,13]. In Chapter 5, the synthesis method is applied to solve design problems subject to not only stress and displacement constraints due to static loads but also frequency constraints[14].

In this Chapter, the optimal synthesis method is extended to solve problems of truss structures subjected to static and seismic loads. The structural optimization dealing with shape, sizing and material variables subjected to static and seismic loads is the first challenge in the world. In the optimum design process, all member elements are assumed to be made of circular steel pipes. By applying the concept of suboptimization, the cross-sectional areas of all member elements are dealt with as sizing variables instead of the diameters and plate thicknesses of circular steel pipes. The objective function is the total construction cost of truss structures considering not only the cost of truss structures but also the cost of land of construction site. The stress, displacement and slenderness ratio constraints are considered as behavior and side constraints. From the practical design viewpoint, the allowable stresses of member elements are taken from the Japanese Specifications for Highway Bridges [JSHB][15]. The stresses of all member elements due to seismic loads are calculated

by a response spectrum method using the acceleration response spectrum which is specified in the JSHB[16].

In the optimum design method, the primary optimum design problem expressed in terms of primary design variables, namely, shape, material and sizing variables, is transformed into an approximate subproblem of convex and separable form by using mixed direct/reciprocal design variables and the sensitivities of behavior constraints with respect to the primary design variables. The sensitivities of stress and displacement constraints due to seismic loads with respect to design variables are calculated analytically by using the sensitivities of eigenvalues, eigenvectors, participation factor and acceleration response spectrum. The separable Lagrangian function is introduced for the approximate subproblem and the Lagrangian function is minimized by the algorithm proposed in Chapters 4 and 5 incorporating suboptimization technique.

In the numerical design examples, the numerical results of minimum-cost design problems of 193-bar transmission tower truss are shown for the three design conditions with different unit costs of land of construction sites. By comparing the optimum solutions, the rigorousness, reliability and efficiency of the optimum design method are demonstrated. It is also emphasized that the optimal configuration, distribution of material kinds and cross-sectional areas of all member elements are significantly influenced by the value of unit cost of land of construction site.

6-2. FORMULATION OF PRIMARY OPTIMUM DESIGN PROBLEM

(1) Design variables

In this study, all member elements are assumed to be made of circular steel pipes with diameter **D** and plate thickness **t** as shown in Fig.6-1. For the reason that the allowable compressive stress of a member element with cross-sectional area A is significantly influenced by the values of slenderness ratio and D/t as specified in the JSHB[15]. Therefore, the design variables with respect to the member size should be primarily D and t. However, by applying the optimum design concept of sub-optimization of structural element presented by Ohkubo et al.[17-20], D and t corresponding to the value of A can be determined quite simply, and this suboptimization concept can simplify the problem formulation of the primary

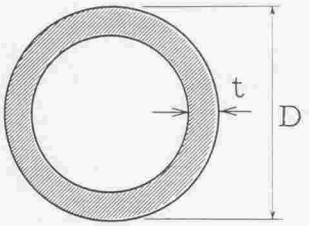

t :Plate thickness (mm)
D:Diameter(cm)

Fig.6-1 Cross section of a member element

Table 6-1 Material set (**MS**)

Material number	σ_{ta} (kgf/cm^2)	E (kgf/cm^2)	ρ_c (yen/cm^3)	ρ_w (kgf/cm^3)	σ_{ta}/ρ_c
1 (SS400)	1400	2.1x10^6	1.6	0.00785	875.
2 (SM490)	1900	2.1x10^6	2.0	0.00785	950.
3 (SM490Y)	2100	2.1x10^6	2.1	0.00785	1000.
4 (SM570)	2600	2.1x10^6	2.5	0.00785	1040.

σ_{ta} : allowable tensile stress　　ρ_c : unit cost

E : modulus of elasticity　　ρ_w : weight density

optimum design problem greatly. For this reason, the cross-sectional areas **A** of all member elements are dealt with as the sizing variables instead of **D** and **t**.

$$\mathbf{A} = [A_1, \cdots, A_n]^T \tag{6-1}$$

where n is the number of member elements.

The detailed determination method for t and D for each member element is stated in section 6-2.(2). Furthermore, the horizontal and vertical coordinates of panel points **S(=X,Y)** and material kinds **M** representing the physical and economical properties of material are considered as design variables.

$$\mathbf{S} = [S_1, \cdots, S_{2P}]^T = [X_1, \cdots, X_P, Y_1, \cdots, Y_P]^T \tag{6-2}$$

$$\mathbf{M} = [M_1, \cdots, M_n]^T \tag{6-3}$$

where P is the number of coordinates of panel points to be taken in to account.

Depending on the characteristics of these design variables, **A** and **S** are dealt with as continuous design variables, while **M** which represent the physical and economical properties of material are dealt with as discrete variables. As the set of available candidate material **MS** used in the design, four steel materials which are usually used for the practical design of steel structures, namely SS400 (material kind 1), SM490 (material kind 2), SM490Y (material kind 3) and SM570 (material kind 4), are taken into account. The allowable tensile stress σ_{ta}, modulus of elasticity E, weight density ρ_w and unit cost ρ_c for each material kind are assumed as Table 6-1 referring to the JSHB[15]. In general, the ratios of σ_{ta}/ρ_c and E/ρ_c represent the effectiveness of the stress and displacement constraints. The material kind 4 which has the largest value of σ_{ta}/ρ_c is the most advantageous material when the stress constraints are dominant, while the material kind 1 which has the largest value of E/ρ_c is the most advantageous material when the displacement constraints are dominant. The allowable axial compressive stress $\sigma^i_{ca}(M_i, t_i, D_i, l_i)$ of the ith member element is given by

$$\sigma^i_{ca}(M_i, t_i, D_i, l_i) = \sigma^i_{cag}(M_i, t_i, D_i, l_i) \cdot \sigma^i_{cal}(M_i, t_i, D_i, l_i) \,/\, \sigma^i_{cao}(M_i, t_i, D_i, l_i) \quad (i = 1, \cdots, n) \tag{6-4}$$

where $\sigma^i_{cag}(M_i, t_i, D_i, l_i)$ is the allowable axial compressive stress not concerning local buckling and it is give as the function of slenderness ratio $l_i / r_i(t_i, A_i)$ for each material kind. $\sigma^i_{cal}(M_i, t_i, D_i, l_i)$ is the allowable axial compressive stress against local buckling and it is expressed as the function of $D_i / 2t_i$ for each material kind. Please refer to the JSHB[15] for the detailed calculation of the allowable axial compressive stress.

(2) Determinations of **t** and **D** by suboptimization[22-25]

As stated in 6-2(1), the plate thickness t_i and diameter D_i corresponding to A_i in the ith member element are determined so as to maximize the allowable compressive stress $\sigma^i_{ca}(t_i)$ for the compressive member element or to minimize the slenderness ratio $l_i / r_i(t_i, A_i)$ for the tensile member element by applying the concept of suboptimization [17-20]. Supposing A_i is a constant value, then the diameter D_i is calculated by using t_i. Therefore, the maximization problem of the allowable

compressive stress $\sigma^{j}_{ca}(t_i)$ for the compressive member element can be stated as follows by considering t_i only as the design variable.

Find t_i which,

maximize $\sigma^{i}_{ca}(t_i) = \sigma^{j}_{cag}(t_i) \cdot \sigma^{i}_{cal}(t_i) / \sigma^{i}_{cao}(t_i)$ (6-5)

subject to $A_i(t_i) =$ constant (6-6)

From the practical design viewpoint, it is assumed that t for each member element should be selected from the following discrete plate thickness set considering the market sizes of steel plate thickness.

$$t_i \in \{2.0, 3.0, 4.0, 5.0, 6.0, 7.0, 8.0, 9.0, 10.0(\text{mm})\}$$

Figs.6-2 and 6-3 show the relationships between plate thickness t and allowable axial compressive stress σ_{ca} for material kinds 1 and 2 obtained by changing t discretely from 2.0mm to 10mm, and also show the process to determine t which maximizes σ_{ca}. In these figures, the member length l and cross-sectional areas **A** are, respectively, assumed as 4m, 50.0cm^2, 100.0cm^2, 150.0cm^2, 200.0cm^2, and 250.0cm^2. As clearly seen from Figs.6-2 and 6-3, **t** which maximize σ_{ca} under the condition of the given cross-sectional areas can be simply determined by comparing the values of σ_{ca} with respect to each plate thickness.

(3) Design constraints

The stress, displacement and slenderness ratio constraints are taken into account as the behavior and side constraints and these constraints are taken from the JSHB [15].

The critical stress constraint $g_j(\mathbf{A},\mathbf{S},\mathbf{M})$ for the jth member element is selected by comparing the values of stress constraints due to static loads, and static and seismic loads, $g^{1}_{\sigma j}(\mathbf{A},\mathbf{S},\mathbf{M})$, $g^{2}_{\sigma j}(\mathbf{A},\mathbf{S},\mathbf{M})$ and $g^{3}_{\sigma j}(\mathbf{A},\mathbf{S},\mathbf{M})$.

$$g^{1}_{\sigma j}(\mathbf{A},\mathbf{S},\mathbf{M}) = |N_{sj}(\mathbf{A},\mathbf{S},\mathbf{M})/A_j| - |\sigma_{aj}(M_j)| \le 0 \tag{6-7}$$

$$g^{2}_{\sigma j}(\mathbf{A},\mathbf{S},\mathbf{M}) = |N_{sj}(\mathbf{A},\mathbf{S},\mathbf{M})/A_j + N_{ej}(\mathbf{A},\mathbf{S},\mathbf{M})/A_j| - 1.5|\sigma_{aj}(M_j)| \le 0 \tag{6-8}$$

$$g^{3}_{\sigma j}(\mathbf{A},\mathbf{S},\mathbf{M}) = |N_{sj}(\mathbf{A},\mathbf{S},\mathbf{M})/A_j - N_{ej}(\mathbf{A},\mathbf{S},\mathbf{M})/A_j| - 1.5|\sigma_{aj}(M_j)| \le 0 \tag{6-9}$$

where $N_{sj}(\mathbf{A},\mathbf{S},\mathbf{M})$ and $N_{ej}(\mathbf{A},\mathbf{S},\mathbf{M})$ are, respectively, the axial forces in the jth

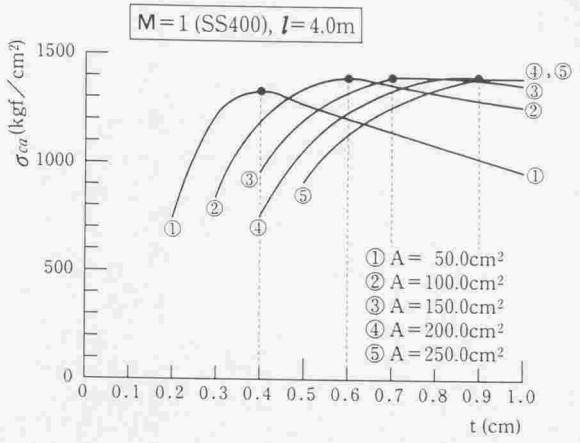

Fig.6-2 Relationships between plate thickness t and allowable compressive stress σ_{ca}
(material kind M=1 (SS400), member length l =4.0m)

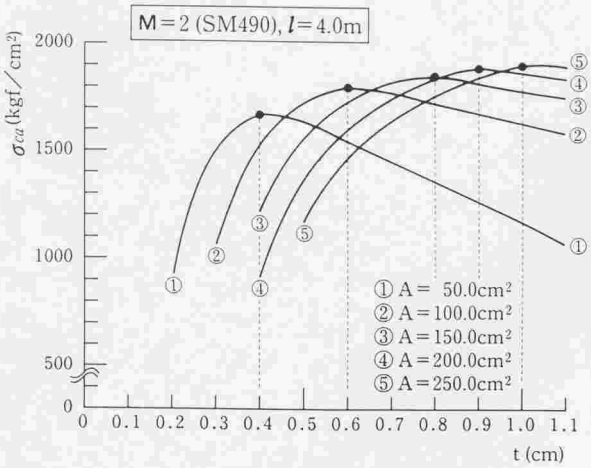

Fig.6-3 Relationships between plate thickness t and allowable compressive stress σ_{ca}
(material kind M=2 (SM490), member length l =4.0m)

member element due to static loads and seismic loads. $\sigma_{aj}(M_j)$ is the maximum allowable axial tensile or compressive stress.

The displacement constraints $g_{\delta d}(\mathbf{A},\mathbf{S},\mathbf{M})$ $(d=1,\cdots,u)$ are given as

$$g_{\delta d}(\mathbf{A},\mathbf{S},\mathbf{M})=|\delta_{sd}(\mathbf{A},\mathbf{S},\mathbf{M})|+|\delta_{ed}(\mathbf{A},\mathbf{S},\mathbf{M})|-|\delta_{ad}|\leq 0 \qquad (d=1,\cdots,u) \tag{6-10}$$

where $\delta_{sd}(\mathbf{A},\mathbf{S},\mathbf{M})$ and $\delta_{ed}(\mathbf{A},\mathbf{S},\mathbf{M})$ are, respectively, the displacements at the dth panel point due to static loads and seismic loads. δ_{ad} is the maximum allowable displacement at the dth panel point. u denotes the number of displacement constraints to be taken into account.

Furthermore, the following constraints on slenderness ratio of the ith member element are considered to hold the minimum member rigidity.

For compressive member $\quad l_i/r_i(t_i, A_i)\leq 120 \qquad (i=1,\cdots,n)$ (6-11)

For tensile member $\quad l_i/r_i(t_i, A_i)\leq 200 \qquad (i=1,\cdots,n)$ (6-12)

In the optimum design process, the above constraints on slenderness ratio are considered as the constraints to determine the lower limit of cross-sectional area of the ith member element A_i^l.

(4) Calculation of displacements and axial forces due to seismic loads

The structural behaviors due to seismic loads, $N_{ej}(\mathbf{A},\mathbf{S},\mathbf{M})$ and $\delta_{ed}(\mathbf{A},\mathbf{S},\mathbf{M})$, are calculated by the response spectrum method in which the standard acceleration spectrum specified by the JSHB [16] is used. The eigenvalues μ^2 and eigenvectors $[\phi]$ of structure which are necessary for the analysis of structural behaviors are obtained by solving the eigenvalue equation of structural dynamics given by eq.(5-12). The total system mass matrix $\overline{\mathbf{M}}_{\mathrm{M}}$ consists of the contributions from structural mass matrix $\overline{\mathbf{M}}_{\mathrm{X}}(\mathbf{A},\mathbf{S},\mathbf{M})$ and nonstructural mass matrix $\overline{\mathbf{M}}_{\mathrm{C}}$.

$$\overline{\mathbf{M}}_{\mathrm{M}}=\overline{\mathbf{M}}_{\mathrm{X}}(\mathbf{A},\mathbf{S},\mathbf{M})+\overline{\mathbf{M}}_{\mathrm{C}} \tag{6-13}$$

In this study, the acceleration response spectrum in the kth vibration mode, $\mathbf{S}_{Ak}$, is calculated by eq.(6-14) considering the dumping ratio of structure and ground condition.

$$\mathbf{S}_{Ak}=1.5\cdot\mathbf{S}_{Ak}^0 \tag{6-14}$$

where $\mathbf{S}_{Ak}^0$ is the standard acceleration response spectrum shown in Fig.6-4 and is

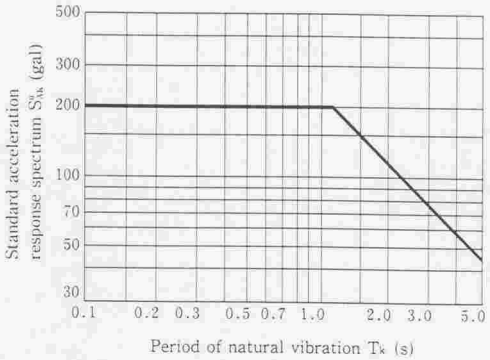

Fig.6-4 Standard acceleration response spectrum specified in JSHB (1990)

taken from the JSHB [16]. The relationship between the period of natural vibration T_k and the standard acceleration response spectrum $\mathbf{S}^0_{Ak}$ is expressed as follows.

$$\left.\begin{array}{lll} \text{if} & T_k < 0.1; & \mathbf{S}^0_{Ak} = 431 T_k^{\frac{1}{3}}(gal) \text{ and } \mathbf{S}^0_{Ak} > 160(gal) \\ \text{if} & 0.1 < T_k < 1.1; & \mathbf{S}^0_{Ak} = 200(gal) \\ \text{if} & 1.1 < T_k; & \mathbf{S}^0_{Ak} = 220/T_k(gal) \end{array}\right\} \quad (6\text{-}15)$$

The displacements $\delta_{e,k}(\mathbf{A},\mathbf{S},\mathbf{M})$ in the kth vibration mode are calculated by the following expression by using the eigenvalue μ_k^2, normalized eigenvector $[\phi]_k$ by eq.(5-19), principal coordinate q_k and participation factor β_k.

$$\delta_{e,k}(\mathbf{A},\mathbf{S},\mathbf{M}) = [\phi]_k q_k \quad (6\text{-}16)$$

where

$$q_k = \frac{\beta_k \mathbf{S}_{Ak}}{\mu_k^2} \quad (6\text{-}17)$$

The axial force of the kth vibration mode in the jth member element, $N_{ej,k}(\mathbf{A},\mathbf{S},\mathbf{M})$, is given by

$$N_{ej,k}(\mathbf{A},\mathbf{S},\mathbf{M}) = \boldsymbol{k}_{mj} \boldsymbol{Q}_j \delta_{ej,k}(\mathbf{A},\mathbf{S},\mathbf{M}) \quad (6\text{-}18)$$

where $\boldsymbol{k}_{mj}$ and $\boldsymbol{Q}_j$ are, respectively, the member stiffness matrix and rotation matrix for the jth member element. $\delta_{ej,k}(\mathbf{A},\mathbf{S},\mathbf{M})$ indicates the displacements at both ends of the jth member element.

Finally, the displacement at the dth panel point, $\delta_{ed}(\mathbf{A},\mathbf{S},\mathbf{M})$, and axial force in the jth member element due to seismic loads, $N_{ej}(\mathbf{A},\mathbf{S},\mathbf{M})$, are obtained by taking the square roots of the summations of squares of $\delta_{ed,k}(\mathbf{A},\mathbf{S},\mathbf{M})$ and $N_{ej,k}(\mathbf{A},\mathbf{S},\mathbf{M})$ $(k=1,\cdots,\nu)$. Namely,

$$\delta_{ed}(\mathbf{A},\mathbf{S},\mathbf{M}) = \sqrt{\sum_{k=1}^{\nu}\{\delta_{ed,k}(\mathbf{A},\mathbf{S},\mathbf{M})\}^2} \tag{6-19}$$

$$N_{ej}(\mathbf{A},\mathbf{S},\mathbf{M}) = \sqrt{\sum_{k=1}^{\nu}\{N_{ej,k}(\mathbf{A},\mathbf{S},\mathbf{M})\}^2} \tag{6-20}$$

where ν indicates the number of eigenvalue taken into account for the response spectrum analysis.

(5) Formulation of primary optimum design problem

The total construction cost is the objective function $\mathbf{W}(\mathbf{A},\mathbf{S},\mathbf{M})$ and it is expressed as the summation of costs of member elements and cost of land of construction site. By considering the design variables, design constraints and objective function stated above, the primary optimum design problem can then be formulated as

Find $\quad \mathbf{A},\mathbf{S},\mathbf{M},$ which

minimize $\quad \mathbf{W}(\mathbf{A},\mathbf{S},\mathbf{M}) = \sum_{i=1}^{n}\rho_{ci}(M_i)\,l_i(\widetilde{\boldsymbol{S}}_i)\,A_i + \rho_L A_L(S_L)$ (6-21)

subject to $\quad g_{cj}(\mathbf{A},\mathbf{S},\mathbf{M}) \le 0 \qquad (j=1,\cdots,n)$ (6-22)

$$g_{dd}(\mathbf{A},\mathbf{S},\mathbf{M}) \le 0 \qquad (d=1,\cdots,u) \tag{6-23}$$

$$\left.\begin{array}{ll} A_i^l \le A_i^l \le A_i^u & (i=1,\cdots,n) \\ S_k^l \le S_k \le S_k^u & (k=1,\cdots,2P) \\ M_i \in \mathbf{MS} & \end{array}\right\} \tag{6-24}$$

where

$$\widetilde{\boldsymbol{S}}_i = [S_{i-}, S_{i-}]^T$$

$\rho_{ci}(M_i)$ is the unit cost of the ith member element with material kind M_i. ρ_L and $A_L(S_L)$ are, respectively, the unit cost and area of land of construction site. S_L is the coordinates of panel points which directly influence the area of land of construction site. S_{i+} and S_{i-} are the horizontal and vertical coordinates of the panel points to which the ith member element is connected. As stated in section 6-2.(3), the lower limit of cross-sectional area A_i^l is determined so as to satisfy the constraints on slenderness ratio in eqs.(6-11) and (6-12) to ensure the minimum member rigidities.

6-3. OPTIMAL STRUCTURAL SYNTHESIS METHOD FOR TRUSS STRUCTURES SUBJECTED TO STATIC AND SEISMIC LOADS[24,25]

(1) Convex and separable approximate subproblem

The objective function and design constraints in eqs. (6-21) to (6-24) are approximated by using the first-order partial derivatives of the objective function and design constraints with respect to design variables. The primary optimum design problem is transformed into the convex and separable approximate subproblem by using the direct and reciprocal design variables considering the signs of partial derivatives. In the approximate optimal design formulation, the change of objective function $\Delta\mathbf{W}$ is taken into account instead of the total objective function, $\mathbf{W}(\mathbf{A},\mathbf{S},\mathbf{M})$, and the changes in material kinds, $\Delta\mathbf{M}=[\Delta M_1,\cdots,\Delta M_n]^T$, are treated as new material variables. Then, the following convex and separable approximate subproblem can be derived.

Find $\quad \mathbf{A}, \mathbf{S}, \Delta\mathbf{M}, \quad$ which

minimize

$$\Delta\mathbf{W}(\mathbf{A},\mathbf{S},\mathbf{M}^0+\Delta\mathbf{M})=\sum_{i=1}^{n}\omega_{Ai}(M_i^0+\Delta M_i)A_i$$
$$+\sum_{k=1}^{2P}[\omega_{Sk(+)}(\mathbf{M}^0+\Delta\mathbf{M})S_k-\omega_{Sk(-)}(\mathbf{M}^0+\Delta\mathbf{M})(S_k^0)^2\frac{1}{S_k}] \qquad (6\text{-}25)$$

subject to

$$\bar{g}_{oj}(\mathbf{A},\mathbf{S},\mathbf{M}^0+\Delta\mathbf{M})=\sum_{i=1}^{n}\left[a_{ji(+)}A_i-a_{ji(-)}(A_i^0)^2\frac{1}{A_i}+m_{ji}\Delta M_i\right]$$
$$+\sum_{k=1}^{2P}\left[s_{jk(+)}S_k-s_{jk(-)}(S_k^0)^2\frac{1}{S_k}\right]+\bar{U}_{oj}\le 0 \qquad (j=1,\cdots,n) \qquad (6\text{-}26)$$

$$\bar{g}_{di}(\mathbf{A},\mathbf{S},\mathbf{M}^0+\Delta\mathbf{M})=\sum_{i=1}^{n}\left[a_{di(+)}A_i-a_{di(-)}(A_i^0)^2\frac{1}{A_i}+m_{di}\Delta M_i\right]$$

$$+\sum_{k=1}^{2P}\left[s_{dk(+)}S_k - s_{dk(-)}(S_k^0)^2\frac{1}{S_k}\right]+\overline{U}_{\delta d}\le 0 \qquad (d=1,\cdots,u) \tag{6-27}$$

$$\left.\begin{aligned} &A_i^l \le A_i^l \le A_i^u \qquad (i=1,\cdots,n)\\ &S_k^l \le S_k \le S_k^u \qquad (k=1,\cdots,2P)\\ &M_i \in \mathbf{MS} \end{aligned}\right\} \tag{6-28}$$

where

$$\overline{U}_{\sigma j}=g_{\sigma j}(\mathbf{A}^0,\mathbf{S}^0,\mathbf{M}^0)-\sum_{i=1}^{n}A_i^0\left[a_{ji(+)}-a_{ji(-)}\right]-\sum_{k=1}^{2P}S_k^0\left[s_{jk(+)}-s_{jk(-)}\right]$$

$$\overline{U}_{\delta d}=g_{\delta d}(\mathbf{A}^0,\mathbf{S}^0,\mathbf{M}^0)-\sum_{i=1}^{n}A_i^0\left[a_{di(+)}-a_{di(-)}\right]-\sum_{k=1}^{2P}S_k^0\left[s_{dk(+)}-s_{dk(-)}\right]$$

$$\omega_{Ai}(M_i^0+\Delta M_i) = \rho_{ei}(M_i^0+\Delta M_i)l_i(\widetilde{\mathbf{S}}_i)$$

$$\omega_{Sk}(\mathbf{M}^0+\Delta\mathbf{M}) = \sum_{i\in K_p}\rho_{ei}(M_i^0+\Delta M_i)A_i\frac{\partial l_i(\widetilde{\mathbf{S}}_i)}{\partial S_k}+\rho_L\frac{\partial A_L(S_L)}{\partial S_k}$$

$$a_{ji} = \frac{\partial g_{\sigma j}}{\partial A_i},\quad s_{jk} = \frac{\partial g_{\sigma j}}{\partial S_k},\quad m_{ji} = \frac{\partial g_{\sigma j}}{\partial M_i},$$

$$a_{di} = \frac{\partial g_{\delta d}}{\partial A_i},\quad s_{dk} = \frac{\partial g_{\delta d}}{\partial S_k},\quad m_{di} = \frac{\partial g_{\delta d}}{\partial M_i}.$$

$$\mathbf{M}=\mathbf{M}^0+\Delta\mathbf{M}$$

In the preceding expressions, the symbols (+) and (−) denote the signs of the first-order partial derivatives, and k_p stands for the set of member elements connected to the kth panel point.

(2) Calculation of sensitivities of displacements and axial forces due to seismic loads

The sensitivities of displacement $\delta_{sd}(\mathbf{A},\mathbf{S},\mathbf{M})$ at the dth panel point and axial force $N_{sj}(\mathbf{A},\mathbf{S},\mathbf{M})$ in the jth member element due to seismic loads which are necessary for the calculations of sensitivities a_{ji}, s_{jk}, m_{ji}, a_{di}, s_{dk}, m_{di} are obtained analytically by using the sensitivities of eigenvalue and eigenvector. On the basis of the Nelson's technique[21], the sensitivities of eigenvalue and eigenvector with respect to design variables are calculated by differentiating the eigenvalue equation of structural dynamics in eq.(5-12). Namely, the sensitivities of eigenvalue, μ_k^2, and eigenvector in the kth vibration mode, $[\phi]_k$, with respect to design variable

$B_i \in \mathbf{B} = [A_1, \cdots, A_n, S_1, \cdots, S_{2P}, M_1, \cdots, M_n]^T$ are given by eqs.(5-14) and (5-21) to (5-23).

The sensitivities of displacements $\delta_{e,k}(\mathbf{A},\mathbf{S},\mathbf{M})$ in the kth vibration mode are calculated as the following expression by differentiating the eqs.(6-16) and (6-17).

$$\frac{\partial \delta_{e,k}(\mathbf{A},\mathbf{S},\mathbf{M})}{\partial B_i} = \frac{\partial [\phi]_k}{\partial B_i} q_k + [\phi]_k \frac{\partial q_k}{\partial B_i} \tag{6-29}$$

where

$$\frac{\partial q_k}{\partial B_i} = \frac{\mathbf{S}_{Ak}}{\mu_k^2} \frac{\partial \beta_k}{\partial B_i} + \frac{\beta_k}{\mu_k^2} \frac{\partial \mathbf{S}_{Ak}}{\partial B_i} - \frac{\beta_k \mathbf{S}_{Ak}}{\mu_k^4} \frac{\partial \mu_k^2}{\partial B_i} \tag{6-30}$$

By differentiating the eq.(6-18), the sensitivities of axial force of the kth vibration mode in the jth member element, $N_{ej,k}(\mathbf{A},\mathbf{S},\mathbf{M})$, with respect to A_i, S_k, M_i are, respectively, given by

$$\frac{\partial N_{ej,k}(\mathbf{A},\mathbf{S},\mathbf{M})}{\partial A_i} = \frac{\partial \boldsymbol{k}_{mj}}{\partial A_i} \boldsymbol{Q}_j \delta_{ej,k}(\mathbf{A},\mathbf{S},\mathbf{M}) + \boldsymbol{k}_{mj} \boldsymbol{Q}_j \frac{\partial \delta_{ej,k}(\mathbf{A},\mathbf{S},\mathbf{M})}{\partial A_i} \tag{6-31}$$

$$\frac{\partial N_{ej,k}(\mathbf{A},\mathbf{S},\mathbf{M})}{\partial S_i} = \frac{\partial \boldsymbol{k}_{mj}}{\partial S_i} \boldsymbol{Q}_j \delta_{ej,k}(\mathbf{A},\mathbf{S},\mathbf{M}) + \boldsymbol{k}_{mj} \frac{\partial \boldsymbol{Q}_j}{\partial S_i} \delta_{ej,k}(\mathbf{A},\mathbf{S},\mathbf{M}) + \boldsymbol{k}_{mj} \boldsymbol{Q}_j \frac{\partial \delta_{ej,k}(\mathbf{A},\mathbf{S},\mathbf{M})}{\partial S_i} \tag{6-32}$$

$$\frac{\partial N_{ej,k}(\mathbf{A},\mathbf{S},\mathbf{M})}{\partial M_i} = \frac{\partial \boldsymbol{k}_{mj}}{\partial A_i} \boldsymbol{Q}_j \delta_{ej,k}(\mathbf{A},\mathbf{S},\mathbf{M}) \cdot \frac{A_i^0}{E_i(M_i^0)} \{E_i(M_i) - E_i(M_i^0)\} + \boldsymbol{k}_{mj} \boldsymbol{Q}_j \frac{\partial \delta_{ej,k}(\mathbf{A},\mathbf{S},\mathbf{M})}{\partial M_i} \tag{6-33}$$

Finally, the sensitivities of displacement $\delta_{ed}(\mathbf{A},\mathbf{S},\mathbf{M})$ at the dth panel point and axial force $N_{ej}(\mathbf{A},\mathbf{S},\mathbf{M})$ in the jth member element due to seismic loads are obtained by taking the first-order partial derivatives of the responses expressed as square roots of the summations of squares of $\delta_{ed,k}(\mathbf{A},\mathbf{S},\mathbf{M})$ and $N_{ej,k}(\mathbf{A},\mathbf{S},\mathbf{M})$ $(k = 1, \cdots, \nu)$. Namely,

$$\frac{\partial \delta_{ed}(\mathbf{A},\mathbf{S},\mathbf{M})}{\partial B_i} = \frac{1}{\sqrt{\sum_{k=1}^{\nu} \{\delta_{ed,k}(\mathbf{A},\mathbf{S},\mathbf{M})\}^2}} \cdot \sum_{k=1}^{\nu} \delta_{ed,k}(\mathbf{A},\mathbf{S},\mathbf{M}) \cdot \frac{\partial \delta_{ed,k}(\mathbf{A},\mathbf{S},\mathbf{M})}{\partial B_i} \tag{6-34}$$

$$\frac{\partial N_{ej}(\mathbf{A},\mathbf{S},\mathbf{M})}{\partial B_i} = \frac{1}{\sqrt{\sum_{k=1}^{\nu} \{N_{ej,k}(\mathbf{A},\mathbf{S},\mathbf{M})\}^2}} \cdot \sum_{k=1}^{\nu} N_{ej,k}(\mathbf{A},\mathbf{S},\mathbf{M}) \cdot \frac{\partial N_{ej,k}(\mathbf{A},\mathbf{S},\mathbf{M})}{\partial B_i} \tag{6-35}$$

(3) Improvements of **A**, **S** and **M** by a two-stage minimization process of the Lagrangian function

(a) Two-stage minimization process of the Lagrangian function

The behaviors of truss structures subjected to static and seismic loads, such as stresses of member elements and displacements at free nodes, are expressed as the functions of **S** and the product of modulus of elasticity E and A, EA, and the objective function is also expressed as the function of **A**, **S** and **M**. As stated in Chapters 4 and 5, in this study **A** and **S** are dealt with as continuous variables and $\Delta\mathbf{M}$ as discrete variables selected from the material set **MS**. Therefore, the design variables **A**, **S** and ΔM are improved by a two-stage minimization process that uses a dual method and incorporate discrete sensitivity analysis. At the first stage of the minimization process, EA is treated as one design variable, but **M** is maintained constant, and the optimal EA and **S** are determined by using a dual method. In the optimization algorithm of first stage minimization process, E is constant and **A** is improved for improvement of EA. Thereafter, at the second stage of the minimization process, **S** is maintained constant and the better combination of A and $\Delta\mathbf{M}$ for each member element is searched independently to reduce the cost of each member element by comparing the value of cost while keeping the activeness of the constraints which are determined by the first stage minimization process.

(b) Lagrangian function

To solve the convex and separable approximate subproblem defined in eqs. (6-25)-(6-28) by using the two-stage minimization process, the following Lagrangian function which is expressed as the separable forms of **A** and **S** is introduced for the subproblem.

$$\mathbf{L}(\mathbf{A},\mathbf{S},\mathbf{M}^0+\Delta\mathbf{M},\lambda)=\sum_{i=1}^{n}L_i(A_i,\Delta M_i,\lambda)+\sum_{k=1}^{2P}L_k(S_k,\Delta\mathbf{M},\lambda)+\sum_{j=1}^{n}\lambda_j^{\sigma}\overline{U}_{\sigma j}+\sum_{d=1}^{u}\lambda_d^{\delta}\overline{U}_{\delta d} \quad (6\text{-}36)$$

where $\lambda_j^{\sigma}\geq 0\ (j=1,\cdots,n)$, $\lambda_d^{\delta}\geq 0\ (d=1,\cdots,u)$

λ_j^{σ} and λ_d^{δ} are, respectively, the Langrange multipliers (dual variables) for $\overline{g}_{\sigma j}$ and $\overline{g}_{\delta d}$. L_i and L_k are, respectively, the element Lagrangian functions with respect to A_i and ΔM_i, S_k and $\Delta\mathbf{M}$, and these are given by

$$L_i(A_i,\Delta M_i,\lambda)=\omega_{Ai}(M_i^0+\Delta M_i)A_i$$
$$+\sum_{j=1}^{n}\lambda_j^{\sigma}\left[a_{ji(+)}A_i-a_{ji(-)}(A_i^0)^2\frac{1}{A_i}+m_{ji}\Delta M_i\right]+\sum_{d=1}^{u}\lambda_d^{\delta}\left[a_{di(+)}A_i-a_{di(-)}(A_i^0)^2\frac{1}{A_i}+m_{di}\Delta M_i\right] \quad (6\text{-}37)$$

$$L_k(S_k,\Delta\mathbf{M},\lambda)=\omega_{Sk(+)}(\mathbf{M}^0+\Delta\mathbf{M})S_k-\omega_{Sk(-)}(\mathbf{M}^0+\Delta\mathbf{M})(S_k^0)^2\frac{1}{S_k}$$
$$+\sum_{j=1}^{n}\lambda_j^{\sigma}\left[s_{jk(+)}S_k-s_{jk(-)}(S_k^0)^2\frac{1}{S_k}\right]+\sum_{d=1}^{u}\lambda_d^{\delta}\left[s_{dk(+)}S_k-s_{dk(-)}(S_k^0)^2\frac{1}{S_k}\right] \quad (6\text{-}38)$$

(c) Improvements of ***EA*** and **S** by the first stage minimization process

In the first stage minimization process of the Lagrangian function, the material kinds of member elements **M** are maintained constant, and ***EA*** and **S** are improved by maximizing $\mathbf{L}(\mathbf{A},\mathbf{S},\mathbf{M}^0+\Delta\mathbf{M},\lambda)$ with respect to λ and minimizing it with respect to ***EA*** and **S**. In the minimization algorithm, ***E*** for each member element is constant and **A** is improved for improvement of ***EA***. Since eq.(6-36) has a simple form of a summation of the separable element Lagrangian functions $L_i(A_i,\Delta M_i,\lambda)$ and $L_k(S_k,\Delta\mathbf{M},\lambda)$, the minimization $\mathbf{L}(\mathbf{A},\mathbf{S},\mathbf{M}^0+\Delta\mathbf{M},\lambda)$ with respect to **A**, **S** and $\Delta\mathbf{M}$ can be accomplished by minimizing L_i and L_k with respect to A_i and S_k independently. A_i^*, which minimizes $L_i(A_i,\Delta M_i,\lambda)$, is given by the following expression derived from the necessary condition of $L_i(A_i,\Delta M_i,\lambda)$, namely, $\partial L_i/\partial A_i=0$, and the side constraint on A_i.

$$\left.\begin{array}{lll}\text{if} & [A_i^l(M_i^0)]^2<Z_{Ai}(M_i^0)<[A_i^u(M_i^0)]^2, & A_i^*=\sqrt{Z_{Ai}(M_i^0)}\\ \text{if} & Z_{Ai}(M_i^0)\le[A_i^l(M_i^0)]^2, & A_i^*=A_i^l(M_i^0)\\ \text{if} & Z_{Ai}(M_i^0)\ge[A_i^u(M_i^0)]^2, & A_i^*=A_i^u(M_i^0)\end{array}\right\} \quad (6\text{-}39)$$

where

$$Z_{Ai}(M_i^0)=\frac{-\left(\sum_{j=1}^{n}\lambda_j^{\sigma}a_{ji(-)}+\sum_{d=1}^{u}\lambda_d^{\delta}a_{di(-)}\right)(A_i^0)^2}{\omega_{Ai}(M_i^0)+\sum_{j=1}^{n}\lambda_j^{\sigma}a_{ji(+)}+\sum_{d=1}^{u}\lambda_d^{\delta}a_{di(+)}} \quad (6\text{-}40)$$

S_k^*, which minimizes $L_k(S_k,\Delta\mathbf{M},\lambda)$, is also given by the following expression derived from the necessary condition $\partial L_k/\partial S_k=0$ and the side constraint on S_k.

$$\left.\begin{array}{lll} \text{if} & [S_k^l]^2 < Z_{Sk}(\mathbf{M}^0) < [S_k^u]^2, & S_k^* = \sqrt{Z_{Sk}(\mathbf{M}^0)} \\ \text{if} & Z_{Sk}(\mathbf{M}^0) \le [S_k^l]^2, & S_k^* = S_k^l \\ \text{if} & Z_{Sk}(\mathbf{M}^0) \ge [S_k^u]^2, & S_k^* = S_k^u \end{array}\right\} \tag{6-41}$$

where

if $\omega_{Sk}(\mathbf{M}^0) \ge 0$,

$$Z_{Sk}(\mathbf{M}^0) = \frac{-\left(\sum_{j=1}^{n} \lambda_j^{\sigma} s_{jk(-)} + \sum_{d=1}^{u} \lambda_d^{\delta} s_{dk(-)}\right)(S_k^0)^2}{\omega_{Sk(+)}(\mathbf{M}^0) + \sum_{j=1}^{n} \lambda_j^{\sigma} s_{jk(+)} + \sum_{d=1}^{u} \lambda_d^{\delta} s_{dk(+)}} \tag{6-42}$$

if $\omega_{Sk}(\mathbf{M}^0) < 0$,

$$Z_{Sk}(\mathbf{M}^0) = \frac{-\left(\omega_{Sk(-)}(\mathbf{M}^0) + \sum_{j=1}^{n} \lambda_j^{\sigma} s_{jk(-)} + \sum_{d=1}^{u} \lambda_d^{\delta} s_{dk(-)}\right)(S_k^0)^2}{\sum_{j=1}^{n} \lambda_j^{\sigma} s_{jk(+)} + \sum_{d=1}^{u} \lambda_d^{\delta} s_{dk(+)}} \tag{6-43}$$

The minimized Lagrangian function with respect to $\mathbf{A}$ and $\mathbf{S}$ is denoted as $l(\lambda)$:

$$l(\lambda) = \min_{\mathbf{A},\mathbf{S}} \mathrm{L}(\mathbf{A},\mathbf{S},\mathbf{M}^0 + \Delta\mathbf{M},\lambda) \tag{6-44}$$

Following the minimization process with respect to A_i and S_k, the Lagrangian function $l(\lambda)$ is maximized with respect to the dual variables λ related to the active constraints by using a Newton-type algorithm. The details of the maximization algorithm of $l(\lambda)$ with respect to λ are described in section 4-3.(3).(c).

After the improvements of the dual variable λ as λ^* by the Newton-type algorithm and $\mathbf{A}$ and $\mathbf{S}$ as $\mathbf{A}^*$ and $\mathbf{S}^*$ using λ^*, the set of active constraints $\boldsymbol{S}_{AG}$ in the currently approximated design space also has to be updated. The min.-max. process described above is iterated until $\mathbf{A}$, $\mathbf{S}$ and λ converge to constant values.

In the first minimization process, it should be noted that if the rate of change in $\mathbf{S}$ is too large in any iteration, the successive solutions oscillate, and in some cases smooth convergence may not be obtained. For this reason, the adaptive move limit constraints are restricted such that the maximum rate of change in $\mathbf{S}$ is limited to less than 15 percent.

(d) Improvements of **A** and **M** by the second stage minimization process

In the second stage minimization process of the Lagrangian function, the values of **S** and λ improved by the first stage minimization process are maintained constant, and the Lagrangian function $\mathbf{L}(\mathbf{A},\mathbf{S},\mathbf{M}^0+\Delta\mathbf{M},\lambda)$ given by eq.(6-36) is minimized with respect to **A** and $\Delta\mathbf{M}$ while keeping the activeness of the constraints which are determined by the first stage minimization process, namely,

Find **A**, $\Delta\mathbf{M}$, which

minimize $\mathbf{L}(\mathbf{A},\overline{\mathbf{S}},\mathbf{M}^0+\Delta\mathbf{M},\overline{\lambda})$ (6-45)

subject to $\overline{g}_{\sigma j}(\mathbf{A},\overline{\mathbf{S}},\mathbf{M}^0+\Delta\mathbf{M}) \le 0 \qquad (j \in \boldsymbol{S}_{AG})$ (6-46)

$\overline{g}_{\delta d}(\mathbf{A},\overline{\mathbf{S}},\mathbf{M}^0+\Delta\mathbf{M}) \le 0 \qquad (d \in \boldsymbol{S}_{AG})$ (6-47)

$$\left.\begin{aligned} A_i^l \le A_i \le A_i^u \qquad & (i=1,\cdots,n) \\ M_i \in \mathbf{MS} \qquad & (i=1,\cdots,n) \end{aligned}\right\} \quad (6\text{-}48)$$

In the above expressions, $\overline{\lambda}$ and $\overline{\mathbf{S}}$ are the solutions obtained by the first stage minimization process and these values are maintained constant during the minimization process.

After the first stage improvements of **A**, **S** and λ, the approximate constrains $\overline{g}_{\sigma j}(\mathbf{A},\overline{\mathbf{S}},\mathbf{M}^0+\Delta\mathbf{M})$ and $\overline{g}_{\delta d}(\mathbf{A},\overline{\mathbf{S}},\mathbf{M}^0+\Delta\mathbf{M})$ in the set of active constrains $\boldsymbol{S}_{AG}$, namely , $j \in \boldsymbol{S}_{AG}$ and $d \in \boldsymbol{S}_{AG}$, become zero, and λ_j^σ and λ_d^δ for the inactive constrains $\overline{g}_{\sigma j}$ and $\overline{g}_{\delta d}$, namely, $j \notin \boldsymbol{S}_{AG}$ and $d \notin \boldsymbol{S}_{AG}$, become zero. By substituting these relations into $\mathbf{L}(\mathbf{A},\overline{\mathbf{S}},\mathbf{M}^0+\Delta\mathbf{M},\overline{\lambda})$ in eq. (6-36), the minimization problem in eqs. (6-45)-(6-48) is solved by minimizing only the term of objective function for each member element in $\mathbf{L}(\mathbf{A},\overline{\mathbf{S}},\mathbf{M}^0+\Delta\mathbf{M},\overline{\lambda})$ independently, namely, $\tilde{L}_i(\tilde{A}_i(M_i^0+\Delta M_i), M_i^0+\Delta M_i)$ $(i=1,\cdots,n)$ given by eq.(6-49), subject to the constraints in eqs.(6-46)-(6-48).

$$\tilde{L}_i(\tilde{A}_i(M_i^0+\Delta M_i), M_i^0+\Delta M_i) = \omega_{Ai}(M_i^0+\Delta M_i)\tilde{A}_i(M_i^0+\Delta M_i) \quad (i=1,\cdots,n) \quad (6\text{-}49)$$

$\tilde{A}_i$ and ΔM_i which minimize $\tilde{L}_i(\tilde{A}_i(M_i^0+\Delta M_i), M_i^0+\Delta M_i)$ are determined by comparing the discrete values of $\tilde{L}_i(\tilde{A}_i(M_i^0+\Delta M_i), M_i^0+\Delta M_i)$ calculated by using the new material kind $(M_i^0+\Delta M_i)$ and $\tilde{A}_i(M_i^0+\Delta M_i)$ improved so as to satisfy the constraints in eqs. (6-46)-(6-48).

For the case where only stress constraints are active, the necessary condition which maintains the stress constraints active for a discrete change ΔM_i in material kind M_i is given by the following expression.

$$\tilde{g}_{\sigma i}(\tilde{A}_i^{\sigma}(M_i^0+\Delta M_i), M_i^0+\Delta M_i) = \frac{|\sigma_i| A_i(M_i^0)}{\tilde{A}_i^{\sigma}(M_i^0+\Delta M_i)}$$

$$-\sigma_{a\max i}(M_i^0+\Delta M_i, \tilde{A}_i^{\sigma}(M_i^0+\Delta M_i), \tilde{t}_i) = 0 \qquad (i=1,\cdots,n) \qquad (6\text{-}50)$$

By solving eq.(6-50) for $\tilde{A}_i^{\sigma}(M_i^0+\Delta M_i)$, the improved $\tilde{A}_i$ for $M_i^0+\Delta M_i$, $\tilde{A}_i(M_i^0+\Delta M_i)$, is given by

$$\tilde{A}_i^{\sigma}(M_i^0+\Delta M_i) = \frac{|\sigma_i| A_i(M_i)}{\sigma_{a\max i}(M_i^0+\Delta M_i, \tilde{A}_i^{\sigma}(M_i^0+\Delta M_i), \tilde{t}_i)} \qquad (i=1,\cdots,n) \qquad (6\text{-}51)$$

where $\qquad A_i^l(M_i^0+\Delta M_i) \le \tilde{A}_i^{\sigma}(M_i^0+\Delta M_i) \le A_i^u(M_i^0+\Delta M_i)$

σ_i and $\sigma_{a\max i}(M_i^0+\Delta M_i, \tilde{A}_i^{\sigma}(M_i^0+\Delta M_i), \tilde{t}_i)$ indicate, respectively, the working stress in the first stage minimization process and the maximum allowable compressive stress or allowable tensile stress for $M_i^0+\Delta M_i$.

In the case that the ith member element is a compressive member, $\sigma_{a\max i}(M_i^0+\Delta M_i, \tilde{A}_i^{\sigma}(M_i^0+\Delta M_i), \tilde{t}_i)$ in eq.(6-51) is expressed as the function of $\tilde{A}_i^{\sigma}(M_i^0+\Delta M_i)$. Therefore, the determinations of accurate values of $\tilde{A}_i^{\sigma}(M_i^0+\Delta M_i)$ and $\tilde{t}_i$ which satisfy eq.(6-50) requires to repeat the calculation of $\sigma_{a\max i}(M_i^0+\Delta M_i, \tilde{A}_i^{\sigma}(M_i^0+\Delta M_i), \tilde{t}_i)$ due to change in $\tilde{A}_i^{\sigma}(M_i^0+\Delta M_i)$ by using the suboptimization stated in 6-2.(2). For this reason, in this study, eq.(6-50) is linearly approximated with respect to $\tilde{A}_i^{\sigma}(M_i^0+\Delta M_i)$ as

$$\hat{g}_{\sigma i}(\tilde{A}_i^{\sigma}(M_i^0+\Delta M_i), M_i^0+\Delta M_i) = \tilde{g}_{\sigma i}(\tilde{A}_{i0}^{\sigma}(M_i^0+\Delta M_i), M_i^0+\Delta M_i)$$
$$+\frac{\partial \tilde{g}_{\sigma i}}{\partial \tilde{A}_i^{\sigma}}\left\{\tilde{A}_i^{\sigma}(M_i^0+\Delta M_i) - \tilde{A}_{i0}^{\sigma}(M_i^0+\Delta M_i)\right\} = 0 \qquad (i=1,\cdots,n) \quad (6\text{-}52)$$

By solving eq. (6-52) for $\tilde{A}_i^{\sigma}(M_i^0+\Delta M_i)$, $\tilde{A}_{i0}^{\sigma}(M_i^0+\Delta M_i)$ is improved by

$$\tilde{A}_i^{\sigma}(M_i^0+\Delta M_i) = -\tilde{g}_{\sigma i}(\tilde{A}_{i0}^{\sigma}(M_i^0+\Delta M_i), M_i^0+\Delta M_i)/\left(\frac{\partial \tilde{g}_{\sigma i}}{\partial \tilde{A}_i^{\sigma}}\right) + \tilde{A}_{i0}^{\sigma}(M_i^0+\Delta M_i)$$

$$(i=1,\cdots,n) \qquad (6\text{-}53)$$

where $\qquad A_i^l(M_i^0+\Delta M_i) \le \tilde{A}_i^{\sigma}(M_i^0+\Delta M_i) \le A_i^u(M_i^0+\Delta M_i)$

$$\frac{\partial \tilde{g}_{\sigma i}}{\partial \tilde{A}_i^{\sigma}} = -\frac{|\sigma_i| A_i(M_i^0)}{\{\tilde{A}_{i0}^{\sigma}(M_i^0+\Delta M_i)\}^2} - \frac{\partial \sigma_{imax}(M_i^0+\Delta M_i, \tilde{A}_i^{\sigma}(M_i^0+\Delta M_i), \tilde{l}_i)}{\partial \tilde{A}_i^{\sigma}} \tag{6-54}$$

By iterating the improvement of $\tilde{A}_{i0}^{\sigma}(M_i^0+\Delta M_i)$ in eq.(6-53), $\tilde{A}_i^{\sigma}(M_i^0+\Delta M_i)$ and $\tilde{l}_i$ which satisfy eq.(6-50) are determined.

For the case when displacement constraints are active, the necessary condition required to maintain the displacement constraints active for a discrete change ΔM_i is to keep the value of $E_i A_i$ constants, namely,

$$E_i(M_i^0) A_i(M_i^0) = E_i(M_i^0+\Delta M_i) \tilde{A}_i^{\delta}(M_i^0+\Delta M_i) \qquad (i=1,\cdots,n) \tag{6-55}$$

Considering eq.(6-55) and the lower and upper limits on $\tilde{A}_i$, the improved $\tilde{A}_i$ for $M_i^0+\Delta M_i$, $\tilde{A}_i^{\delta}(M_i^0+\Delta M_i)$, is calculated as follows:

$$\left.\begin{array}{ll} \text{if } A_i^l(M_i^0+\Delta M_i) < A_\delta < A_i^u(M_i^0+\Delta M_i); & \tilde{A}_i^{\delta}(M_i^0+\Delta M_i) \\ \text{if } A_\delta \le A_i^l(M_i^0+\Delta M_i); & \tilde{A}_i^{\delta}(M_i^0+\Delta M_i) = A_i^l(M_i^0+\Delta M_i) \\ \text{if } A_\delta \le A_i^l(M_i^0+\Delta M_i); & \tilde{A}_i^{\delta}(M_i^0+\Delta M_i) = A_i^u(M_i^0+\Delta M_i) \end{array}\right\} \tag{6-56}$$

$$\text{where} \quad A_\delta = \sqrt{Z_{Ai}(M_i^0)}\, E_i(M_i^0) / E_i(M_i^0+\Delta M_i) \tag{6-57}$$

$Z_{Ai}(M_i^0)$ in eq.(6-57) is given by eq.(6-40).

In the case where both stress and displacement constraints are active, a larger value of $\tilde{A}_i^{\sigma}(M_i^0+\Delta M_i)$ and $\tilde{A}_i^{\delta}(M_i^0+\Delta M_i)$ obtained by eqs.(6-53) and (6-56) is chosen.

The discrete changes in the mechanical and economic properties of materials considerably affect the design space. Therefore, in the minimization of $\tilde{L}_i(\tilde{A}_i(M_i^0+\Delta M_i), M_i^0+\Delta M_i)$ the range of ΔM_i in one iteration is restricted to the nearest stronger($\Delta M_i=+1$) and weaker($\Delta M_i=-1$) material only and ΔM_i which minimizes $\tilde{L}_i$ is determined by comparing the discrete values of $\tilde{L}_i$ for $\Delta M_i=+1, 0, -1$.

In the optimization process, the followings are noteworthy when the structural behaviors due to not only static loads but also seismic loads are taken into account in the optimum design problem considering shape, material and sizing variables. As described in Chapter 5, the vibration mode and period of natural vibration of truss

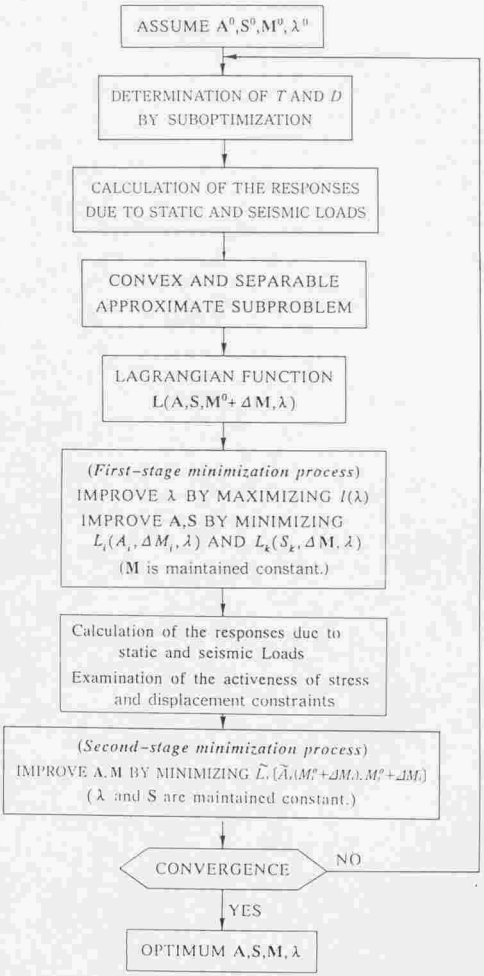

Fig.6-5 Flowchart of the proposed optimal structural synthesis method for truss structures subjected to static and seismic loads

structures are very sensitive to the distribution of EA and $\mathbf{S}$, and the stress for each member element and displacement at each panel point due to seismic loads might be changed considerably as a result of the improvements of EA and $\mathbf{S}$ in the first stage minimization process. If the vibration mode and period of natural vibration are indeed changed after the first stage minimization process, the sensitivities of stress and displacement constraints due to seismic loads calculated using the initial EA and $\mathbf{S}$ in the first stage minimization process become ineffective to satisfy the stress and displacement constraints with the improved EA and $\mathbf{S}$. For this reason, it is necessary to calculate the accurate vibration mode and structural behaviors due to seismic loads by using the response spectrum method and to examine the activeness of stress and displacement constraints after the first stage minimization process. If the activeness of the constraints is changed, the set of active constraints S_{AG} must be modified before performing the second stage minimization process.

In the two-stage minimization process, the iterative improvements of $\mathbf{A},\mathbf{S},\mathbf{M}$ and λ described in this section are repeated until the convergence criteria are satisfied. Thus the optimal solution $\mathbf{A}^*,\mathbf{S}^*,\mathbf{M}^*$ and λ^* to the optimum design problem are obtained. The flowchart of the propose optimal structural synthesis method for truss structures subjected to static and seismic loads is depicted in Fig. 6-5.

6-4. NUMERICAL DESIGN EXAMPLES

The proposed optimal structural synthesis method is applied to various minimum-cost designs of truss structures subjected to static and seismic loads to demonstrate the rigorousness, efficiency and reliability of the optimal design method. In this section, the numerical results for a 193-bar transmission tower truss shown in Fig.6-6 are discussed.

The nonstructural lumped masses $\overline{M}_{C1}$ to $\overline{M}_{C7}$ and structural lumped masses $\overline{M}_{Xi}$ ($i=1,\cdots,86$) as shown in Fig.6-6 are taken into account for the response spectrum analysis. The structural configuration and cross-sectional area for each member element are assumed to be symmetrical about the vertical center line. The horizontal distances from the center line, X_1 and X_2, and the heights in the cantilever trusses, Y_1-Y_9, are considered as the shape design variables. The cross-sectional areas and material kinds for 100 member elements which locate on the one

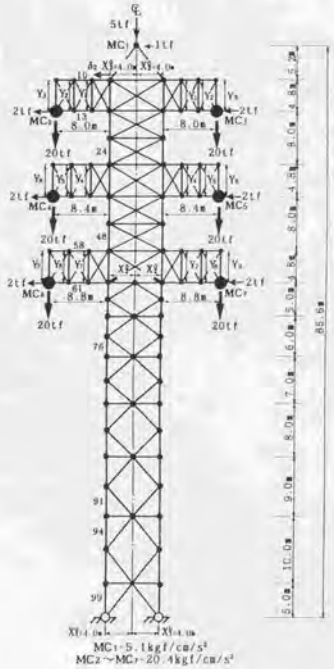

Fig.6-6 Initial 193-bar Transmission tower truss

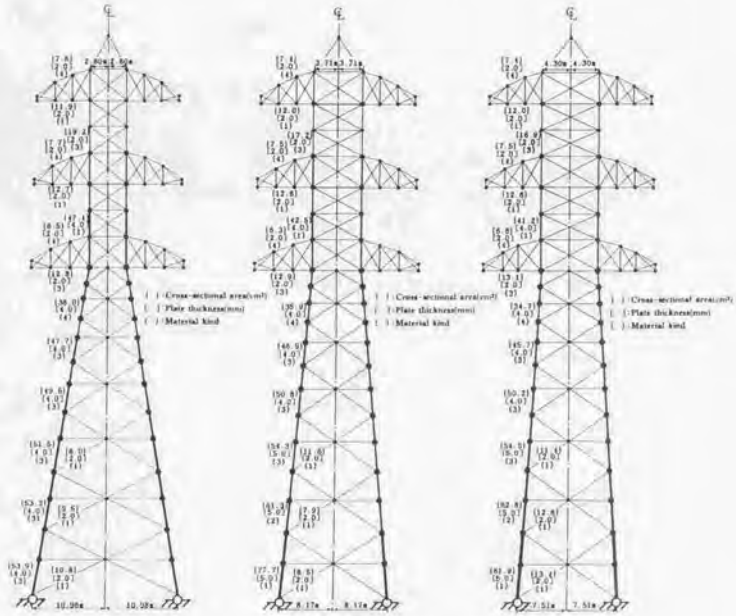

(a) P_L/P_c(SS400)=0.00 (b) P_L/P_c(SS400)=0.06 (c) P_L/P_c(SS400)=0.12

Fig.6-7 Comparison of optimum solutions of 193-bar transmission tower truss for P_L/P_c(SS400)= 0.00, 0.06, 0.12

side of the structure to the centerline are considered as the sizing and material design variables. The critical stress constraint for a member element is determined by comparing the stresses of two member elements which are symmetrical about the centerline each other. Therefore, the numbers of design variables and design constraints considered in the optimization process are, respectively, 211 and 201. The vibration modes from 1st to 8th modes, in which the summation of effective masses of these vibration modes becomes 95 percent lager than the total mass of structural, are taken into account for the response spectrum analysis to obtain the accurate behaviors. The area of land of construction site $A_L(S_L)$ is assumed as a square in which the length of one side is $2(X_1+200)$cm. By comparing the optimum solutions in which the ratio of the unit cost of construction site to the unit cost of steel material SS400 (material kind 1), ρ_L/ρ_c(SS400), are, respectively, assumed as 0.00, 0.06 and 0.12, the effects of the unit cost of land of construction site ρ_L on the optimal configuration and distribution of cross-sectional areas and material kinds are investigated in addition to the rigorousness, efficiency and reliability of the optimal synthesis method.

The comparison of optimum solutions for ρ_L/ρ_c(SS400)=0.00, 0.06 and 0.12 are summarized in Table 6-2 in which the initial **A** and **M** are, respectively, assumed as $50cm^2$ and material kind 4 and the maximum allowable horizontal displacement at panel point 2, δ_2, is set at 45cm. In this table, T.COST of Truss indicates the cost of truss not including the cost of land of construction site. The optimal configurations, distributions of cross-sectional areas and material kinds for three cases are, respectively, shown in Figs.6-7 (a), (b) and (c). In these figures, the thickness of a member element indicates the cross-sectional area, and the values with { }, [ ] and ( ) indicate, respectively, the cross-sectional area, plate thickness and material kind at the optimal solutions.

For the case where ρ_L/ρ_c(SS400) is set at 0.00, namely, the cost of land of construction site is not considered, the optimum solution is obtained after 15 iterations efficiently. At the optimum solution, both stress and displacement constraints due to static and seismic loads are active. Since the cost of land of construction site does not need to take into account in this problem, X_1 and X_2 can take the most economical values for the stress and displacement constraints due to static and seismic loads. The optimum material kinds for main member elements are selected as material kinds 3 and 4 which are more advantageous for problem in

Table 6-2 Comparison of optimum solutions of 193-bar transmission tower truss for ρ_L/ρ_c(SS400)=0.00, 0.06, 0.12 (A^0=50cm^2, M^0=4, δ_a=45cm)

Design Variables	ρ_L/ρ_c(SS400)=0.00	ρ_L/ρ_c(SS400)=0.06	ρ_L/ρ_c(SS400)=0.12
X_1	1097.5(cm)	817.0 (cm)	751.2 (cm)
X_2	279.8	371.2	429.6
Y_1	399.5	413.0	413.4
Y_2	277.5	275.5	275.9
Y_3	69.0	117.9	115.7
$\{A_{10}\}^{1)},[t_{10}]^{2)},(M_{10})^{3)}$	{7.6},[2.0],(4)	{7.4},[2.0],(4)	{7.4},[2.0],(4)
$\{A_{13}\},[t_{13}],(M_{13})$	{11.9},[2.0],(1)	{12.0},[2.0],(1)	{12.0},[2.0],(1)
$\{A_{24}\},[t_{24}],(M_{24})$	{19.2},[2.0],(3)	{17.2},[2.0],(3)	{16.9},[2.0],(3)
$\{A_{48}\},[t_{48}],(M_{48})$	{47.1},[4.0],(1)	{42.5},[4.0],(1)	{41.2},[4.0],(1)
$\{A_{58}\},[t_{58}],(M_{58})$	{6.5},[2.0],(4)	{6.3},[2.0],(4)	{6.6},[2.0],(4)
$\{A_{61}\},[t_{61}],(M_{61})$	{12.8},[2.0],(3)	{12.9},[2.0],(3)	{13.1},[2.0],(3)
$\{A_{76}\},[t_{76}],(M_{76})$	{50.0},[4.0],(4)	{45.5},[4.0],(3)	{44.3},[4.0],(3)
$\{A_{91}\},[t_{91}],(M_{91})$	{51.9},[4.0],(3)	{56.1},[5.0],(3)	{57.6},[5.0],(3)
$\{A_{94}\},[t_{94}],(M_{94})$	{53.3},[4.0],(3)	{61.3},[5.0],(2)	{62.8},[5.0],(2)
$\{A_{99}\},[t_{99}],(M_{99})$	{53.9},[4.0],(3)	{77.7},[5.0],(1)	{81.9},[5.0],(1)
$\{A_{100}\},[t_{100}],(M_{100})$	{10.8},[2.0],(1)	{8.5},[2.0],(1)	{13.4},[2.0],(1)
Iteration	15	10	10
Active constraints	σ, δ	σ, δ	σ, δ
T.COST of truss(yen)	7.310×10^6	7.524×10^6	7.815×10^6
T.C.COST I (yen)[4]	$\underline{7.310\times10^6}$	8.765×10^6	9.986×10^6
T.C.COST II (yen)[5] (ρ_L/ρ_c(SS400)=0.06)	9.330×10^6	$\underline{8.765\times10^6}$	8.901×10^6
T.C.COST III (yen)[6] (ρ_L/ρ_c(SS400)=0.12)	11.350×10^6	10.006×10^6	$\underline{9.986\times10^6}$

1){ }: Cross section (cm^2) 2)[ ]: Plate thickness (mm) 3)( ): Material kind
4) Costs of truss + costs of land of construction site for ρ_L/ρ_c(SS400)=0.00, 0.06, 0.12
5) Costs of truss + costs of land of construction site for ρ_L/ρ_c(SS400)=0.06
6) Costs of truss + costs of land of construction site for ρ_L/ρ_c(SS400)=0.12

which the stress constraints are dominant. For examples, the active constraint for the member element 99 which has a largest cross-sectional area is the stress constraint $g^1_{\sigma 99}$ due to static loads and its optimum material kind is selected as material kind 3. Furthermore, the optimum material kinds for the upper chords in the cantilever trusses are selected as material kind 4. On the contrary, the cross-sectional areas of diagonal member elements which are not fully stressed are determined by the lower limits of cross-sectional areas to satisfy the constraint on slenderness ratio. The plate thicknesses and material kinds of diagonal member elements are, respectively, 2mm and 1 which are the minimum plate thickness and the most economical material kind. X_1, X_2 and T.COST of Truss at the optimum

Table 6-3 Active constraints of main member elements numbered in Fig 6-6 and active constraints as whole structual system for ρ_L/ρ_c(SS400)= 0.00, 0.06, 0.12

No. of member element	ρ_L/ρ_c(SS400)=0.00	ρ_L/ρ_c(SS400)=0.06	ρ_L/ρ_c(SS400)=0.12
10	g_σ^1, (4)	g_σ^1, (4)	g_σ^1, (4)
13	g_σ^1, (1)	g_σ^1, (1)	g_σ^1, (1)
24	g_σ^3, (3)	g_σ^1, g_σ^3, (3)	g_σ^1, (3)
48	g_σ^3, (1)	g_σ^1, g_σ^3, (1)	g_σ^1, (1)
58	g_σ^1, (4)	g_σ^1, (4)	g_σ^1, (4)
61	g_σ^1, (3)	g_σ^1, (3)	g_σ^1, (3)
76	g_σ^1, (4)	g_σ^1, (3)	g_σ^1, (3)
91	g_σ^1, (3)	g_σ^1, g_σ^3, (3)	g_σ^3, (3)
94	g_σ^1, (3)	g_σ^1, g_σ^3, (2)	g_σ^3, (2)
99	g_σ^1, (3)	g_σ^1, g_σ^3, (1)	g_σ^3, (1)
100	g_{SL}, (1)	g_{SL}, (1)	g_{SL}, (1)
system[1)]	g_δ	g_δ	g_δ

1) Active constraints as whole structual system
g_σ^1 : stress constraint due to static and seiamic loads
g_σ^3 : compressive stress constraint due to static and seismic loads
g_{SL} : constraint on slenderness ratio
g_δ : displacement constraint due to static and seismic loads

solution are, respectively, 1097.5cm, 279.8cm and 7.310×10^6yen.

For the case where ρ_L/ρ_c(SS400) is set at 0.06, the optimum solution is obtained after 10 iterations quite efficiently. As the same as the case of ρ_L/ρ_c(SS400)=0.00, both stress and displacement constraints are active at the optimum solution. In this problem, the cost of land of construction site influences the total construction cost. Therefore, the optimum value of X_1 is 817.0cm and it is 280.5cm smaller than that for the case of ρ_L/ρ_c(SS400)=0.00, on the contrary, the optimum value of X_2 is 371.2cm and it is 91.4cm larger than that for the case of ρ_L/ρ_c(SS400)=0.00. With regard to member element 99, by the changes of X_1 and X_2, the two stress constraints due to not only static loads but also static and seismic loads, $g_{\sigma 99}^1$ and $g_{\sigma 99}^3$, become active. The optimum plate thickness and material kind for the case of ρ_L/ρ_c(SS400) =0.00 were 4mm and 3, but the optimum plate thickness for the case of ρ_L/ρ_c(SS400)=0.06 is 5mm and the optimum material kind is selected as 1. The cross-sectional area of member element 99 is 44.2% larger than that for the case of ρ_L/ρ_c(SS400)=0.00. In the comparison of the cost of truss not including the cost of

ρ_L / ρ_c(SS400) =0.00. In the comparison of the cost of truss not including the cost of land of construction site, T.COST of Truss for the case of ρ_L / ρ_c(SS400) =0.06 is 2.93% higher than that for the case of ρ_L / ρ_c(SS400) =0.00.

For the case where ρ_L / ρ_c(SS400) is set at 0.12, the optimum solution is also obtained after 10 iterations quite efficiently. As the same as two cases mentioned previously, both stress and displacement constraints are also active at the optimum solution. The optimum value of X_1 is 751.2cm and 65.8cm reduction of X_1 is observed compared with that for the case of ρ_L / ρ_c(SS400) =0.06, while the optimum value of X_2 is 429.6cm and 58.4cm increase of X_2 is observed. The active constraints of member element 99 is the stress constraint due to seismic loads, $g^3_{\sigma 99}$. The optimum cross-sectional area of member element 99 for the case of ρ_L / ρ_c(SS400) =0.12 is 81.9cm^2 and it is 5.4% larger than that for the case of ρ_L / ρ_c(SS400) =0.06. However, the optimum plate thickness and material kind for member element 99 are identical to those for the case of ρ_L / ρ_c(SS400) =0.06. As the result, T.COST of Truss for the case of ρ_L / ρ_c(SS400) =0.12 is 3.87% higher than that for the case of ρ_L / ρ_c(SS400) =0.06.

Table 6-3 summarizes the active constraints of main member elements numbered in Fig.6-6 and the active constraints as whole structural systems for ρ_L / ρ_c(SS400) = 0.00, 0.06 and 0.12 at the optimum solutions. As clearly seen from Table 6-3, according to the values of ρ_L / ρ_c(SS400) the active constraints of main member elements become g^1_σ or g^3_σ or both g^1_σ and g^3_σ except the member element 100 whose cross-sectional area is determined in order to satisfy the constraint on slenderness ratio. The combination of stress constraints, g^1_σ or g^3_σ or both g^1_σ and g^3_σ, are also active for the other member elements of transmission tower truss shown in Fig.6-6. As the whole structural system, the displacement constraint due to static and seismic loads is also active for three cases. From these results, the optimum configurations, optimum arrangements of cross-sectional areas and material kinds are determined such that the working stresses for main member elements are equal to the allowable stresses of corresponding material kinds and the maximum horizontal displacement in whole structural system due to static and seismic loads is equal to the maximum allowable displacement.

To investigate the reliability of optimum solution stated above, the total construction costs which are expressed as the summations of the costs of land of construction site and the costs of truss are depicted in the column of T.C.COST I

in Table 6-2 for ρ_L / ρ_c(SS400) = 0.00, 0.06 and 0.12. The column of T.C.COST Ⅱ in Table 6-2 indicates the summation of the costs of truss for ρ_L / ρ_c(SS400) = 0.00, 0.06 and 0.12 and the costs of land of construction site for ρ_L / ρ_c(SS400) = 0.06. Namely, in the calculation of the costs of land of construction site, the value of ρ_L / ρ_c(SS400) is assumed as 0.06 and the areas of land of construction site are calculated by using the optimum values of $\mathbf{X}_1$ for ρ_L / ρ_c(SS400) = 0.00, 0.06 and 0.12. The column of T.C.COST Ⅲ in Table 6-2 indicates the summation of the costs of truss for ρ_L / ρ_c(SS400) = 0.00, 0.06 and 0.12 and the costs of land of construction site for ρ_L / ρ_c(SS400) = 0.12. In the calculation of the costs of land of construction site, the value of ρ_L / ρ_c(SS400) is assumed as 0.12 and the areas of land of construction site are calculated by using the optimum values of $\mathbf{X}_1$ for ρ_L / ρ_c(SS400) = 0.00, 0.06 and 0.12. As clearly seen from Table 6-2, the most economical total construction costs for ρ_L / ρ_c(SS400) = 0.00, 0.06 and 0.12 indicate, respectively, 7.310×10^6 in T.C.COST Ⅰ, 8.765×10^6 in T.C.COST Ⅱ and 9.986×10^6 in T.C.COST Ⅲ. This results emphasize the reliability of the proposed method. As stated previously, the optimum configuration of transmission tower truss and optimum arrangements of material kinds and cross-sectional areas for each ρ_L / ρ_c(SS400) are quite reasonable. Therefore, it is clarified that the proposed optimum design method can determine the optimum configuration and optimum arrangements of material kinds and cross-sectional areas of truss structures subjected to static and seismic loads quite efficiently and rationally.

6-5. CONCLUSIONS

This Chapter presents an efficient optimal synthesis method for truss structures subjected to static and seismic loads. The optimum design method is developed by utilizing the algorithm developed in Chapters 4 and 5 and suboptimization techniques. The coordinates of panel points, cross-sectional dimensions and discrete material kinds of all member elements are dealt with as the design variables. Constraints on stresses and displacements caused by static and seismic loads and constraints on slenderness ratio are considered, respectively, as behavior and side constraints. The behaviors and their sensitivities due to earthquake motions are calculated, respectively, by the response spectrum analysis and Nelson's method. As the design examples the cost-minimization problems of 193-bar transmission tower

truss are shown for the three design conditions with different unit costs of land of construction sites to demonstrate the rigorousness, efficiency and reliability of the proposed optimum design method.

The following conclusions can be drawn from this study:

(1) The proposed optimal synthesis method can obtain the optimum shape of structure, discrete material kinds and cross-sectional dimensions of member elements of large scale truss structures subject to stress and displacement constraints due to static and seismic loads within 15 iterations quite efficiently.

(2) By investigating and comparing the optimum solutions for various unit prices of land of construction site, it has been confirmed that the optimal shape and distribution of material kinds and sizing variables in the whole structure are considerably affected by the unit price of land of construction site.

(3) The proposed two-stage optimization process for minimizing the Lagrangian function can determine the optimum material kinds of all member elements of truss structures subjected to static and seismic loads in a systematic and efficient manner even when the algorithm is initialized with the worst material distribution.

(4) The suboptimization concept on cross-sectional dimensions can simplify the formulation of optimum design problem greatly. The optimum cross-sectional dimensions of each member elements can be determined simply by using the optimum cross-sectional areas and suboptimization process.

(5) In the optimization process, the vibration mode and period of natural vibration of truss structures are very sensitive to the distribution of $\boldsymbol{EA}$ and $\mathbf{S}$, and the stress for each member element and displacement at each panel point due to seismic loads might be changed considerably as a result of the improvements of $\boldsymbol{EA}$ and $\mathbf{S}$ in the first stage minimization process. Therefore, it is necessary to calculate the accurate vibration mode and structural behaviors due to seismic loads by using the response spectrum method and to examine the activeness of stress and displacement constraints after the first stage minimization process. If the activeness of the constraints is changed, the set of active constraints must be modified before performing the second stage minimization process.

REFERENCES

1. Pierson,B.L., "A survey on optimal structural design under dynamic constrains", *Int. J. Numer. Methods Engng.*, Vol.4, 1972, pp.491-499.
2. Cheng,F.Y. and Botkin,M.E., "Nonlinear optimum design of dynamic damped frames", *J. Struct. Div. ASCE*, Vol.102(ST3), 1976, pp.609-627.
3. Zagjeski,S.W. and Bertero,V.V., "Optimum seismic-resistant design of R/C frames", *J. Struct. Div. ASCE*, Vol.105(ST5), 1979, pp.829-845.
4. Davidsion,J.W., Felton,L.P. and Hart,G.C., "On reliability-based structural optimization for earthquakes", *Computers and Structures*, Vol.12, 1980, pp.99-105.
5. Balling,R.J., Pister,K.S. and Ciampi,V., "Optimal seismic resistant design of a planar steel frame", *Earthquake Engineering and Structural Dynamics*, Vol.11, 1983, pp.541-556.
6. Austin,M.A. and Pister,K.S., "Design of seismic-resistant friction-braced frames", *J. Struct. Engng. ASCE*, Vol.111, No.12, 1985, pp.2751-2769.
7. Austin,M.A., Pister,K.S. and Mahin,S.A., "Probabilistic design of earthquake-resistant structures", *J. Struct. Engng. ASCE*, Vol.113, No.8, 1987, pp.1642-1659.
8. Austin,M.A., Pister,K.S. and Mahin,S.A., "Probabilistic design of moment-resistant frames under seismic loading", *J. Struct. Engng. ASCE*, Vol.113. No.8, 1987, pp.1660-1677.
9. Cheng,F.Y. and Juang,D.S., "Recursive optimization for seismic steel frames", *J. Struct. Engng. ASCE*, Vol.115, No.2, 1989, pp.445-466.
10. Gulay,G. and Boduroglu,H., "An algorithm for the optimum design of braced and unbraced steel frames under earthquake loading", *Earthquake Engineering and Structural Dynamics*, Vol.18, 1989, pp.121-128.
11. Hwang,H.H.M. and Hsu,H.M., "Seismic LRFD criteria for RC moment-resisting frame buildings", *J. Struct. Engng. ASCE*, Vol.119, No.6, 1993, pp.1807-1824.
12. Ohkubo,S. and Asai,K., "A hybrid optimal synthesis method for truss structures considering shape, material and sizing variables", *Int. J. Numer. Methods Engng.*, Vol.34, 1992, pp.839-851.
13. Ohkubo,S., Taniwaki,K. and Asai,K., "Optimal structural synthesis utilizing shape, material and sizing sensitivities", in Kleiber,M. and Hisada,T. eds., *Design Sensitivity Analysis*, Atranta Technology Publications, Atlanta, 1993, pp.164-188.
14. Ohkubo,S. and Taniwaki,K., "Total optimal synthesis method for truss structures subject

to static and frequency constraints", *Microcomputers in Civil Engineering*, Vol.10, 1995, pp.39-50.

15. Japan Road Association, *Specifications for highway bridges*, Part II *steel bridges*, Maruzen Co.Ltd., Tokyo, 1995. (in Japanese)
16. Japan Road Association, *Specifications for highway bridges, steel bridges, Part V seismic design*, Maruzen Co.Ltd., Tokyo, 1990. (in Japanese)
17. Ohkubo,S., "Optimization of truss using suboptimization of member", *Transactions of JSCE*, Vol. 2, Part I, 1970, pp.111-118.
18. Okumura,T. and Ohkubo,S., "Optimum design of steel continuous girders using suboptimization of girder elements", *Proc. of JSCE*, No.215, 1973, pp.1-14. (in Japanese)
19. Ohkubo,S. and Okumura,T., "Structural system optimization based on suboptimizing method of member elements", *Preliminary Report of Tenth Congress*, IABSE, 1976, pp.163-168.
20. Ohkubo,S. and Taniwaki.K., "Optimum design of truss by dual approach and element suboptimization", *Proc. of JSCE*, No.350/I-2, 1984, pp.331-340. (in Japanese)
21. Nelson,R.B., "Simplified calculation of eigenvector derivatives", *AIAA Journal*, Vol.14, No.9, 1976, pp.1201-1205.
22. Ohkubo,S. and Taniwaki,K., "Optimum earthquake-resistant design of truss structures considering configuration and sizing variables", *Proc. of the Int'l Conf. on Computational Engineering Science*, ICES, 1995, pp.193-198.
23. Ohkubo,S. and Taniwaki,K., "Structural optimization dealing with shape, material and sizing variables subjected to static and seismic loads", *Proc. of the Tools and Methods for Concurrent Engineering*, TMCE'96, 1996, pp.59-74.
24. Ohkubo,S. and Taniwaki,K., "Total optimal synthesis method for earthquake-resistant design of truss structures", *Proc. of First World Congress of Structural and Multidisciplinary Optimization*, WCSMO-1, 1995, pp.629-634.
25. Ohkubo,S. and Taniwaki,K., "Optimal earthquake-resistant design of truss structures considering configuration, material and sizing variables", *J. Structural Mechanics and Earthquake Engineering*, JSCE, No.570/I-40, 1997, pp.47-61. (in Japanese)

Chapter 7 CONCLUSIONS

In Chapter 2, a rigorous and efficient optimum design method for steel cable-stayed bridges is presented. In this design method, not only the cross-sectional dimensions of cables, main girder and pylon elements but also the cable anchor positions on the main girder and the heights of pylons are dealt with as the design variables. The proposed optimum design method has been applied to the minimum-cost design problem of steel cable-stayed bridge with 48 cable stays and the practical design problem of the Swan Bridge at the Tokiwa Park. The theoretical rigorousness, efficiency and practical usefulness of the proposed optimum design method are demonstrated by investigating the optimum solutions at various design conditions.

The following conclusions can be drawn from this study:

(1) The global optimum solutions can be determined in 9-15 iterations quite efficiently by the proposed optimum design method.

(2) The optimum values of pylon height, cable anchor positions on the main girder, steel plate thicknesses of each main girder and pylon elements, and cross-sectional area of each cable appear to be reasonable and well balanced.

(3) In the numerical examples of steel cable-stayed bridge with 48 cable stays, the reduction of total cost from 2.7%-8.6% can be observed by dealing with the cable anchor positions on the main girder and the height of pylon as the design variables. Therefore, the treatment of cable arrangement as the design variables is extremely significant in the optimum design problem of steel cable-stayed bridges.

(4) From structural mechanics consideration, with regard to the optimum cable arrangement in the numerical example of steel cable-stayed bridge with 48 cable stays, the top two cables are parallel and are anchored at the end support in the side span, on the other hand, the cables are distributed as the geometric series in the center span. The cross-sectional areas of top two cables in the side and center spans are determined to be 3.6-1.4 times larger than those of the middle cables. The cross-sectional areas of unnecessary cables at the optimum solutions are found to be the imposed lower limit automatically by the proposed optimum design method.

(5) By applying the proposed method to the practical design of the Swan Bridge at the Tokiwa Park, the final decision-making could be accomplished quite easily and efficiently from the standpoint of total optimization considering not only the cost minimization but also the aesthetic feeling. Therefore, we can conclude that the proposed design method is quite useful in the practical design of steel cable-stayed bridges.

In Chapter 3, a general purpose, rigorous and efficient optimum design system for steel cable-stayed bridges is developed. In this design system, not only can the cable anchor positions on the main girder $\mathbf{X}_C$ and the height of pylon $\mathbf{Y}_C$, and the cross-sectional dimensions $\mathbf{Z}$ of cables, main girder and pylon elements be dealt with as design variables, but also the pseudo-loads $\mathbf{P}_P$ applied to the cables which induce the prestresses into the cables. The cost-minimization problem is solved by a powerful two-stage optimum design process. The proposed optimum design method has been applied to the minimum-cost design problems of practical-scale steel cable-stayed bridge with 64 cable stays. The theoretical rigorousness, efficiency and practical usefulness of the proposed optimum design system are demonstrated by giving several numerical design examples and investigating the optimum solutions at various design conditions.

The conclusions that can be drawn from this study are:

(1) The global optimum solutions of steel cable-stayed bridges for various design conditions and combinations of the design variables $\mathbf{Z}$, $\mathbf{X}_C$, $\mathbf{Y}_C$ and $\mathbf{P}_P$ can be determined quite rigorously and efficiently by the proposed two-stage optimum design method.

(2) The significance of dealing with cable anchor positions on the main girder $\mathbf{X}_C$ and the height of pylon $\mathbf{Y}_C$ as the design variables in the optimum design of steel cable-stayed bridges is also confirmed from the design examples in this Chapter.

(3) The optimum solutions of $\mathbf{Z}$ only or $\mathbf{Z}$, $\mathbf{X}_C$ and $\mathbf{Y}_C$ can be obtained in 6-19 iterations of the first stage optimization process theoretically and efficiently. Following the optimum solutions in the first stage optimization process, after 10-14 iterations of the second stage optimization process the theoretical optimum solutions of $\mathbf{Z}$ and $\mathbf{P}_P$ can be obtained quite efficiently.

(4) The optimum cable anchor positions on the main girder $\mathbf{X}_C$ and the height of pylon $\mathbf{Y}_C$ determined during the first stage optimization process by considering only the design loads are found to be scarcely affected by the optimum pseudo-loads from the design example. Therefore, we can obtain the final optimum solutions of $\mathbf{Z}$, $\mathbf{X}_C$, $\mathbf{Y}_C$ and $\mathbf{P}_P$ after only one repetition of two-stage optimization process, namely determination of the optimum solutions of $\mathbf{Z}$, $\mathbf{X}_C$, $\mathbf{Y}_C$ subjected to only the design loads by the first stage optimization process and determination of the optimum solutions of $\mathbf{Z}$ and $\mathbf{P}_P$ subjected to design loads and pseudo-loads by the second stage optimization process.

(5) By giving the optimum prestresses to the cables, the local peaks of min. and max. bending moments at the middle support in the main girder are reduced to 53.6 −40.5% and the cross-sectional areas of cables change to the range from +42.7% to -84.5%, and all nontrivial cables are fully stressed. As a result, 2.9% reduction in the total cost of the bridge is observed by giving the optimum cable prestresses in the design examples. From various design examples, it can be said that we can save 2.6%-4.1% of the total cost of the bridge by giving the optimum prestress in the cables.

(6) The proposed optimum design system is quite useful for practical design of the steel cable-stayed bridge at all design stages, from the planning stage to the detailed design stage.

In Chapter 4, an optimal structural synthesis method is presented to determine the optimum solutions for design problems of truss structures considering the coordinates of panel points, cross-sectional areas and discrete material kinds of all member elements simultaneously as design variables. The stress and displacement constraints due to static loads are taken into account in the optimization process. The optimal structural synthesis method has been developed by using the concept of convex and linear approximation, dual method, two-stage minimization process of the Lagrangian function and discrete sensitivity analysis. The generality, rigorousness, reliability and efficiency of the proposed optimal structural synthesis method are illustrated by applying the method to various minimum-cost design problems of 31-bar truss subjected to stress and displacement constraints and investigating the optimum solutions at various design conditions.

The conclusions that can be drawn from this study are:

(1) The design method can deal with any combinations of design variables such as shape of the structure, discrete material kinds and cross-sectional areas of member elements, and can optimize the design variables as well as the topological member arrangement simultaneously.

(2) The two-stage minimization process of the Lagrangian function can solve the mixed discrete/continuous variable problems quite systematically and efficiently.

(3) The rigorousness and reliability of the proposed design method have been confirmed by various numerical experiments of 31-bar trusses. The convergence to the optimum solutions is quite excellent and the optimum solutions can be obtained after 15-25 iterations quite efficiently even when the algorithm is initialized with the worst possible material distribution.

(4) Adaptive move limit constraint on **Y** is required to ensure the successive solutions converge to the optimum solution when the displacement constraints are active in the design problem.

In Chapter 5, the systematic synthesis method proposed in Chapter 4 is applied to determine the optimum solutions of shape, material and sizing variables, **S**, **M**, **A**, of truss structures subject to not only stress and displacement constraints due to static loads but also frequency constraints. The design method is developed by utilizing the two-stage minimization process of the Lagrangian function, the concept of convex and linear approximation, dual method and discrete sensitivity analysis. The rigorousness, reliability and efficiency of the proposed design method have been confirmed by various numerical experiments on statically indeterminate trusses.

The following conclusions can be drawn from this study:

(1) The proposed optimal synthesis method can deal with any combinations of design variables such as shape of structure, discrete material kinds and cross-sectional areas of member elements of truss structure subject to both static and frequency constraints. The application of this method, also, leads to an optimum member topology.

(2) The proposed two-stage optimization process for minimizing the Lagrangian function can also solve the mixed discrete/continuous variable problem subject

to stress, displacement and frequency constraints in a systematic and efficient manner.

(3) Adaptive move limit constraint on **S** is necessary to ensure that successive solutions converge to the optimum solution when displacement or frequency constraints are active in the design problem.

(4) The vibration mode and frequency of truss structure are very sensitive to the distribution of EA (the product of modulus of elasticity E and cross-sectional are A) and **S**, and the vibration mode might be changed by improvements of EA and **S** at the first stage of the minimization process. Therefore, it is necessary to calculate the exact vibration mode and frequency and to examine the activeness of frequency constraint at the end of first stage minimization process to ensure the smooth convergence to the optimum solution.

Chapter 6 presents an efficient optimal synthesis method for truss structures subjected to static and seismic loads. The optimum design method is developed by utilizing the algorithm developed in Chapters 4 and 5 and suboptimization techniques. The coordinates of panel points, cross-sectional dimensions and discrete material kinds of all member elements are dealt with as the design variables. Constraints on stresses and displacements caused by static and seismic loads and constraints on slenderness ratio are considered, respectively, as behavior and side constraints. The behaviors and their sensitivities due to earthquake motions are calculated, respectively, by the response spectrum analysis and Nelson's method. As the design examples the cost-minimization problems of 193-bar transmission tower truss are shown for the three design conditions with different unit costs of land of construction sites to demonstrate the rigorousness, efficiency and reliability of the proposed optimum design method.

The following conclusions can be drawn from this study:

(1) The proposed optimal synthesis method can obtain the optimum shape of structure, discrete material kinds and cross-sectional dimensions of member elements of large scale truss structures subject to stress and displacement constraints due to static and seismic loads within 15 iterations quite efficiently.

(2) By investigating and comparing the optimum solutions for various unit prices of land of construction site, it has been confirmed that the optimal shape and

distribution of material kinds and sizing variables in the whole structure are considerably affected by the unit price of land of construction site.

(3) The proposed two-stage optimization process for minimizing the Lagrangian function can determine the optimum material kinds of all member elements of truss structures subjected to static and seismic loads in a systematic and efficient manner even when the algorithm is initialized with the worst material distribution.

(4) The suboptimization concept on cross-sectional dimensions can simplify the formulation of optimum design problem greatly. The optimum cross-sectional dimensions of each member elements can be determined simply by using the optimum cross-sectional areas and suboptimization process.

(5) In the optimization process, the vibration mode and period of natural vibration of truss structures are very sensitive to the distribution of $\boldsymbol{EA}$ and $\mathbf{S}$, and the stress for each member element and displacement at each panel point due to seismic loads might be changed considerably as a result of the improvements of $\boldsymbol{EA}$ and $\mathbf{S}$ in the first stage minimization process. Therefore, it is necessary to calculate the accurate vibration mode and structural behaviors due to seismic loads by using the response spectrum method and to examine the activeness of stress and displacement constraints after the first stage minimization process. If the activeness of the constraints is changed, the set of active constraints must be modified before performing the second stage minimization process.

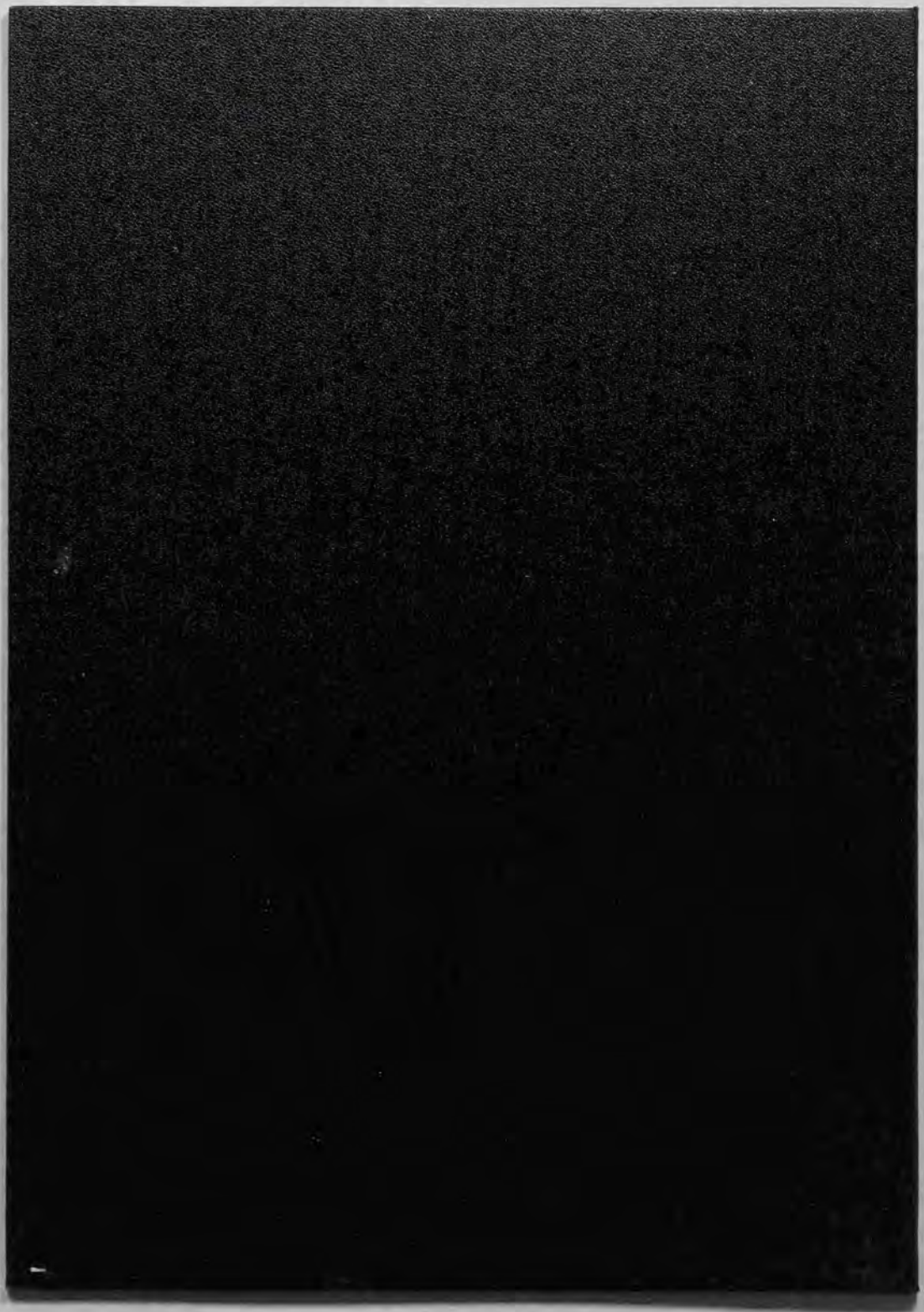

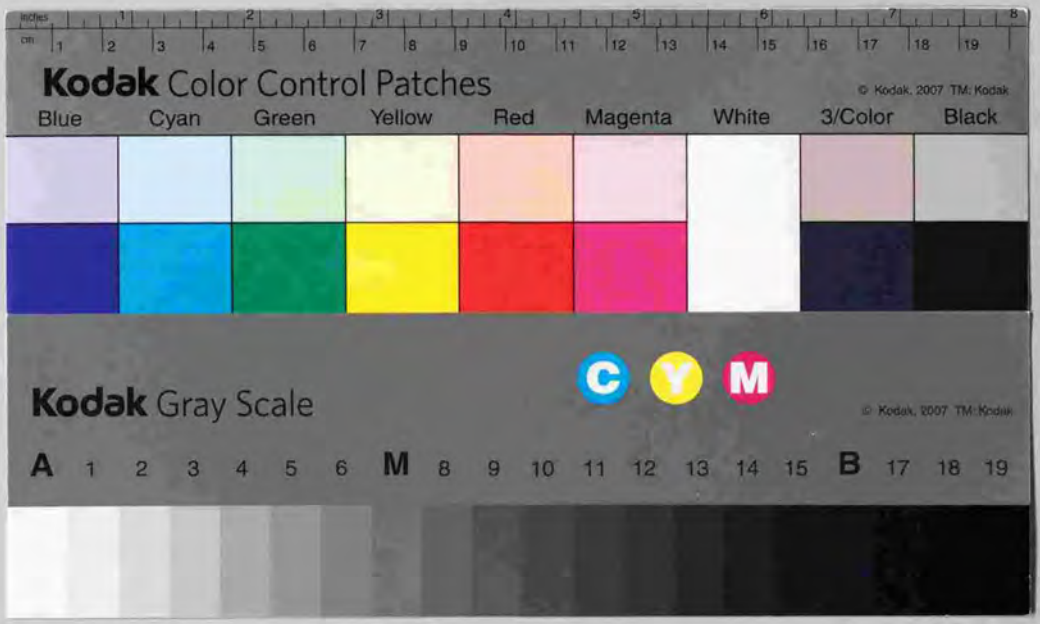
inches
cm
Kodak Color Control Patches
© Kodak, 2007 TM: Kodak
Blue
Cyan
Green
Yellow
Red
Magenta
White
3/Color
Black
Kodak Gray Scale
C
Y
M
© Kodak, 2007 TM: Kodak
A 1 2 3 4 5 6 M 8 9 10 11 12 13 14 15 B 17 18 19